National Library of Canada
Bibliothèque nationale du Canada

Canadian Theses Service
Service des thèses canadiennes

Ottawa, Canada
K1A 0N4

NOTICE

The quality of this microform is heavily dependent upon the quality of the original thesis submitted for microfilming. Every effort has been made to ensure the highest quality of reproduction possible.

If pages are missing, contact the university which granted the degree.

Some pages may have indistinct print especially if the original pages were typed with a poor typewriter ribbon or if the university sent us an inferior photocopy.

Reproduction in full or in part of this microform is governed by the Canadian Copyright Act, R.S.C. 1970, c. C-30, and subsequent amendments.

AVIS

La qualité de cette microforme dépend grandement de la qualité de la thèse soumise au microfilmage. Nous avons tout fait pour assurer une qualité supérieure de reproduction.

S'il manque des pages, veuillez communiquer avec l'université qui a conféré le grade.

La qualité d'impression de certaines pages peut laisser à désirer, surtout si les pages originales ont été dactylographiées à l'aide d'un ruban usé ou si l'université nous a fait parvenir une photocopie de qualité inférieure.

La reproduction, même partielle, de cette microforme est soumise à la Loi canadienne sur le droit d'auteur, SRC 1970, c. C-30, et ses amendements subséquents.

NL-339 (r. 88/04) c

Canada

University of Alberta

Imino-Functionalized Phosphines and Bisphosphines and their Metal Complexes

by

Robert William Reed ©

A thesis
submitted to the Faculty of Graduate Studies and Research
in partial fulfilment of the requirements
for the degree of Doctor of Philosophy

Department of Chemistry

Edmonton, Alberta
Spring, 1992

National Library
of Canada

Bibliothèque nationale
du Canada

Canadian Theses Service

Service des thèses canadiennes

Ottawa, Canada
K1A 0N4

The author has granted an irrevocable non-exclusive licence allowing the National Library of Canada to reproduce, loan, distribute or sell copies of his/her thesis by any means and in any form or format, making this thesis available to interested persons.

The author retains ownership of the copyright in his/her thesis. Neither the thesis nor substantial extracts from it may be printed or otherwise reproduced without his/her permission.

L'auteur a accordé une licence irrévocable et non exclusive permettant à la Bibliothèque nationale du Canada de reproduire, prêter, distribuer ou vendre des copies de sa thèse de quelque manière et sous quelque forme que ce soit pour mettre des exemplaires de cette thèse à la disposition des personnes intéressées.

L'auteur conserve la propriété du droit d'auteur qui protège sa thèse. Ni la thèse ni des extraits substantiels de celle-ci ne doivent être imprimés ou autrement reproduits sans son autorisation.

ISBN 0-315-73030-7

Canada

University of Alberta

Release form

Name of Author: Robert William Reed

Title of Thesis: **Imino-Functionalized Phosphines and Bisphosphines and their Metal Complexes.**

Degree: Doctor of Philosophy

Year this Degree Granted: 1992

Permission is hereby granted to the University of Alberta Library to reproduce single copies of this thesis and to lend or sell such copies for private, scholarly or scientific research purposes only.

The author reserves other publication rights, and neither the thesis nor extensive extracts from it may be printed or otherwise reproduced without the author's written permission.

(Signed) Rob W Reed

Robert W. Reed

Permanent Address:
132 Mary Street
Guelph, Ontario N1G 2B3

Date: November 25, 1991

" Just say what you have to say and then stop."

David Eddings

University of Alberta

Faculty of Graduate Studies and Research

The undersigned certify that they have read, and recommend to the Faculty of Graduate Studies and Research for acceptance, a thesis entitled **Imino-Functionalized Phosphines and Bisphosphines and their Metal Complexes** submitted by Robert W. Reed in partial fulfilment of the requirements for the degree of Doctor of Philosophy.

(Supervisor) Dr. R. G. Cavell

Dr. A. Hunter

Dr. H. J. Liu

Peter Sporns.

Dr. P. Sporns

Dr. J. Takats

(External Examiner) Dr. A. Norman
University of Colorado

Date: November 22, 1991

For my family

John Harold Reed DVM, Ph.D.

Shirley Elizabeth Reed R.N.

Susan Elizabeth Reed Tanaka P. Arch., OAA

John Kenneth Reed MD, FRCS(C)

Bruce Hunter Reed Ph.D.

Abstract

The imino-functionalized phosphines, Ph-CH=N-PPh_2 and Ph-C(N($SiMe_3$)$_2$)=N-PPh_2 have been synthesized by reaction of the corresponding trimethylsilyl derivatives with chlorodiphenylphosphine *via* elimination of trimethylsilyl chloride. Both phosphines form complexes with $PdCl_2(PhCN)_2$, $[Rh(CO)_2Cl]_2$ and $[Rh(COD)Cl]_2$. For the former phosphine, analysis of the second order multiplet for the imine proton in the ^1H NMR spectra demonstrated that the phosphines were *trans* in the complex $L_2Rh(CO)Cl$ (L = Ph-CH=N-PPh_2) with a very large $^2J_{PP}$ (= approx. 400 Hz) and *cis* in the complex $PdCl_2L_2$ (L = Ph-CH=N-PPh_2) with a very small $^2J_{PP}$ (= approx. 7 Hz). The complex LRh(COD)Cl (L = Ph-CH=N-PPh_2) was prepared. Through NMR spectroscopy it was demonstrated that the imine-proton-rhodium coupling was too small to resolve and was not a significant factor in the appearance of the second order multiplets observed for the previous two complexes. For the latter phosphine, (Ph-C(N($SiMe_3$)$_2$)=N-PPh_2) initial complexation was followed by trimethylsilylchloride elimination to produce five membered ring P,N metallacycles, PdL_2 and Rh(COD)L (L = Ph-C(N-$SiMe_3$)=N-PPh_2).

The reaction of bisphosphines with azides yields, when only one phosphine is oxidized, the heterodifunctional P,N-ligands (Ph_2P-E-P(Ph_2)=N-R). The utilization of a variety of azides has given access to a range of substituents on nitrogen (R=Me_3Si-, $(PhO)_2P(=O)$-, C_6H_5-CH_2-, or NC-C_6F_4-). A variety of bisphosphines have also been explored (E=CH_2, $CHCH_3$, C_6H_4, CH_2CH_2, CH=CH). For the derivatives Ph_2P-E-P(Ph_2)=N-R, where E=CH_2 or $CHCH_3$, the bridging carbon protons readily undergo deuterium exchange with deuterochloroform when R=Me_3Si and $CH_2C_6H_5$. For the derivatives Ph_2P-E-PPh_2 where E is a rigid linkage (C_6H_4 or *cis* CH=CH) the reaction with azides proceeds efficiently to yield the mono-oxidized bisphosphine Ph_2P-E-P(Ph_2)=N-R. When E=CH_2 or $CHCH_3$, the reaction with azides is less efficient

producing mixtures of compounds (Ph_2P-E-PPh_2, Ph_2P-E-P(Ph_2)=N-R and R-N=(Ph_2)P-E-P(Ph_2)=N-R), but the major product is the desired compound Ph_2P-E-P(Ph_2)=N-R. When E=CH_2CH_2 or *trans* CH=CH, the reaction with azides displays little selectivity for the formation of the mono-oxidized product (Ph_2P-E-P(Ph_2)=N-R) versus the doubly oxidized product (R-N=(Ph_2)P-E-P(Ph_2)=N-R).

The heterodifunctional ligands, Ph_2P-E-P(Ph_2)=N-R, readily form metal complexes upon reaction with $[Rh(CO)_2Cl]_2$. In all cases the complexes are square-planar about rhodium with the carbonyl ligand *cis* to the P(III) centre of the ligand as determined by spectroscopic means and, for one example, a single crystal X-ray structure determination.

Acknowledgements

I wish to thank Dr. Ronald G. Cavell for supervising this work and giving me all of the rope I could handle. I don't think I got tangled too badly. Thank you Ron.

To Dr. Pat Cavell I wish to point out that hockey season is a good time to have a thesis defence and thanks are due to Mrs. Powers who introduced me to Edmonton and supplied the tea.

Thank you to Dr. Bernie Santarsiero for the X-ray structure determinations and the opportunity to practice my home renovation skills.

For the friendship and assistance of group members past and present : Dr. Ian Phillips, Dr. Kattesh V. Katti, Dr. Dietmar Kennepohl (I havn't broken your vacuum line......yet!), Dr. Janos Takacs, Dr. Kal Mahadev, Dr. David Law, Dr. Ingrid Bartz, Dr. M. S. Balakrishna, Vivian Mozol, Rodney Gagne and Mike Mikoluk, I thank you all!

A special thank you to Paul Collins for his dedication and determination....for golf, but especially for his able assistance.

Honourable mention for certain events is rewarded to the following: Dr. Jim Jenkins for stopping on the ski run to watch me ski over that drop-off into the mogul field and then picking up the pieces (Thank you for reading my thesis too!). We must have that two-stepping snow-ball contest some day. Jeannette Loiselle for being brave and quick footed during all those dance lessons. Dr. Bahb McDonald for always making sure that hockey maintains its proper priority. Dietmar, Dr. Margaret Sisley, Lauren Warrack and Dr. Jim Hoyano for all those 10:30 coffee breaks. Thank you Jackie Jorgensen for letting me print those pages and smiling when you look up even if to make me sing a different tune (literally). Bill Henry (Genetics) for breaking my thumb in the first period of that hockey game and Nachum the beggar.

For the brave men and women of the spectral services: Glen Bigham, Tom Brisbane, Tom Nakashima, Gerdy Aarts, Lai (NMR), Andrew Jodhan (throw my golf club further into the briar patch this time!) (M.S.), Andrea Dunn, Darlene Mahow (Microanalysis), Diane Formanski and Jim Hoyle (FTIR), a sincere thank you.

Thank you Cor for letting me use your glass blowing lathe.

My sanity has been maintained since 1987 by Dr. Leonard Ratzlaff and the University of Alberta Chamber Choir (The Madrigal Singers) (That's why I have the tuxedo).

If I have not listed your name, I'll try to remember to send you a post card from France.

Thank you Mom and Dad, once again, for your patience and love.

Table of Contents

Chapter One

1 Introduction: Recent Developements 2

1.1 Synthesis 2

1.2 Structure and Bonding 3

1.3 Transition Metal Chemistry 6

1.4 Coordination Chemistry 7

1.5 Metal-Nitrogen Bonded Compounds 10

1.6 Coordination and Metal-Nitrogen Bond Chemistry 11

1.7 References 17

Chapter Two Imino-functionalized Phosphines 18

2.1 Introduction 19

Imines 20

Amidines 24

2.2 Results and Discussion 29

2.3 Summary 46

2.4 Experimental 47

2.5 References 57

Chapter Three Deuterium Exchange in Bis(diphenylphosphino)methane Derivatives 59
3.1 Introduction 60
3.2 Results and Discussion 62
3.3 Summary 70
3.4 Experimental 70
3.5 References 71

Chapter Four Oxidation of *ortho*-Bis(diphenylphosphino)benzene with Azides 73
4.1 Introduction 74
4.2 Results and Discussion 82
4.3 Summary 104
4.4 Experimental 105
4.5 References 112

Chapter Five The Selectivity of Oxidation of *cis* and *trans* Bis(diphenylphosphino)ethylene with *p*-Cyanotetrafluorophenyl Azide 115
5.1 Introduction 116
5.2 Results and Discussion 118
5.3 Summary 122
5.4 Experimental 122
5.5 References 124

Chapter Six When Phosphorus Spins Collide: The Unusual Temperature Dependence of Coupling in an ABMX Spin System. 125

6.1 Introduction 126

6.2 Results and Discussion 128

6.3 Summary 142

6.4 Experimental 143

6.5 References 145

Chapter Seven The Control of Oxidation: A Discussion 146

References 155

Chapter Eight Conclusions 156

References 160

Appendix 161

List of Tables.

Table 1.1	Structural features.	4
Table 2.1	Summary of spectroscopic data.	32
Table 3.1	Summary of compounds tested for deuterium exchange.	69
Table 4.1	^{31}P NMR spectroscopy data for the ligands.	89
Table 4.2	Selected ^{31}P NMR and I.R. data for the rhodium complexes.	98
Table 4.3	Structural data for rhodium complexes.	102
Table 6.1	Multinuclear NMR data for **1** at +55°C (CD_2Cl_2/CD_3CN).	129
Table 6.2	Matrix of the significant coupling constants for **1**.	130
Table 7.1	^{31}P NMR chemical shifts and coupling constants.	154
Table 8.1	The carbonyl carbon ^{13}C NMR data for the rhodium complexes possessing *cis* carbonyl and phosphine ligands.	159

Table A.1 Solvents and drying agents. 162

Table A.2 Instrumentation. 163

Table A.3 Crystallographic experimental details: $C_{33}H_{33}NP_2Si$. 164

Table A.4 Table of atomic coordinates (x 10^{-4}) and equivalent isotropic Gaussian parameters (Å, x 10^{-3}). 165

Table A.5 Table of selected interatomic bond lengths (in Å). 167

Table A.6 Table of selected interatomic angles (in degrees). 168

Table A.7 Crystallographic experimental details: $C_{34}H_{33}ClNOP_2RhSi$. 170

Table A.8 Table of atomic coordinates (x 10^{-4}) and equivalent isotropic Gaussian parameters (x 10^{-3}). 171

Table A.9 Table of selected interatomic lengths (in Å). 173

Table A.10 Table of selected interatomic angles (in degrees). 175

List of Figures.

Figure 2.1 The ^{1}H NMR spectra of the imine protons for compounds **30** and **31** demonstrating the second order AA'XX' spectral features. 33

Figure 2.2 The simulated ^{1}H NMR spectrum for the imine protons of **31** as $^2J_{PP}$ increases demonstrating the effect of large $^2J_{PP}$ coupling upon the AA'XX' spectrum. 34

Figure 2.3 The simulated ^{1}H NMR spectrum for the imine protons of **30** demonstrating the effect of small $^2J_{PP}$ coupling upon the AA'XX' spectrum. 36

Figure 2.4 The variation of AA'XX' spectra with coupling constant values. 38

Figure 2.5 The observed and simulated mass spectrum signals for the parent ion of **38** (m/e=856). 46

Figure 3.1 The ^{31}P NMR spectra demonstrating the evolution of the signals with time as the methylene protons are exchanged for deuterium. 66

Figure 3.2 The ^{1}H NMR spectra demonstrating the disappearing signals with time as the methylene protons are exchanged for deuterium. 67

Figure 3.3 The ^{31}P NMR spectra demonstrating the evolution of the P(III) signal with time as the methylene deuterons are exchange for protons. 68

Figure 4.1 The ORTEP representation of **11**. Structure courtesy of Dr. B. D. Santarsiero, Structure Determination Laboratory, University of Alberta. 92

Figure 4.2 The ^{31}P NMR spectrum of **19**. 97

Figure 4.3 The ORTEP representation of **19** (two views). Structure courtesy of Dr. B. D. Santarsiero, Structure Determination Laboratory, University of Alberta. 100

Figure 5.1 The ^{31}P NMR spectrum of the reaction solution of **3**. 119

Figure 5.2 The ^{31}P NMR spectrum of the reaction solution of **4**. 120

Figure 6.1 Variable temperature ^{31}P NMR spectra of **1.** 134

Figure 6.2 Simulation of the variable temperature ^{31}P NMR spectra demonstrating the effect of changing phosphorus chemical shifts on the ^{31}P NMR spectral features. 135

Figure 6.3 Variable temperature ^{13}C NMR spectra of **1**. 136

Figure 6.4 Simulation of the variable temperature ^{13}C NMR spectra demonstrating the effect of changing phosphorus chemical shifts on the ^{13}C NMR spectral features. 137

Figure 6.5 The ^{31}P and ^{13}C NMR spectra at the two temperatures at which the differences of the phosphorus chemical shifts is approximately one-half of the large phosphorus-rhodium coupling constant. 138

Figure 6.6 The equations describing the ^{13}C NMR spectral behavior. 141

Figure 7.1 A ^{31}P NMR spectrum of the reaction mixture of trimethylsilylazide with bis(diphenylphosphino)methane (dppm) demonstrating the three compounds; **A**=dppm, **B**=$Ph_2PCH_2P(Ph_2)$=N-$SiMe_3$, **C**=Me_3Si-N=$(Ph_2)PCH_2P(Ph_2)$=N-$SiMe_3$. 148

Figure 7.2 A ^{31}P NMR spectrum of the reaction mixture of trimethylsilylazide with bis(diphenylphosphino)ethane (diphos) demonstrating the three compounds; (Note the overlapping signals) **A**=diphos, **B**=$Ph_2PCH_2CH_2P(Ph_2)$=N-$SiMe_3$, **C**=Me_3Si-N=$(Ph_2)PCH_2CH_2P(Ph_2)$=N-$SiMe_3$.

List of Schemes.

Scheme 1.1	5
Scheme 1.2	12
Scheme 1.3	13
Scheme 2.1	32
Scheme 4.1	76
Scheme 4.2	78
Scheme 4.3	83
Scheme 7.1	151

Abbreviations

br	broad (IR and NMR)
C	Celsius
cm	centimetres
COD	1,5-cyclooctadiene
δ	chemical shift in NMR
dppbz	1,2-bis(diphenylphosphino)benzene
dppe	1,2-bis(diphenylphosphino)ethane
dppm	bis(diphenylphosphino)methane
Et_2O	diethyl ether
g	grams
Hz	hertz
IR	infrared
J	NMR coupling constant in hertz
M^+	parent ion in M.S.
M	molar
m	medium (IR), multiplet (NMR)
m/e	mass to charge ratio (M.S.)
Me	methyl, CH_3-
mg	milligrams
mL	millilitres
mmol	millimoles
mol	mole
M.S.	mass spectroscopy
NMR	nuclear magnetic resonance
Ph	phenyl, C_6H_5-

ppm	parts per million
s	strong (IR), singlet(NMR)
THF	tetrahydrofuran
TMS	tetramethylsilane
ν	frequency, cm^{-1} in IR
vs	very strong (IR)
w	weak (IR)

Chapter One

Introduction

1 Introduction: Recent Developments Concerning Phosphinimines.

1.1 Synthesis

The chemistry of phosphinimines, or formally, phosphine imides ($R_3P=N\text{-}R$), has received considerable interest recently. Their synthetic use ranges from reagents for Wittig-like reactions[1], through the formation of polymers[2], coordination compounds[3], to organometallic complexes[1]. The Staudinger reaction[4] (Equation 1.1) is still the favoured method of synthesis, but, this versatile unit can also be prepared by a variety of synthetic methods. The Kirsanov reaction (Equation 1.2) depends on the elimination of hydrogen chloride from a dichlorophosphorane and an amine[5]. A more recent synthesis utilizes diethyl azodicarboxylate to link a phosphine and an amine[6] (Equation 1.3) while a straight forward approach involves the deprotonation of an aminophosphonium salt[1] (Equation 1.4).

Equation 1.1

$$R_3P + RN_3 \longrightarrow R_3P=N\text{-}R + N_2$$

Equation 1.2

$$R_3PCl_2 + RNH_2 \longrightarrow R_3P=N\text{-}R + 2HCl$$

Equation 1.3

$$R_3P + RNH_2 \xrightarrow{\text{Et-O-CO-N}_2\text{-CO-O-Et}} R_3P=N\text{-}R$$

Equation 1.4

$$R_3P\text{-}NH_2^+X^- \quad + \quad 2RLi \longrightarrow R_3P{=}N\text{-}Li$$

$$R_3P{=}N\text{-}Li \quad + \quad RX \longrightarrow R_3P{=}N\text{-}R \quad + \quad LiX$$

1.2 Structure and Bonding

The structure of the phosphinimine unit appears to be straightforward. The phosphorus atom is approximately tetrahedral with five bonds and the nitrogen atom is two coordinate with three bonds and one pair of non-bonding electrons. Examination of the structures of compounds with *N*-carbon based phosphinimine units reveals bond lengths and angles of expected magnitudes (Table 1.1). There is, however, a striking difference in structural features when heavier elements are attached to the nitrogen atom of the phosphinimine unit. The P=N bond length shortens and the phosphorus-nitrogen-substituent angle increases. This effect reaches a maximum when a transition metal of high oxidation state (*i.e.* an atom with low lying, empty d-orditals) is attached to nitrogen. Furthermore, when the nitrogen centre (Lewis base) is coordinated to a Lewis acid, the P=N bond lengthens and the bonding angle decreases. The trend demonstrated by this data is that a short P=N bond is associated with a large P=N-R angle, and a long P=N bond is associated with a smaller P=N-R angle. The lone pair of electrons on nitrogen must therefore be actively involved in the bonding to stabilize the observed structural features. Similar structural features are observed in metal-imido linkages[7]. Such linear linkages are depicted with a metal-nitrogen triple bond and the same reasoning can be applied to a phosphinimine unit possessing a large P=N-R angle[8] (Scheme 1.1).

Table 1.1 Structural features.

	d(P=N)Å	d(N-R)Å	(P=N-R)°	Ref.
$Ph_2FP{=}N{-}Me$	1.641	1.469	119	9
$Ph_3P{=}N{-}C_6H_4Br$	1.567	1.417	124	10
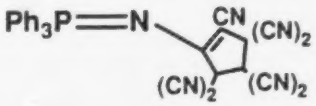	1.615	1.317	130	11
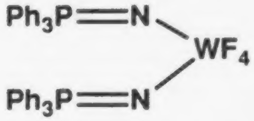	1.59	1.83	157	12
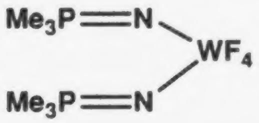	1.62	1.82	139	12
$Me_3P{=}N{-}SiMe_3$	1.542	1.705	145	13
$Ph_3P{=}N{-}MoCl_4Py$	1.65	1.72	177	12
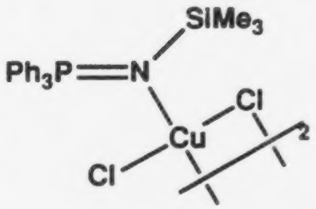	1.598	1.751	127	14
$Cl_3V{=}N{-}SiMe_3$	1.59	1.79	177	15

Scheme 1.1

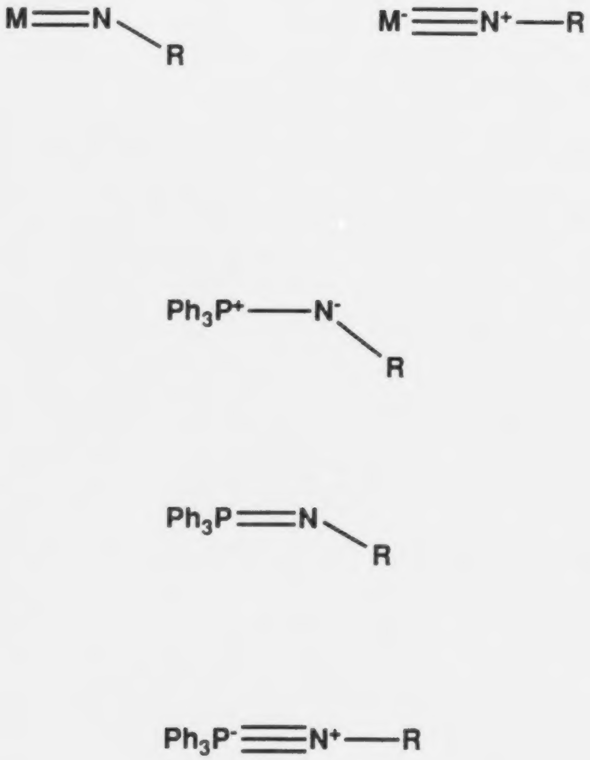
M=N–R
M⁻≡N⁺–R
Ph3P⁺–N⁻–R
Ph3P=N–R
Ph3P⁻≡N⁺–R

The above observations are further supported by theoretical examination[16]. Calculations[17] on the model compounds $H_3P{=}NH$, $H_3P{=}N\text{-}SiH_3$, and $[H_3P{=}N\text{-}PH_3]^+$ were carried out to examine the frontier molecular orbitals. The bond lengths and angles follow the expected trends from Table 1.1 and the charge distributions are reasonable. In particular, the highest occupied orbitals of $H_3P{=}NH$ are separated by 1.14eV. The photoelectron spectrum of $Me_3P{=}NH$ reveals that the two lowest ionization potentials are separated by 1eV[8]. For $H_3P{=}N\text{-}SiH_3$, the calculated energy difference between the highest occupied orbitals is 0.18eV but the ionization potentials cannot be resolved in the photoelectron spectrum of $Me_3P{=}N\text{-}SiMe_3$[8]. The comparison of the theoretical and experimental results indicate that inductive substituent effects are operative in this system. These effects are particularly pronounced when substituents with empty d-orbitals are involved. Therefore, modifying the nitrogen substituent of the phosphinimine unit in order to control the Lewis basicity of the nitrogen and hence the binding strength to transition metals is a reasonable proposition.

1.3 Transition Metal Chemistry

Linking two phosphinimine units together, through the phosphorus atoms, produces chelating ligands for transition metal coordination chemistry. If a reactive functional group at nitrogen is present, precursors to polymers or heterocyclic compounds are produced (See Chapter Two, Introduction). For example, the use of the Staudinger reaction between bis(diphenylphosphino)methane and azides has generated both chelating ligands and metallocyclic precursors. Appel and coworkers[18], from reactions of trimethylsilyl azide with phosphines prepared phosphinimine derivatives with a reactive trimethylsilyl group on nitrogen. These derivatives have been utilized by Roesky[19] to prepare cyclic species. In other work, Elsevier and coworkers[20] have examined the coordination chemistry of phosphinimine derivatives with aryl substituents on nitrogen.

1.4 Coordination Chemistry

The presence of aromatic rings on nitrogen blocks further substitution chemistry at nitrogen and allows the coordination chemistry of phosphinimines to be examined. Deprotonation of *N*-tolyl-diphenylmethylphosphinimine and reaction with $[ML_2Cl]_2$ (M=Rh, L_2=COD, L=CO; M=Ir, L_2=COD) produces stable complexes **1**[21] in which the ligand is bound to the metal *via* a sigma bond. In an analogous fashion, deprotonation of bis(*N*-tolyl-diphenylphosphinimine)methane and reaction with $[ML_2Cl]_2$ (M=Rh, L_2=COD, L=CO) produces similar complexes **2**[20].

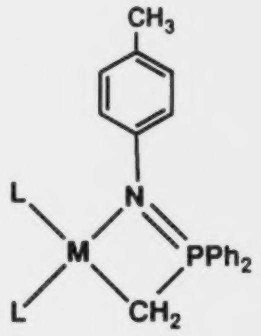

1

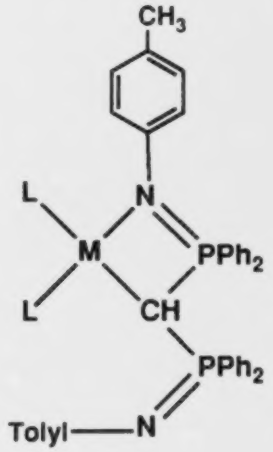

2

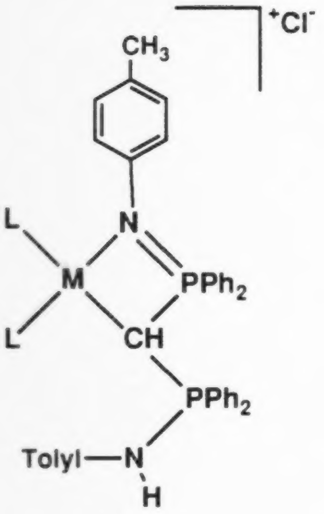

3

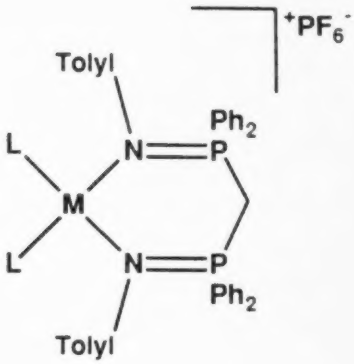

4

Reaction of bis(*N*-tolyl-diphenylphosphinimine)methane with $[ML_2Cl]_2$ (M=Rh, L_2=COD, L=CO) in the absence of a deprotonating agent also produces four membered ring complexes **3**, but, one of the methylene protons has migrated to the dangling phosphinimine nitrogen[20]. In addition, anion exchange of chloride for PF_6^- or BF_4^- reveals a new coordination mode **4** in which the labile proton has migrated back to the methylene carbon. The compounds **3** and **4** are simultaneously generated under the reaction conditions but the product distribution can be skewed by changing the metal, ligand, solvent, or anion[22]. When the aryl substituent on nitrogen is 4-methoxyphenyl the chemistry is identical to the tolyl derivative, however, the 4-nitrophenyl derivative (bis(*N*-4-nitrophenyl-diphenylphosphinimine)methane) does not form metal complexes under these conditions[22]. In addition, deprotonation of the nitro-ligand derivatives and reaction with $[ML_2Cl]_2$ (M=Rh, L_2=COD, L=CO) fails to produce complexes of the type **2** or **4**[21,22]. These results clearly indicate that the Lewis basicity and complexation ability of the phosphinimine nitrogen is, again, susceptible to inductive effects.

A curious feature illustrated by the complexes **3** and **4** is the reversible transfer of the methylene proton to the nitrogen atom. Both tautomeric forms of the ligand exist when bound to a metal centre (**3** and **4**), but in solution or the solid state, only the tautomer **5** of the free ligand can be detected[20]. But, since the methylene protons of **5** will readily exchange for deuterium with D_2O, CD_3OD, or $CDCl_3$, the other tautomer **6** must also be present in order to facilitate the exchange[23].

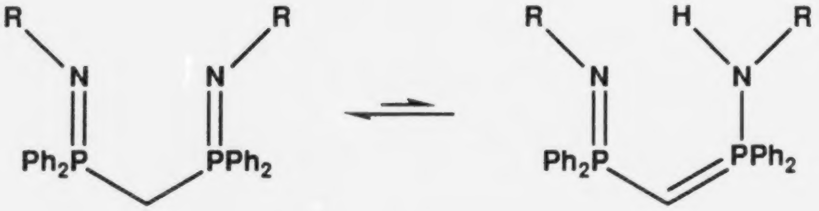

5 **6**

1.5 Metal - Nitrogen Bonded Compounds

The reaction of *N*-trimethylsilyl-triphenylphosphinimine with WF_6 produces the compound **7**[19] and reaction of bis(*N*-trimethylsilyl-diphenylphosphinimine)methane with metal halides produces metallocycles of the form **8**[24]. Reaction of either phosphinimine reagent with K_2ReO_7 replaces the trimethylsilyl group with ReO_3 functionalities through the elimination of hexamethyldisiloxane (**9** and **10**)[25].

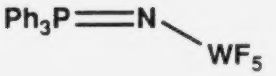

7

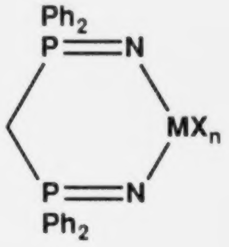

8

MX_n=WF_4, WCl_4, $SeCl_2$,$TeCl_2$.

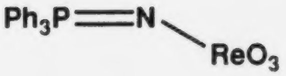

9

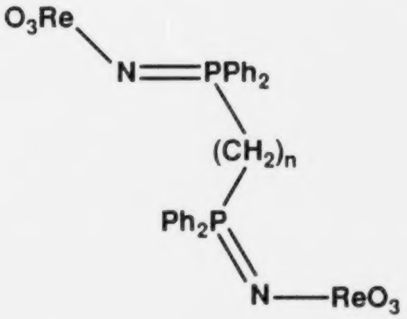

10 n = 1, 2.

1.6 Coordination and Metal - Nitrogen Bond Chemistry

In our research group, we have combined the features of both systems. We have discovered that bisphosphines, such as those listed in Scheme 1.2, react with azides under controlled conditions to produce a new class of heterodifunctional phosphorus-nitrogen chelating ligands[26]. This approach produces a versatile ligand system. The final size of the chelate can be modified simply by changing the linkage between the two phosphorus centres[27]. The substituent on nitrogen can be readily exchanged allowing the basicity of the nitrogen, and hence the binding strength, to be altered at will. The combination of a soft phosphine centre and a hard nitrogen centre confers on the ligand the ability to form complexes with a wide range of transition metals in a wide range of oxidation states[28]. Furthermore, a reactive functional group, trimethylsilyl, on nitrogen provides the potential to form metal-nitrogen sigma bonds through trimethylsilyl halide elimination[29]. Scheme 1.3 outlines these features and summarizes some of the chemistry previously done in our laboratory.

This thesis describes the exploration of a variety of these factors. Chapter two details the preparation of two imino-functionalized phosphines and representative metal complexes. One of these ligands is a monodentate phosphine while the other is a heterodifunctional phosphorus-nitrogen chelate with reactive trimethylsilyl groups for metal nitrogen bond formation. In chapter three the suprizingly facile deuterium exchange between deutero-chloroform and dppm derivatives is presented. In chapters four and five the effect of placing a rigid linkage between two phosphines is explored with respect to reaction with azides and metal complex formation. Chapter six documents a highly unusual NMR spectroscopic study in which all observed spectral transformations are due to second order NMR effects and not a dynamic molecular process. An overview of the reaction of an azide with a bisphosphine is provided in chapter seven; chapter eight concludes this thesis.

Scheme 1.2 The bisphosphines[26,27].

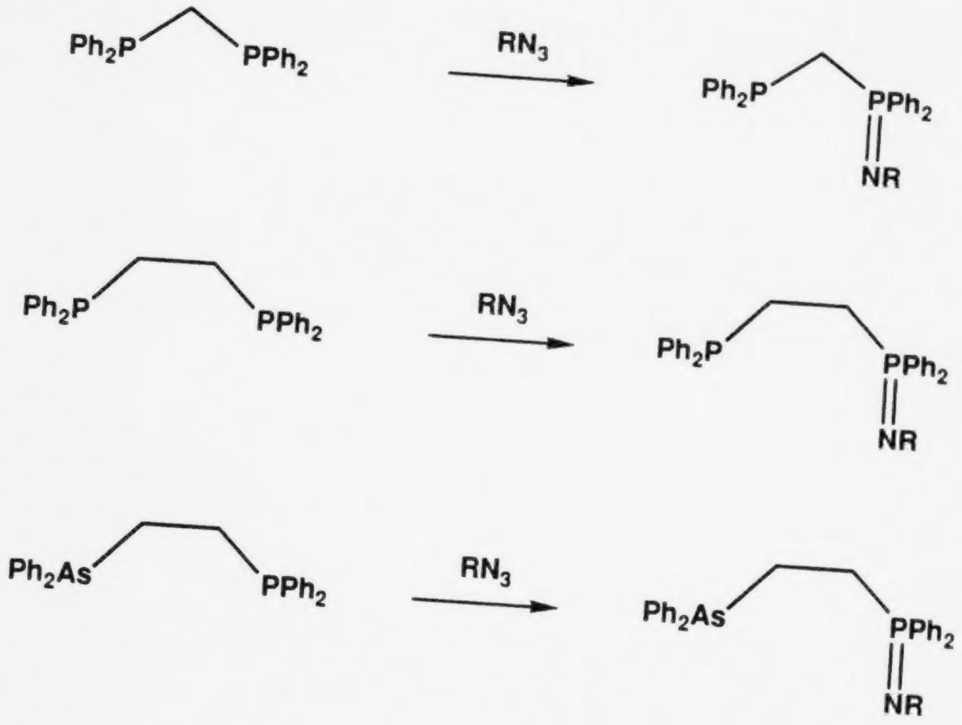
Ph2P
PPh2
RN3
NR
Ph2As

R = Me_3Si, Me_3Ge, C_6F_4CN, $C_6H_2F(NO_2)_2$

Scheme 1.3 Summary of the previously prepared complexes[26-29].

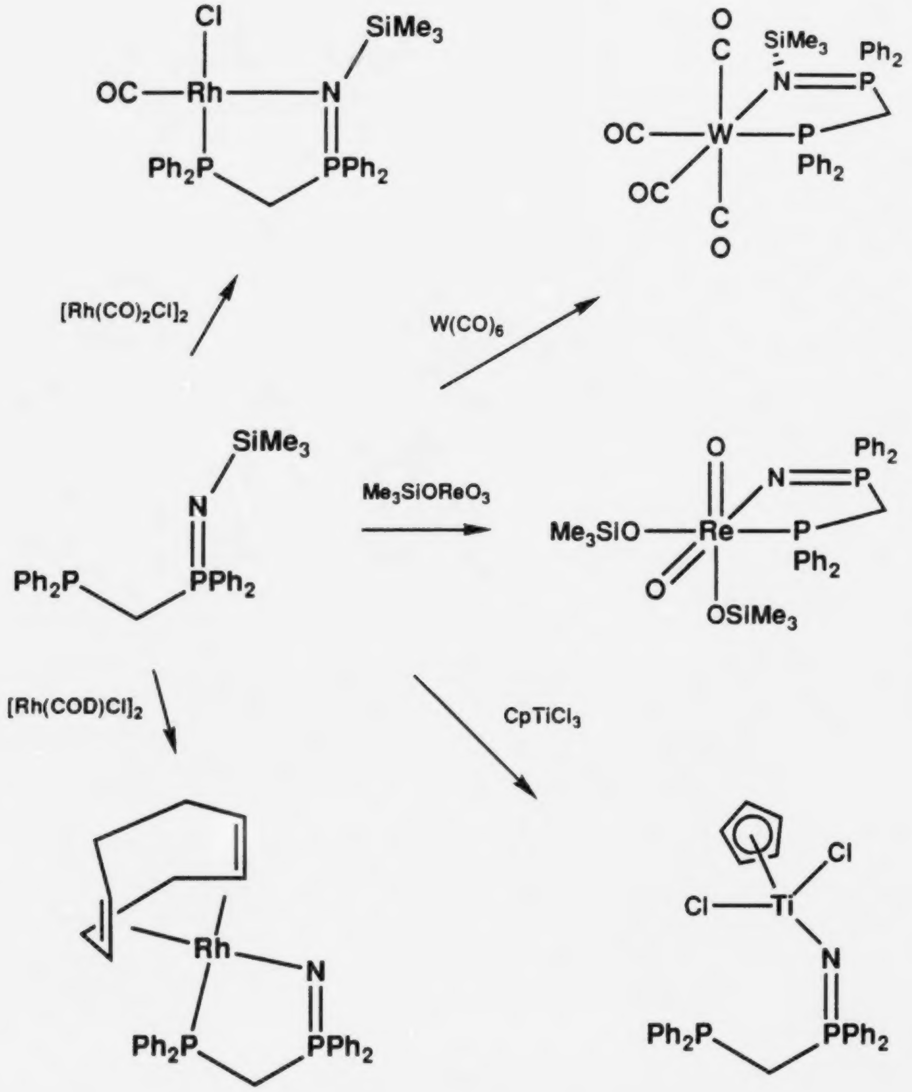
[Rh(CO)$_2$Cl]$_2$
W(CO)$_6$
Me$_3$SiOReO$_3$
[Rh(COD)Cl]$_2$
CpTiCl$_3$

The reaction of an azide with a phosphine produces a phosphinimine and dinitrogen (Staudinger reaction, Equation 1.1). The mechanism of this reaction is not fully understood. It is known that the alpha nitrogen of the azide is retained in the phosphinimine product and two possible mechanisms[1] are outlined by Scheme 1.4. Whether the reaction proceeds *via* the cyclic intermediate or not is debatable, but both intermediates require space. It can therefore be anticipated that steric crowding about the phosphine will inhibit the reaction. This is the focus of chapter seven, 'the control of oxidation, a discussion'.

Scheme 1.4

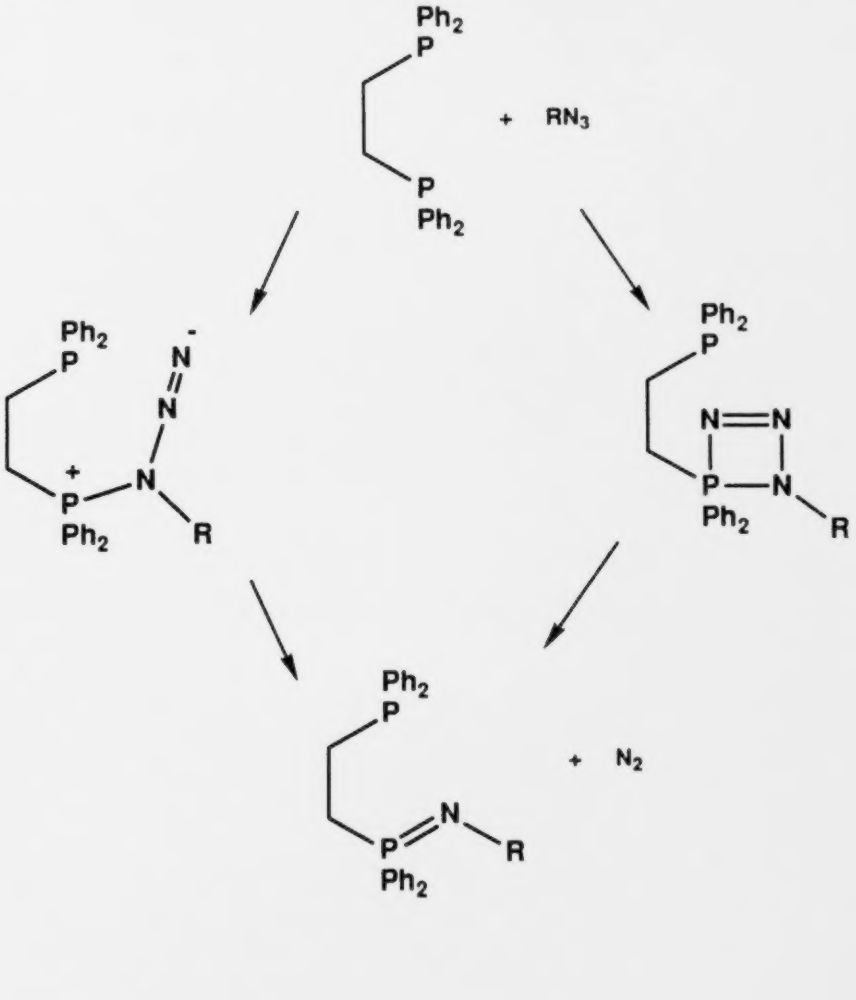

The chemistry of the Staudinger reaction[30] and phosphinimines[1] has been extensively reviewed.

Perhaps the most informative, but least investigated, aspect of complexation chemistry, with phosphorus containing ligands, is second-order NMR spectra. In many instances complex spectra are justifiably labelled as multiplets and forgotten. In this thesis the analysis of complex spectra has revealed valuable chemical information. Complete analysis of second-order NMR spectra is often realized by calculating an exact duplicate spectrum. In this work, exact simulation has often been impossible, instead simulation has been used to demonstrate the source of the observed second order spectra.

In chapter two, 'imino-functionalized phosphines', analysis of the X-portion of an AA'XX' spectra reveals the magnitude of $J_{AA'}$ which cannot be observed directly. The magnitude of the coupling constant then clearly indicated the arrangement of the ligands in the metal complexes. In chapter six, 'when phosphorus spins collide', analysis of a spin system containing an AB sub-spin system in which A and B have opposite chemical shift temperature dependence again provided substantial structural information. The complex spectra were not the result of a dynamic molecular process but simply the result of the phosphorus nuclei (A and B) 'exchanging' chemical shifts. The detailed descriptions of the equations describing these spin systems can be found in reference 31(a,b,c,d).

1.7 References

1. E. W. Abel and S. A. Mucklejohn. *Phosphorus and Sulphur*, **9**, 235 (1981).
2. R. H. Neilson and P. Wisian-Neilson. *Chem. Rev.*, **88**, 541 (1988).
3. K. Dehnicke and J. Strähle. *Polyhedron* , **8**, 707 (1989).
4. H. Staudinger and J. Meyer. *Helv. Chim. Acta.*, **2**, 635 (1919).
5. A. V. Kirsanov. *Izv. Akad. Nauk SSSR, Otd. Khim. Nauk*, 426 (1950).
6. S. Bittner, Y. Assaf, P. Krief, M. Pomerantz, B. T. Ziemnicka and C. G. Smith. *J. Org. Chem.*, **50**, 1712 (1985).
7. W. A. Nugent and B. L. Haymore. *Coordination Chemistry Reviews.*, **31**, 123 (1980).
8. K. A. O. Starzewski and H. T. Dieck. *Inorg. Chem.*, **18**, 3307 (1979).
9. G. W. Adamson and J. C. J. Bart. *Chemical Communications.*, 1036 (1969).
10. M. J. E. Hewlins. *J. Chem. Soc.B.*, 942 (1971).
11. P. J. Butterfield, J. C. Tebby and T. J. King. *J. C. S. Perkin I*, 1237 (1978).
12. K. Völp, F. Weller and K. Dehnicke. *Z. Naturforsch*, **42b**, 947 (1987).
13. E. E. Astrup, A. M. Bouzga and K. A. O. Starzweski. *J. Mol. Str.*, **51**, 51 (1987).
14. D. Fenske, E. Böhm, K. Dehnicke and J. Strähle. *Z. Naturforsch*, **43b**, 1 (1988)
15. E. Schweda, K. D. Scherfise and K. Dehnicke. *Z. anorg. allg. Chem.*, **528**, 117 (1985).
16. a) R. A. Wheeler, R. Hoffmann and J. Strähle. *J. Am. Chem. Soc.*, **108**, 5381 (1986). b) M. W. Schmidt and M. S. Gordon. *Inorg. Chem.*, **25**, 248 (1986). c) W. W. Schoeller, T. Busch and E. Niecke. *Chem. Ber.*, **123**, 1653 (1990).
17. Calculations were carried out using MONSTERGAUSS (closed shell, SCF, ab-initio calculations) The basis set was STO-3G* (d-orbitals for phosphorus) with full geometry optimization for non-hydrogen atoms.
18. R. Appel and I. Ruppert. *Z. anorg. allg. Chem.*, **406**, 131 (1979).

19. H. W. Roesky. *Chem. Soc. Rev.*, **15**, 309 (1986).

20. P. Imhoff and C. J. Elsevier. *J. Organomet. Chem.*, **361**, C61 (1989).

21. P. Imhoff, S. C. A. Nefkens, C. J. Elsevier, K. Goubitz and C. H. Stan. *Organometallics,* **10**, 1421 (1991).

22. P. Imhoff, R. Van Asselt, C. J. Elsevier, M. C. Zoutberg and C. H. Stan. *Inorganica Chimica Acta,* **184**, 73 (1991).

23. P. Imhoff, R. Van Asselt, C. J. Elsevier, K. Vrieze, K. Goubitz, K. F. Van Malssen and C. H. Stan. *Phosphorus, Sulphur and Silicon*, **47**, 401 (1990).

24. K. V. Katti, U. Seseke and H. W. Roesky. *Inorg. Chem.*, **26**, 814 (1987).

25. H. W. Roesky, D. Hesse, M. Rietzel and M. Noltemeyer. *Z. Naturforsch*, **45b**, 72 (1990).

26. a) K. V. Katti and R. G. Cavell. *Inorg. Chem.*, **28**, 413 (1989).

    b) K. V. Katti and R. G. Cavell, *Comments Inorg. Chem.*, **10**, 55 (1990).

27. K. V. Katti, R. J. Batchelor, F. W. B. Einstein and R. G. Cavell. *Inorg. Chem.*, **29**, 808 (1990).

28. a) K. V. Katti and R. G. Cavell. *Organometallics*, **8**, 2147 (1989).

    b) K. V. Katti and R. G. Cavell. *Inorg. Chem.*, **28**, 3033 (1989).

29. K. V. Katti and R. G. Cavell. *Organometallics*, **7**, 2236 (1988).

30. Yu. G. Gololobov, I. N. Zhmurova and L. F. Kasukhin. *Tetrahedron*, **37**, 437 (1981).

31. a) E. D. Becker. "High Resolution NMR Theory and Chemical Applications", Academic Press, (1980).

    b) J. A. Pople and T. Schaefer. *Mol. Phys.*, **3**, 547 (1960).

    c) R. J. Abraham and H. J. Bernstein. *Can. J. Chem.*, **39**, 216 (1961).

    d) T. Schaefer. *Can. J. Chem.*, **40**, 1678 (1962).

Chapter Two

Imino-functionalized Phosphines.

2.1 Introduction.

The recent publication of the efficient synthesis of *N*-trimethylsilyl-benzalimine[1] and *N*-persilylated benzamidine[2] prompted our utilization of these compounds as reagents for the preparation of imino-functionalized phosphines, **1** and **2**.

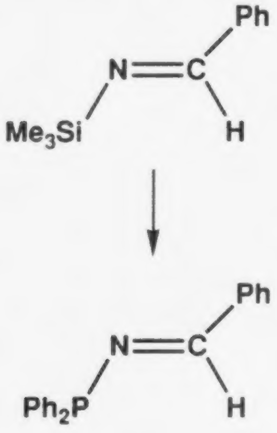

1

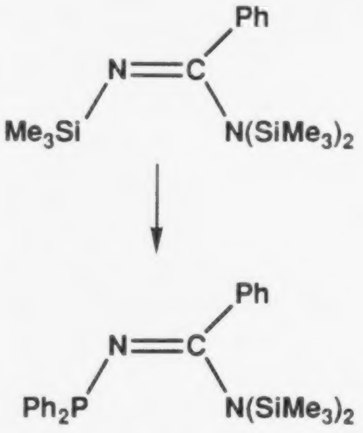

2

This chapter describes the synthesis, characterization and reaction chemistry of these compounds. The following section describes the literature related to the chemistry of imines, R-CH=N-R', and amidines, R-C(=NR)-NR$_2$, as well as representative examples of their transition metal chemistry.

Imines.

The traditional method for the preparation of imine derivatives involves the condensation reaction of an aldehyde with a primary amine and elimination of a water molecule to produce a Schiff base[3]. The subsequent chemistry of these imine derivatives is often limited due to the presence of an alkyl or aryl group on nitrogen. Hart *et al.* [1] prepared imine derivatives by the condensation of aldehydes with lithium hexamethyldisilazane producing *N*-trimethylsilyl imine derivatives *via* elimination of lithium trimethylsiloxide (Equation 2.1). This reaction is applicable to all aldehydes that do not possess an alpha hydrogen. The presence of alpha hydrogens allows keto-enol tautomerism to occur and under these conditions the reaction proceeds to form the lithium salt of the aldehyde and hexamethyldisilazane[4].

Equation 2.1

$$\text{R-CH=O} \quad + \quad \text{LiN(SiMe}_3)_2 \longrightarrow \text{R-CH=N-SiMe}_3 \quad + \quad \text{LiOSiMe}_3$$

The advantage of this synthesis arises from the presence of a trimethylsilyl group on nitrogen which allows further chemistry to be performed on these derivatives through the elimination of trimethylsilyl halide from a variety of metal or main group halides.

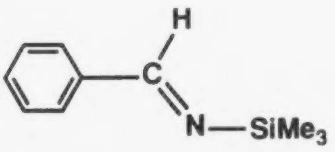

3

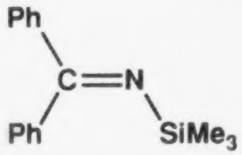

4

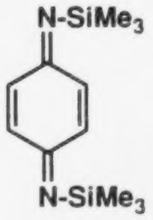

5

For example, Krüger *et al.* [4] utilized the sodium salt of hexamethyldisilazane to convert benzaldehyde, benzophenone and *p*-quinone to the corresponding *N*-trimethylsilyl imine derivatives (**3-5**).

Although, the utilization of *N*-trimethylsilyl imine derivatives in transition metal chemistry has not been extensively explored, other imine derivatives prepared *via* the elimination of water from an aldehyde and a primary amine have been complexed to a variety of transition metals (*vide infra*). For example, Drolet *et al.*[5] prepared pyridine-2-carboxaldehyde imine derivatives and employed these compounds in the study of the reaction kinetics of the photolysis of $W(CO)_6$ (Equation 2.2).

Equation 2.2

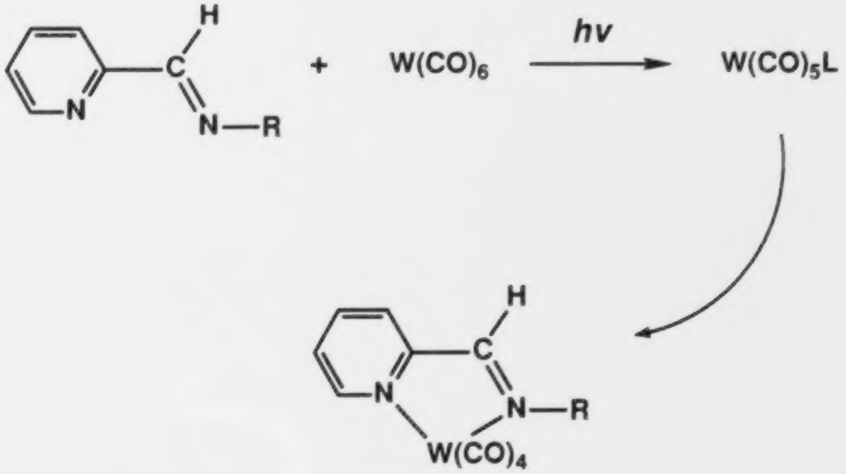

Cullen *et al.* [6] utilized a chiral amine to prepare the imine derivative **6** for use with [Rh(COD)Cl]$_2$ in an asymmetric hydrosilylation catalyst system. The addition of diphenylsilane to acetophenone proceeded in high yield, but, subsequent hydrolysis produced a racemic mixture of the alcohol product. Brunner *et al.* [7] found the imine derivative **7** to be an excellent ligand for the hydrosilylation of ketones (87% conversion, optical yield = 51% e.e.). Hussein *et al.* [8] found that the reaction of arylamidoximes with Li$_2$[PdCl$_4$] yielded orthometalated compounds **8** and Blake *et al.*[9] found that the bis-imine **9** is an excellent ligand for stabilizing nickel in oxidation states I to III.

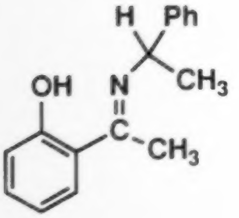

6

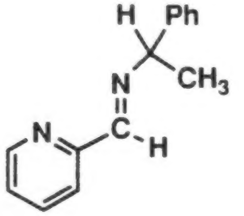

7

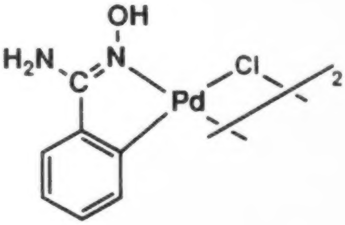

8

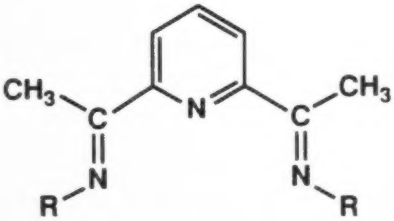

9

As a final example, Anderson *et al.*[10] prepared the imine **10** which when complexed with $[PtMe_2(\mu\text{-}SMe_2)]_2$ produced **11**. The compound **11** can then react further in two different ways. When the ortho substituent **X** on the phenyl group was hydrogen or fluorine orthometallation was observed with the elimination of methane (**12**) (the carbon-fluorine bond is not activated), but, for the chlorine and bromine derivatives (X=Cl, Br), oxidative addition of the carbon-halogen bond to platinum resulted to produce the derivatives **13**.

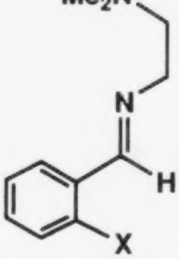

10

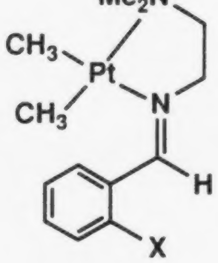

11

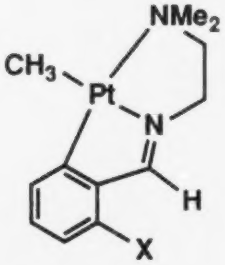

12

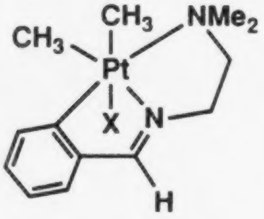

13

The versatility of compounds containing an imine unit, R-CH=N-R', is clearly demonstrated by the above examples and their subsequent organometallic chemistry. These results suggested that the incorporation of a phosphine unit utilizing the *N*-trimethylsilyl derivatives and chlorodiphenylphosphine would lead to a rich area of relatively unexplored chemistry. To date there are few examples of N-phosphine-imine derivatives (*cf* **14**[11]) and no examples of the application of these compounds in transition metal chemistry have been found in the literature.

$(R_2C{=}N\text{-})_n\text{-}PX_{3-n}$

14 **R= Ph, ^{t}Bu, tolyl, CF_3.**

X= Ph, Cl, Me, OMe, OEt.

Amidines.

The first report of a persilylated benzamidine was by Sanger in 1973[12]. A later paper by Boeré *et al.* [2] described the preparation of a series of persilylated amidines and the acid hydrolysis of these compounds to the corresponding amidine hydrochloride salts. Since that time (1987), persilylated benzamidines, prepared as outlined by Equation 2.3, have been reacted with a wide range of halogen containing compounds (*vide infra*).

Equation 2.3

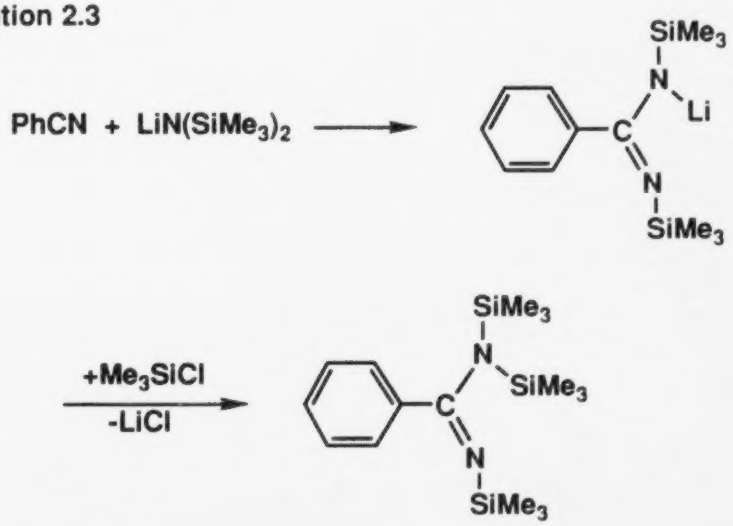

The reactions of compounds containing metal halogen bonds with persilylated benzamidine are summarized by the following representative examples. Roesky *et al.*[13] reacted lithium *N,N'*-bis(trimethylsilyl)-benzamidate with $SiCl_4$, $SnCl_4$, Me_2SnCl_2, Ph_2SnCl_2, $TiCl_4$, $ZrCl_4$, MoO_2Cl_2, and WO_2Cl_2. The elimination of lithium chloride in one to one reaction with $SiCl_4$ produced compound **15**. Two to one reactions with $SnCl_4$, $TiCl_4$, and $ZrCl_4$ produced compounds of the type **16** and reaction with MoO_2Cl_2 and WO_2Cl_2 produced compounds **17**.

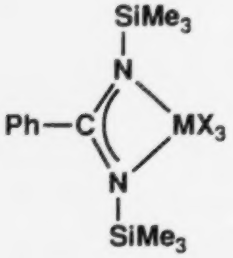

15

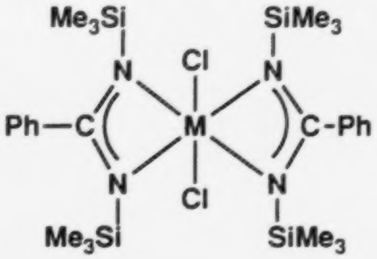

16

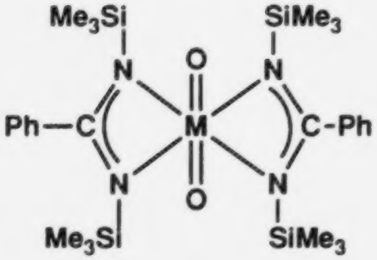

17

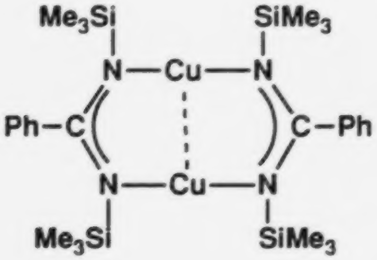

18

Dehnicke and coworkers[14] have paralleled these results by synthesizing the corresponding one to one amidinato complexes corresponding to **15** from the trichlorides of aluminum, gallium, and indium, from boron tribromide and from the tetrachlorides of tin, titanium and zirconium[15]. The reaction with anhydrous copper(I) chloride produced the bridging compound **18**[16].

The main group chemistry of phosphorus and sulphur is less extensive, however, a few representative examples are listed below. The reaction of persilylated benzamidine with dichlorophenylphosphine produces **19**[17] and reaction with sulphur dichloride produces **20** or **21** depending upon the reaction conditions[18].

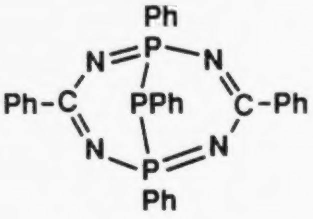

19

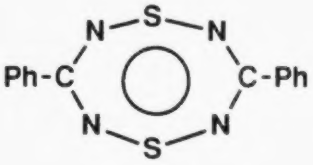

20

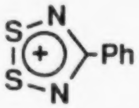

21

As part of this thesis, persilylated benzamidine was reacted with $CpTiCl_3$ producing the compound **22**[19]. Additionally, the reaction of persilylated benzamidine with chlorodiphenylphosphine produced *N*-diphenylphosphino-*N′*,*N′*-bis(trimethylsilyl)-benzamidine **2**.

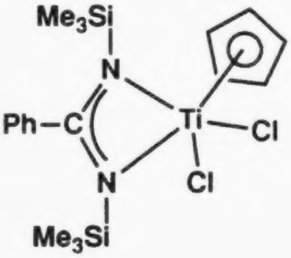

22

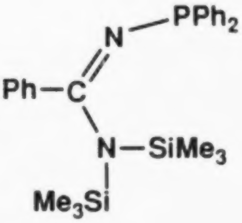

2

There have now been several reports in the literature of the existence of *N*-diphenyl-phosphino-*N′*,*N′*-bis(trimethylsilyl)benzamidine **2**. In one of the first reports[20], this compound was an unisolated intermediate in a reaction sequence for the preparation of the 'phosphinimine-amidine' (Equation 2.4) **23**.

Equation 2.4

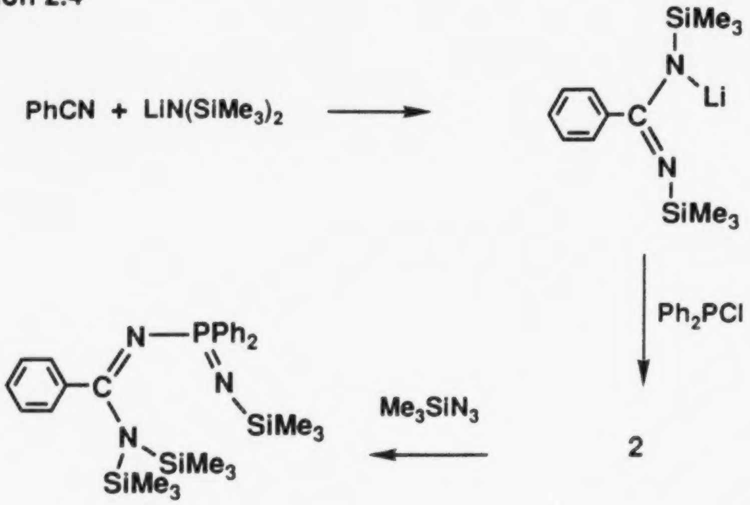
PhCN + LiN(SiMe3)2
SiMe3
N
Li
C
N
SiMe3
Ph2PCl
2
Me3SiN3
N—PPh2
C
N
SiMe3
N
SiMe3
SiMe3

23

The reaction of **23** with $MoOCl_4$ produced the unusual metallacycle **24**[21], while reactions with sulphur or selenium chlorides produced the six membered ring compounds **25**[22].

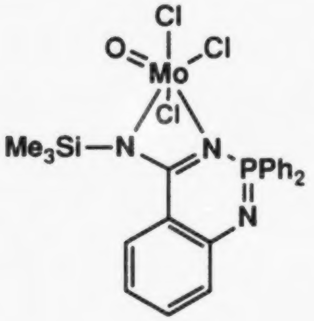
Cl
O
Cl
Mo
Cl
Me3Si—N
N
PPh2
N

24

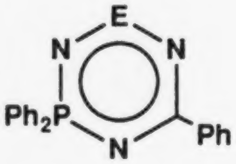
E
N
N
Ph2P
N
Ph

25

Sanchez and coworkers[23] claimed the preparation of **2** as an unpublished result on the basis of a ^{31}P NMR chemical shift. The subsequent reaction with a chlorophosphinium salt produced **26**.

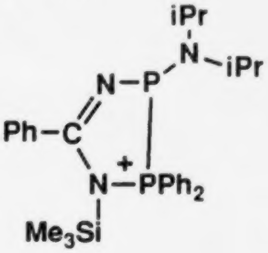

26

Based upon the reactivity of persilylated benzamidine with metal and main group halides it was believed by our research group that **2** would be a good chelating ligand with the additional potential to form metal nitrogen bonds *via* trimethylsilyl chloride elimination. Furthermore the phosphine centre and the trimethylsilyl functional groups would aid in the characterization of such complexes *via* multinuclear NMR spectroscopy.

2.2 Results and Discussion

N-Diphenylphosphinobenzalimine, 1.

The synthesis of *N*-diphenylphosphinobenzalimine **1** is achieved by the reaction of *N*-trimethylsilylbenzalimine with chlorodiphenylphosphine *via* the elimination of chlorotrimethylsilane. This compound and its derivatives have three structural features that facilitate characterization. Proton NMR spectroscopy detects the 'imine' proton (for **1**, 8.28 ppm, $^3J_{HP}$ = 22 Hz) which is very sensitive to the environment of the phosphorus centre. Large chemical shift changes in the ^{31}P NMR spectra from that of **1** (49.38 ppm) are diagnostic of oxidation or complexation of the phosphorus centre and infrared spectroscopy allows the strong 'imine' (-CH=N-) double bond absorption (for **1** ν(C=N) = 1610 cm^{-1}) to be monitored. Scheme 2.1 summarizes the reaction chemistry of *N*-diphenylphosphino-benzalimine **1**.

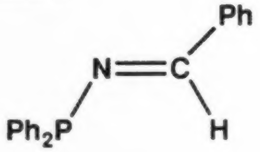

1

Oxidation of the phosphine centre of **1** with *p*-cyanotetrafluorophenyl azide or sulphur proceeds cleanly in good yield and the products are highly crystalline materials (**27** and **28**). The reaction with trimethylsilyl azide also proceeds cleanly as monitored by ^{1}H and ^{31}P NMR spectroscopy to yield compound **29**, however, the crude product was an oil and crystals obtained from an acetonitrile solution proved to be the cyclic phosphazene $(Ph_2P{=}N)_3$. Subsequent attempts to isolate **29** as a crystalline solid through slow crystallization met with equal failure as **29** readily rearranges to $(Ph_2P{=}N)_3$.

Complexation of two equivalents of *N*-diphenylphosphino-benzalimine per metal centre with $PdCl_2(PhCN)_2$ and $1/2[Rh(CO)_2Cl]_2$ afforded the corresponding complexes **30** and **31**, while the one to one reaction with $1/2[Rh(COD)Cl]_2$ produced **32**.

Scheme 2.1

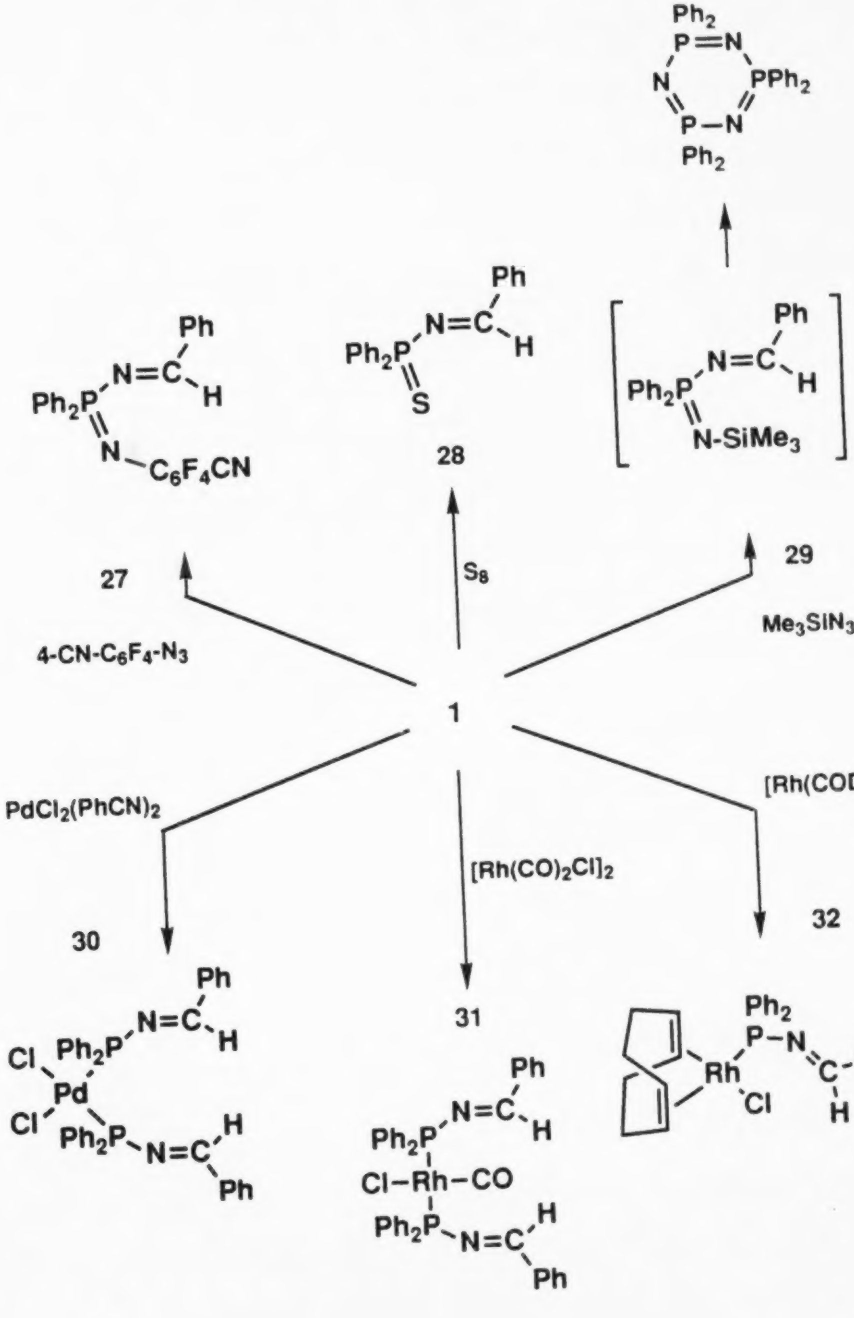
27
28
29
1
4-CN-C6F4-N3
S8
Me3SiN3
PdCl2(PhCN)2
[Rh(CO)2Cl]2
[Rh(COD)Cl]2
30
31
32

The three structural features of the compounds in Scheme 2.1: the imine proton (^{1}H NMR), the phosphorus centre (^{31}P NMR), and the imine double bond (infrared spectroscopy), are listed in Table 2.1. In the ^{1}H NMR spectra, oxidation of **1** with azides or sulphur deshields the imine proton chemical shift by approximately one ppm from 8.28 ppm to 9.13-9.43 ppm and the $^3J_{HP}$ coupling constants increase from 22 Hz to 34-40 Hz. For the metal complexes the effect of complexation of the phosphine on the imine proton chemical shift (8.28 ppm to 8.38-8.82 ppm) and on the $^3J_{HP}$ coupling constant (22 Hz to 28-32.5 Hz) is less dramatic. For **30** and **31** the presence of two phosphines on one metal centre produces a more complicated ^{1}H NMR spectrum (a doublet with 'satellites' for **30** and a pseudo-triplet for **31**) (Figure 2.1). The AA'XX' spin systems (A=H, X=P) for these two complexes arises from the unobserved $^2J_{PP}$ coupling constant. In addition, the "triplet" observed for the imine proton in complex **31** is *not* the result of rhodium coupling since phosphorus decoupling the ^{1}H NMR spectrum was found to produce a singlet for both complexes **31** and **32.**

Simulation of the multiplets observed for the imine proton in **30** and **31** allows the estimation of the unobserved $^2J_{PP}$ coupling constant. A series of simulations is shown in Figure 2.2 demonstrating that the $^2J_{PP}$ coupling for **31** is very large (300-500 Hz). For square planar complexes trans coupling across the metal centre is much larger than cis coupling and comparable trans-$^2J_{PP}$ coupling constants of 400 and 435 Hz are observed for the complexes **33** and **34**[25].

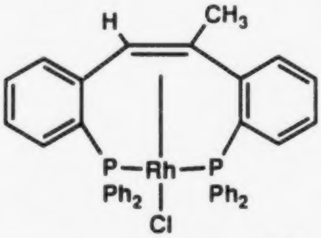

33

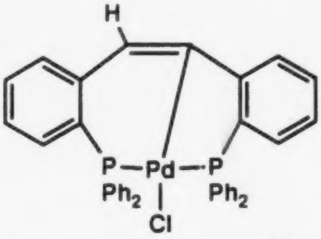

34

Table 2.1 Summary of spectroscopic data.

Compound	**NMR Data**				**Infrared Data**
	^{31}**P** (ppm)	^{1}**JPRh** (Hz)	^{1}**H** (ppm)	^{3}**JHP** (Hz)	ν(C=N) cm^{-1}
1	49.38		8.28 d	22	1610
27	15.41		9.13 d	34	1615
28	61.14		9.43 d	40	1615
29[a]	6.66		9.37 d	36	
30	72.73		8.38 m[b]	32.5	1624
31	70.72	130	8.82 m[b]	30	1625
32	73.00	161	8.42 d	28	1624

a =compound not isolated. *b* = $^{3}J_{HP} + ^{5}J_{HP'}$. d= doublet. m= multiplet.

Figure 2.1 The ^{1}H NMR spectra of the imine protons for compounds **30** and **31** demonstrating the second order AA'XX' spectrum.

30

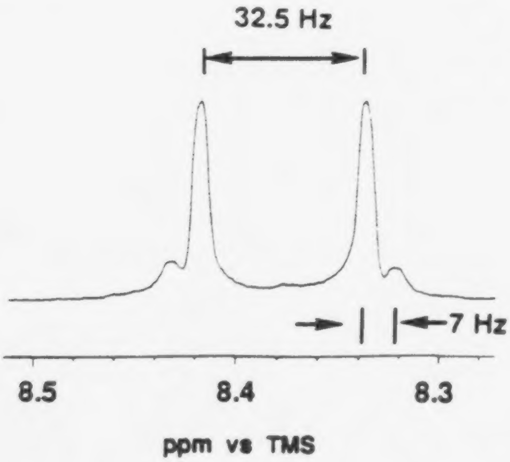

31

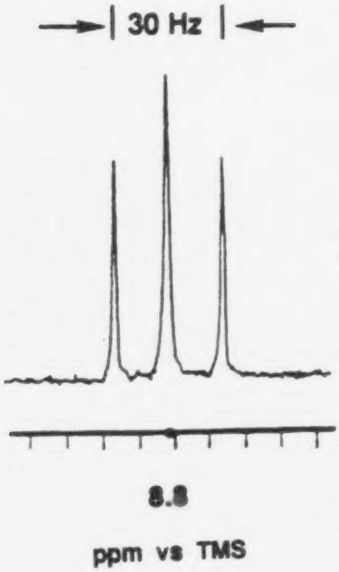

Figure 2.2 The simulated ^{1}H NMR spectra for the imine protons of **31** as $^{2}J_{PP}$ increases demonstrating the effect of large $^{2}J_{PP}$ coupling upon the AA'XX' spectrum. J_{HP} = 30 Hz, $J_{HP'}$ = 0 Hz, $J_{HH'}$ = 0 Hz, J_{PRh} = 130 Hz

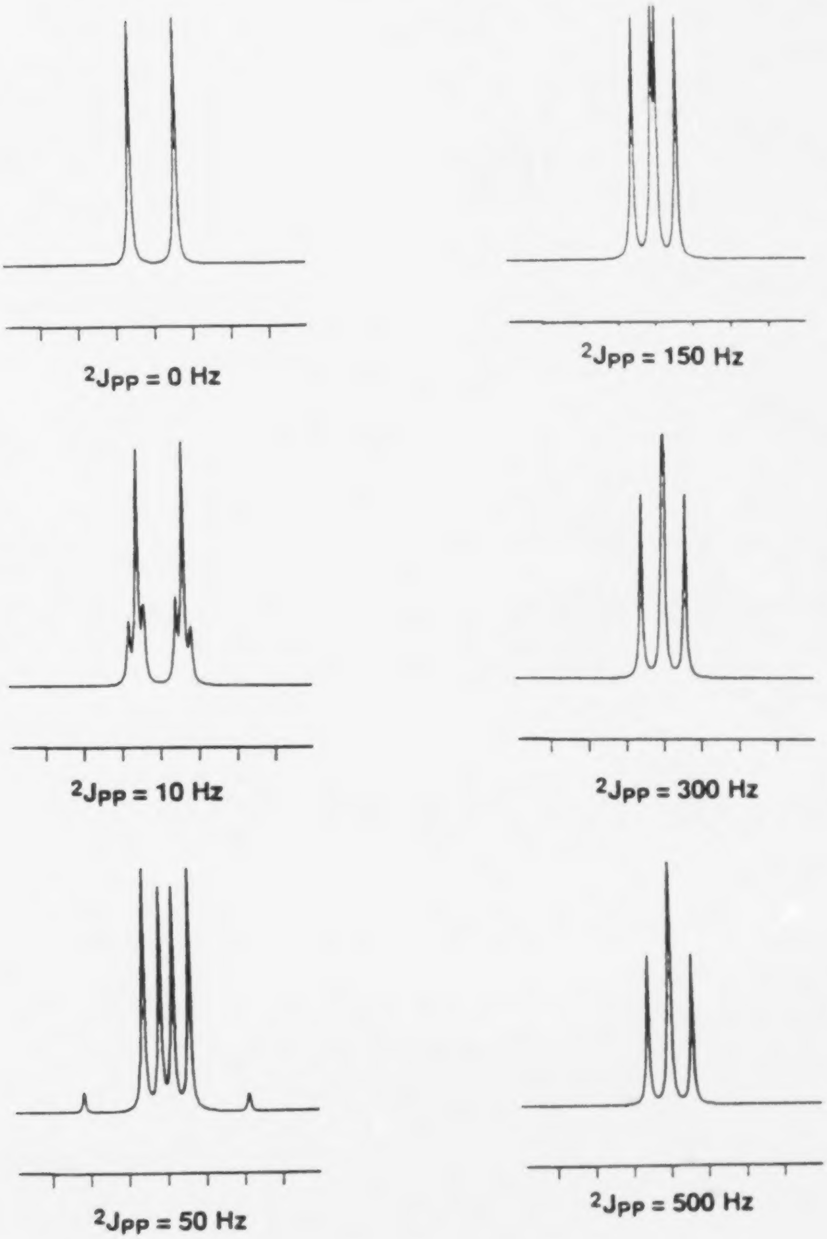

$^{2}J_{PP}$ = 0 Hz

$^{2}J_{PP}$ = 150 Hz

$^{2}J_{PP}$ = 10 Hz

$^{2}J_{PP}$ = 300 Hz

$^{2}J_{PP}$ = 50 Hz

$^{2}J_{PP}$ = 500 Hz

In addition, the doublet of triplets detected by ^{13}C NMR spectroscopy for the rhodium complex **31** (186.7 ppm, $^{1}J_{CRh}$=74.7 Hz, $^{2}J_{CP}$=15.1 Hz) clearly indicates two equivalent phosphines reinforcing the conclusion that the phosphines in this complex are trans to each other.

The simulation of the imine proton multiplet for **30** is equally unusual. This is an example of a limiting case of an AA'XX' spin system in which several coupling constants are very small resulting in a highly symmetric, simplistic multiplet. The simulation of this multiplet and appropriate coupling constants are shown in Figure 2.3. Typically one-half of an AA'XX' spectrum has as many as 12 transitions but in this case $J_{AA'}$ (J_{HH}) is essentially zero and $J_{XX'}$ (J_{PP}) is small (<10 Hz). In this situation most of the transitions overlap to form the most intense lines which are separated by $J_{AX} + J_{AX'}$ ($J_{AX} >> J_{AX'}$). The small side peaks are separated from the intense peaks by $J_{AA'} + J_{XX'}$ (or $J_{AA'} - J_{XX'}$). Assuming that the $J_{HH'}$ coupling is zero (no through space interaction), this separation is the $^{2}J_{PP}$ coupling constant of only 7 Hz. Literature examples of $^{2}J_{PP}$ coupling constants this small belong to cis-phosphine substituted palladium complexes such as **35** ($^{2}J_{PP}$=10 Hz)[25] and thus **30** must have cis-phosphines.

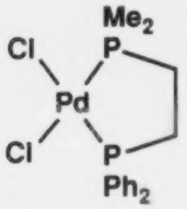

35

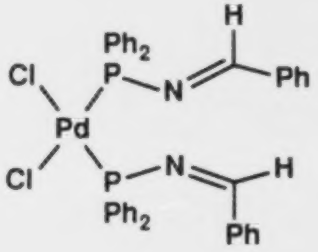

30

Figure 2.3 The simulated ^{1}H NMR spectra for the imine protons of **30** demonstrating the effect of small $^2J_{PP}$ coupling upon the AA'XX' spectrum.

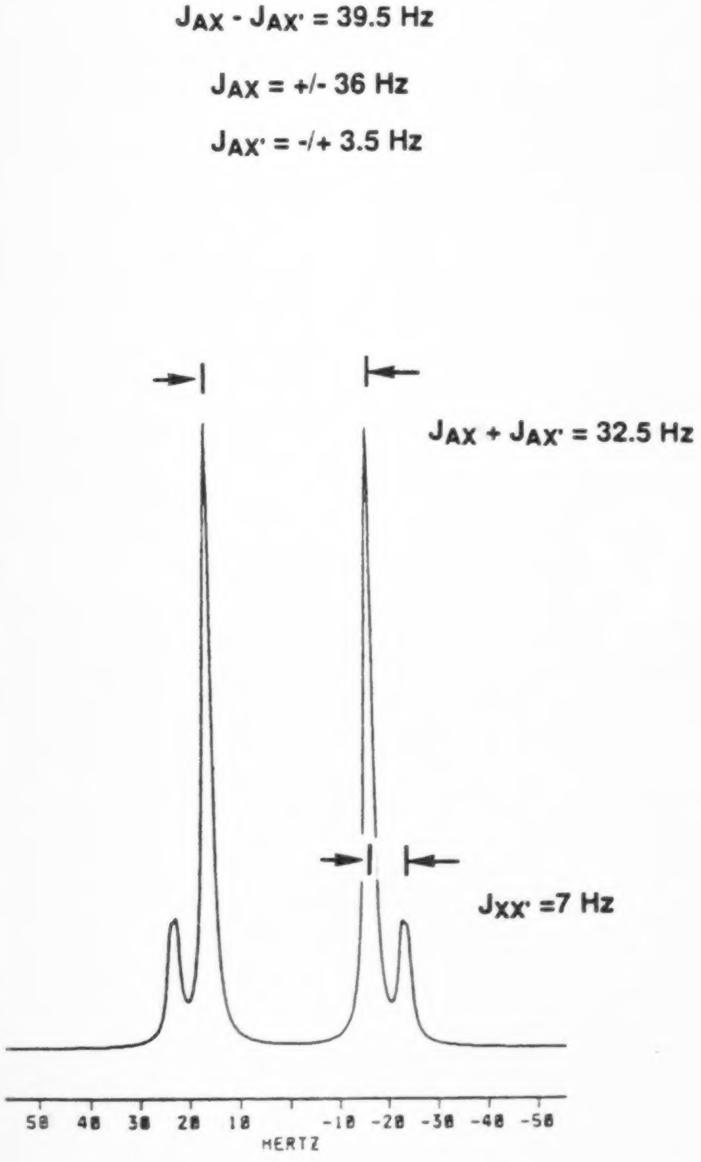

The multiplets observed in the ^{1}H NMR spectra of **30** and **31** are extreme examples of AA'XX' spin systems in which $J_{XX'}$ is very small and very large respectively. The effects of these values on the appearance of the AA'XX' spectrum is illustrated in Figure 2.4.

Phosphorus NMR spectroscopy is very effective in monitoring the effects of oxidation or complexation of the phosphine. The phosphine (**1**) has a chemical shift of 49.38 ppm and upon oxidation with azides the chemical shifts are 15.41 ppm for **27** and 6.66 ppm for **29.** Oxidation of **1** with sulphur has the opposite effect and **28** has a chemical shift of 61.14 ppm . The chemical shifts for the complexes **30**, **31** and **32** are similarly affected with resonances of 72.73, 70.72, and 73.00 ppm respectively.

Finally, infrared spectroscopy (Table 2.1) clearly demonstrates that the absorption by the imine double bond (ν 1610 cm^{-1}) is essentially unaffected by the changes occuring at the phosphorus centre.

Figure 2.4 The variation of AA'XX' spectra with coupling constant values.

a) All coupling constants non-zero[28].

$N=J_{AX}+J_{AX'}$, $M=J_{AA'}-J_{XX'}$, $K=J_{AA'}+J_{XX'}$, $L=J_{AX}-J_{AX'}$, $2P=(K^2+L^2)^{1/2}$ and $2R=(M^2+L^2)^{1/2}$.

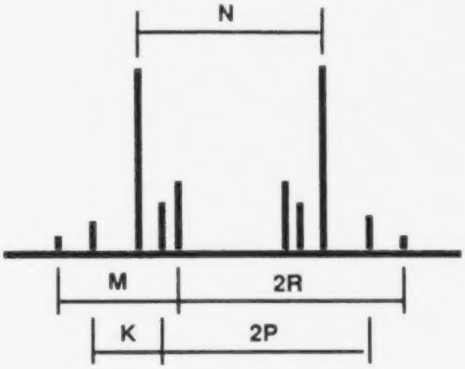

b) $J_{AA'}=0$ Hz. $K=M=J_{XX'}$, $2P=2R$.

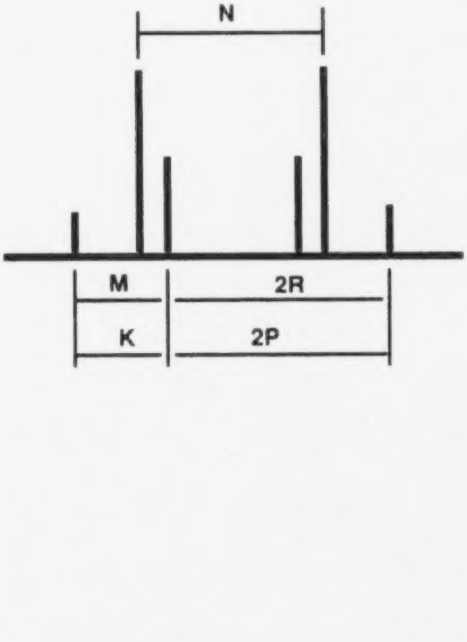

c) $J_{XX'} >> N$, $J_{AA'} = 0$ Hz, $K = M = J_{XX'} = 2P = 2R$.

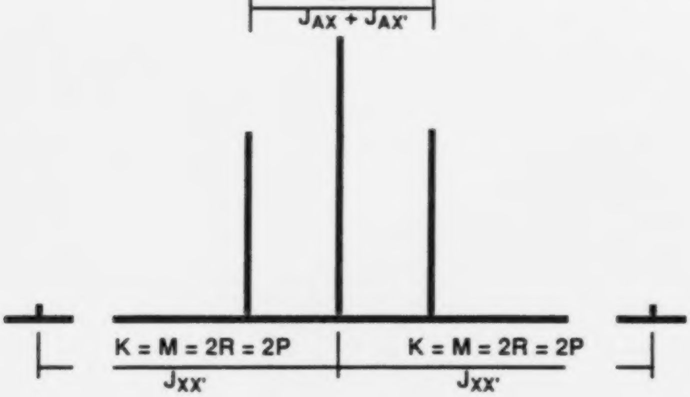
N
JAX + JAX'
K = M = 2R = 2P
JXX'
K = M = 2R = 2P
JXX'

d) $J_{XX'} < N$, $J_{AA'} = 0$ Hz.

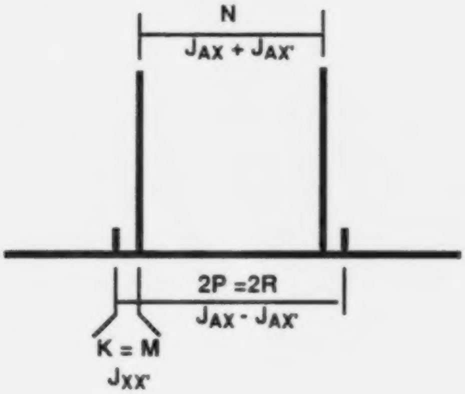
N
JAX + JAX'
2P =2R
JAX - JAX'
K = M
JXX'

N-Diphenylphosphine-*N'*,*N'*-bis(trimethylsilyl)benzamidine.

The synthesis of *N*-diphenylphosphino-*N'*,*N'*-bis(trimethylsilyl)-benzamidine **2** is described in the experimental section and has already been outlined in the introduction (Equation 2.4). A single resonance for the protons of the trimethylsilyl group is observed in the ^{1}H NMR spectrum with no observed coupling to phosphorus. At room temperature this compound displays broad singlets in the ^{31}P and ^{29}Si NMR spectra. Upon cooling to approximately -60°C the signal in the ^{31}P NMR spectrum broadens further. Cooling to -90°C produces a sharp ^{31}P signal. Considering the lack of coupling between the ^{1}H or the ^{29}Si nuclei with the ^{31}P nucleus (at ambient temperature), the assignment of structure **2** is favoured over that of **2'**.

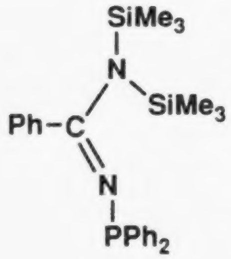

2

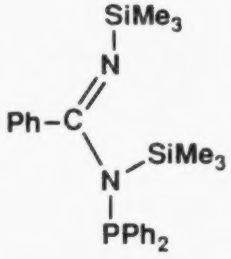

2'

In a similar fashion, the trimethylsilyl groups of compound **23** are equivalent as indicated by a single resonance in the ^{1}H NMR spectrum[2]. It is possible that in this compound the trimethylsilyl groups are able to migrate between the nitrogen centres. Furthermore, the compound **36**[21] is observed as two isomers (**36a** and **36b**) at room temperature in the ^{1}H, ^{29}Si and ^{31}P NMR spectra. The ability of these two isomers to inconvert is unknown. Thus the source of the broadening of the ^{31}P NMR signal with temperature observed for **2** is unlikely to be due to trimethylsilyl group migration unless the isomers **2** and **2'** have the same ^{31}P NMR chemical shift. A more reasonable explanation would involve the slowing of a process such as inversion of a pyramidal nitrogen or a C-N bond rotation.

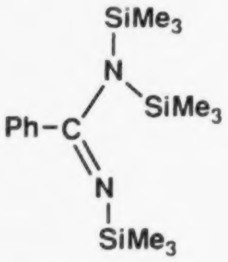

23

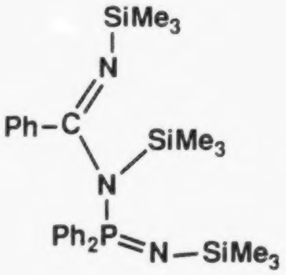

36a

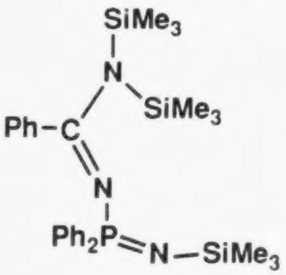

36b

Single crystal X-ray structure determinations for **23**[26] and **36**[20] reveal that one silyl group is asymmetrically bridging the amidine nitrogens in the former while in the latter compound the central nitrogen atom does not possess a trimethylsilyl group (**36b**). In the solid state, both compounds possess near planar nitrogen centres with two trimethylsilyl groups. This suggests the possibility that in solution at low temperature a planar nitrogen environment is preferred and hence supports the source of the observed temperature variation of the ^{31}P NMR signal for **2** as a pyramidal nitrogen inversion process in which a trigonal planar nitrogen environment is thermodynamically favoured. A C-N bond rotation is still required to equilibrate the trimethylsilyl groups and the low temperature ^{29}Si NMR spectrum of **2** needs to be studied.

Complexation reactions of **2** with a variety of transition metals were investigated. Overall, most transition metal halides and organometallic compounds attempted were either too reactive and destroyed the ligand, or, no reaction was observed. The reactions with $TiCl_4$ and $CpTiCl_3$ produced glassy solids which could not be identified spectroscopically. In related work, a recent paper by Roesky and co-workers[27] describes the preparation of a compound incorporating a titanium-nitrogen double bond stabilized by coordinated pyridine molecules **37**. It is conceivable that reactions of **2** with high oxidation state metal halides has occurred producing similar metal-nitrogen double bonds which subsequenty undergo further reaction.

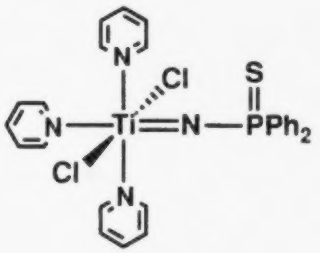

37

Titanocene dichloride and zirconocene dichloride do not react with **2** at room temperature in dichloromethane solution while tungsten hexachloride and **2** stirred at room temperature in dichloromethane react to produce a variety of unidentified products. Tungsten hexacarbonyl does not react with **2** after 4 days in refluxing acetonitrile. Complexation reactions of **2** with one equivalent of $PdCl_2(PhCN)_2$ or $1/2[Rh(CO)_2Cl]_2$ produced unstable compounds which were briefly observable by ^{31}P NMR spectroscopy.

The reaction of two equivalents of **2** with $PdCl_2(PhCN)_2$ proceeded cleanly to yield one product **38**. The product was identified as the dichloromethane solvate from the elemental analysis and the presence of a strong signal at 5.32 ppm (CH_2Cl_2) in the ^1H NMR spectrum. The geometry at palladium (cis or trans) and the site of attachment of the remaining trimethylsilyl groups could not be determined by spectroscopic means. The mass spectrum, however, does show the parent ion at $M^+=856$ with 100 % intensity verifying the molecular composition. Furthermore, the isotopic distribution of the signal detected for the parent ion and the simulation (Figure 2.5) are identical.

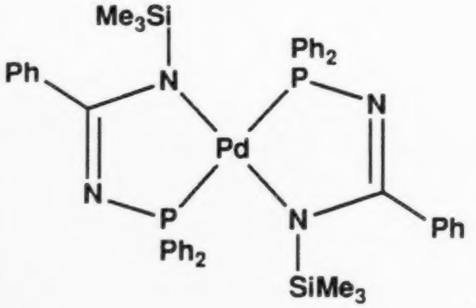

38

The reaction of **2** with 1/2[Rh(COD)Cl]$_2$ produces **39** which was prepared by simply combining the reagents in methylene chloride at -78°C for one hour and removing the solvent *in vacuo*. The possibility of further reaction was suggested by the mass spectrum. Indeed, **39** was not observed in the mass spectrum, instead a signal at mass 586 (38 %) **40** was observed indicated that trimethylsilyl chloride had been eliminated from **39**. In solution, prolonged stirring of **39** in methylene chloride (or gentle reflux) produced the compound **40** as an impure oily-solid. The further deshielding of the ^{31}P NMR signal (from 59.1 ppm for **39** to 88.0 ppm for **40**) is characteristic of ring formation[25] and is similar to the ^{31}P NMR chemical shift for **38** at 85.5 ppm . The $^{1}J_{PRh}$ coupling constant has increased from 154.7 Hz to 165.9 Hz. The ^{1}H NMR spectrum integrates correctly for **40**, but until firmer characterization is achieved, the existence of **40** is tentative.

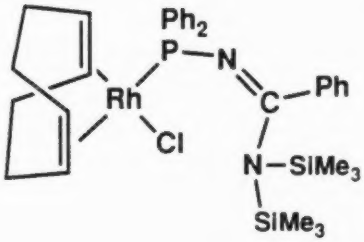
Ph$_2$
P
N
C
Ph
Rh
Cl
N
SiMe$_3$
SiMe$_3$

39

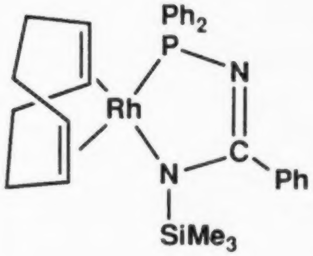
Ph$_2$
P
N
Rh
C
N
Ph
SiMe$_3$

40

Figure 2.5 The observed and simulated mass spectrum signals for the parent ion of **38** (M/e=856).

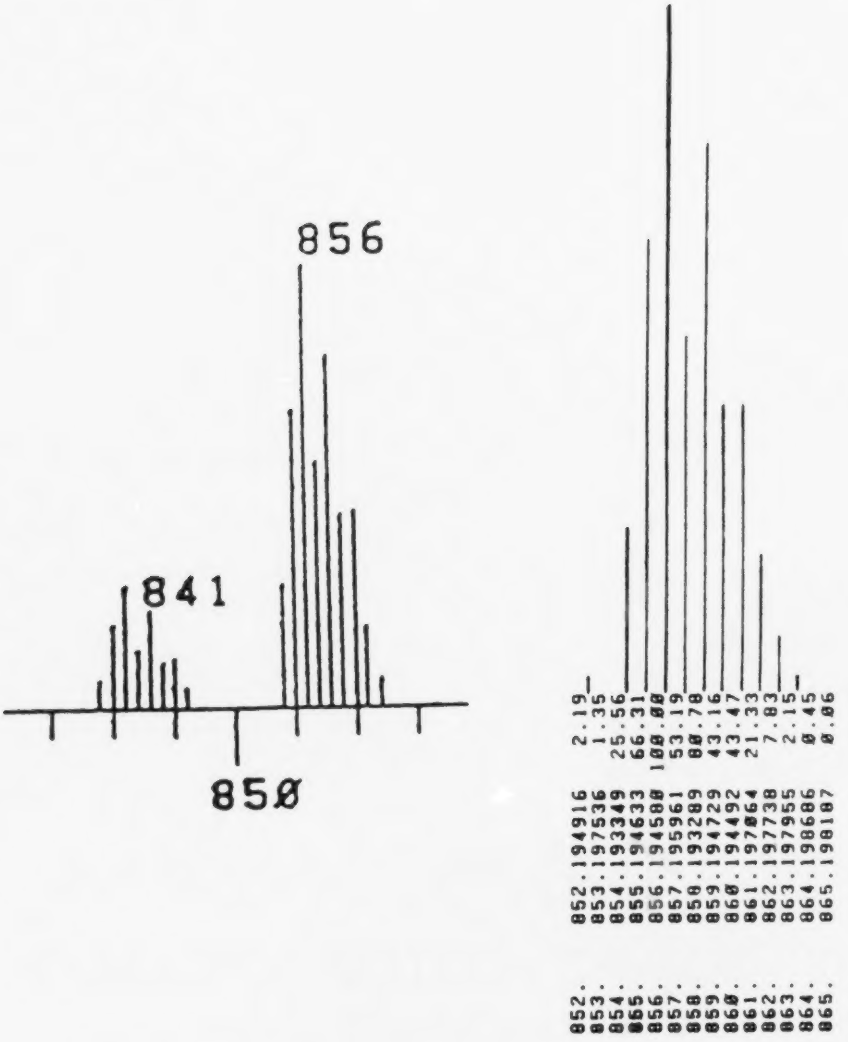

```
852.   852.194916     2.19
853.   853.197536     1.35
854.   854.193349    25.56
855.   855.194633    66.31
856.   856.194580   100.00
857.   857.195961    53.19
858.   858.193289    80.78
859.   859.194729    43.16
860.   860.194492    43.47
861.   861.197064    21.33
862.   862.197738     7.83
863.   863.197955     2.15
864.   864.198686     0.45
865.   865.198187     0.06
```

2.3 Summary

In conclusion it has been demonstrated that *N*-diphenylphosphino-benzalimine can be synthesized in good yield utilizing the elimination of trimethylsilyl chloride from *N*-trimethylsilylbenzalimine and chlorodiphenylphosphine. The product phosphine, derivatives and metal complexes are easily identified by characteristic ^{1}H and ^{31}P NMR spectroscopic features. The second order appearance of the imine protons in the ^{1}H NMR spectra of the metal complexes **30** and **31** reveals valuable structural information. Although the $^2J_{PP}$ coupling constant was not observed directly, simulation of the ^{1}H NMR spectrum through an iterative process allowed this coupling constant to be approximated ($^2J_{PP}$ for **30** = approx. 7 Hz (*cis*), $^2J_{PP}$ for **31** = 300 - 500 Hz). The magnitude of this coupling constant indicated that the phosphines were *cis* in the palladium complex and reinforced the deduction, from the ^{13}C NMR, that the phosphines were *trans* in the rhodium complex.

In addition, *N*-diphenylphosphino-*N'*,*N'*-bis(trimethylsilyl)-benzamidine **2** is readily synthesized from persilylated-benzamidine and chlorodiphenylphosphine. Compound **2** is highly soluble in all organic solvents and the trimethylsilyl groups display fluxional behavior in solution. This compound is a poor heterodinuclear ligand seeming to favour decomposition over complexation. The presence of two reactive trimethylsilyl groups complicates reactions with metal halides possessing more than one halide; from reactions of these many products are formed. Presumably, trimethylsilyl chloride elimination occurs followed by rupture of the P-N bond which leads to the destruction of the ligand. When a relatively unreactive metal chloride, such as Pd(II) or Rh(I), is utilized, complexation is achieved cleanly prior to trimethylsilyl chloride elimination. Compounds, **38** and **40** are cyclic heterocycles possessing a metal-nitrogen sigma bond. They still possess one trimethylsilyl group resulting in relatively low melting points and increased volatility which aids in their detection by mass spectroscopy.

2.4 Experimental

This section describes the synthesis and subsequent chemistry of *N*-diphenylphosphinobenzalimine **1** and *N*-diphenylphosphino-*N'*,*N'*-bis(trimethylsilyl)benzamidine **2**. General techniques, reagents, solvents and instrumentation are listed in the appendix.

Section A. Synthesis of the Phosphine Derivatives.

A.1. Synthesis of *N*-diphenylphosphinobenzalimine, 1.

A.1.i Preparation of *N*-trimethylsilylbenzalimine.

This procedure was modified from that of Hart.[1] In a typical reaction, 25.00 g (103.7 mmol) of $LiN(SiMe_3)_2{\cdot}Et_2O$[2] was placed in a 500 mL 24/40 round bottom flask and an atmosphere of argon was introduced. Freshly distilled tetrahydrofuran, 100 mL, (diethyl ether can also be used with no noticable difference in the result) was then added to dissolve the solid lithium salt and the reaction flask was cooled to 0 °C. Benzaldehyde (11.0 g, 103.8 mmol) was then placed in a pressure equalizing dropping funnel and slowly added to the reaction flask. The reaction mixture was allowed to stir overnight and warm slowly to room temperature during which time the colourless solution turned pale yellow. The solvent was then stripped off *in vacuo* and the yellow residual oil was vacuum distilled (0.5 torr) leaving the side product, $LiOSiMe_3$, behind. The product was collected between 55 to 60 °C (9.38 g, 53.0 mmol, 51 %). ^1H NMR (δ, $CDCl_3$,TMS) 8.9 ppm (s, 1H, -CH=N-), Lit.[1] 8.9 (s,1H,-CH=N-).

A.1.ii. Synthesis of *N*-diphenylphosphinobenzalimine.

In a 500 mL 24/40 round bottom flask was placed 8.82 g (49.8 mmol) of *N*-trimethylsilylbenzalimine and 150 mL of toluene. The reaction flask was cooled to 0 °C and 10.99 g (49.73 mmol) of chlorodiphenylphosphine in 50 mL of toluene was added dropwise. The reaction mixture was allowed to stir overnight. Removal of the solvent *in vacuo* (caution: this compound is thermally unstable in solution, for best yields avoid exposure to unnecesssary heat) produces a yellow sticky solid (approx. 14 g, 97 %) which can be carefully recrystallized from acetonitrile or diethylether. M.P.=72-73 °C, Analysis: $C_{19}H_{16}NP$: Calculated: C=78.88, H=5.57, N=4.84% . Found: C=76.22, H=5.53, N=4.88%. I.R. (CH_2Cl_2 cast) 3054w, 2850w, 1625m, 1611m, 1577w, 1477w, 1449w, 1433m, 1308w, 1214w, 1092w, 1067w, 1025w, 844w, 775m, 741s, 694s, 516w, 502m. M.S.: M^+ 289 (100 %). ^1H NMR (δ, $CDCl_3$, TMS) 8.28 ppm, d, 1H, $^3J_{PP}$=22 Hz.; 8.0-7.3 ppm, m, 15H. ^{31}P NMR (δ, $CDCl_3$, H_3PO_4) 49.38 ppm, s.

A.2. Synthesis of *N*-diphenylphosphino-*N'*,*N'*-bis(trimethylsilyl)benzamidine, 2.

In a 500 mL three neck 24/40 round bottom flask was placed 30.0 g (124 mmol) of $LiN(SiMe_3)_2 \cdot Et_2O$ and 300 mL of dry diethyl ether. To this solution was added dropwise 13 mL (130 mmol) of benzonitrile and the mixture was stirred at room temperature and monitored by ^1H NMR until the signal at 0 ppm disappeared and a signal at -0.4 ppm reached a maximum ($Ph-C(=NLi)N(SiMe_3)_2$. Chlorodiphenylphosphine (24.3 g, 110 mmol) was then added dropwise and the reaction mixture was stirred at room temperature overnight. The ^{31}P NMR spectrum of the reaction mixture demonstrated that Ph_2PCl was completely converted to the product **2**. The LiCl precipitate was allowed to settle for several hours before the solution was filtered under argon and approximately 75 % of the solvent was removed *in vacuo*. Acetonitrile was added (50 mL) to the oily amber solution. A few seed crystals of the product were added (when available) and the flask was left in the freezer (-20 °C) until crystallization occured (1-7 days). Filtration of the yellow waxy crystals under argon (while still cold) and drying under vacuum produced 40 g (89 mmol, 81 %) of N-diphenylphosphino-N',N'-Bis(trimethylsilyl)benzamidine. M.P.=63-65°C. Analysis: $C_{25}H_{33}N_2Si_2P$. Calculated: C=66.92, H=7.41, N=6.24 %. Found: C= 66.35, H=7.56, N=6.43 %. I.R. (CH_2Cl_2 cast) 3120m, 2950m, 1640w, 1555vs, 1480m, 1435s, 1250vs,br, 1150w, 1120m, 1080w, 1040m, 1020m, 875m,br, 840vs,br, 770s, 740m, 700s, 515m. M.S. M^+, 448 (5 %). ^1H NMR (δ, $CDCl_3$, TMS) 7.9-7.4, m, 15H; 0.1, s, 9H. ^{31}P NMR (δ, $CDCl_3$, H_3PO_4) 34.8 ppm, s, broad. ^{29}Si (δ, $CDCl_3$, TMS) 5.8 ppm, s, broad.

Section B. Chemistry of the Phosphine Derivatives.

B.1. Oxidation of *N*-diphenylphosphinobenzalimine, 1.

B.1.i. Reaction with trimethylsilyl azide to form 29.

Into a 250 mL 24/40 round bottom flask was placed: 5.20 g (18.0 mmol) of *N*-diphenylphosphinobenzalimine (**1**), 2.20 g (19.1 mmol) of trimethylsilyl azide, and 50 mL of dry toluene. The reaction mixture was refluxed overnight. The ^{31}P NMR spectrum of the reaction solution demonstrated that the reaction was complete; no signal was observed for the starting material. The product showed a single peak at 6.66 ppm. Removal of the solvent *in vacuo* and recrystallization of the thick syrup from acetonitrile afforded a small quantity of a white crystalline material which proved to be $[Ph_2PN]_3$[24]. M.S. M^+=597. Subsequent attempts to isolate **29** as a crystalline solid met with equal failure.

B.1.ii. Reaction with *p*-cyanotetrafluorophenyl azide to form 27.

Into a 100 mL side arm round bottom flask was placed 1.0017 g (3.466 mmol) of N-diphenylphosphinobenzalimine (**1**) and 30 mL of dichloromethane. The flask was cooled to 0 °C and 0.7600 g (3.518 mmol) of *p*-cyanotetrafluorophenyl azide in 10 mL of dichloromethane was added dropwise. After several hours the solvent was removed *in vacuo* and the product recrystallized from a minimum of acetonitrile producing 0.91 g (1.9 mmol, 55 %) of pale yellow crystals. M.P.=188-190 °C. Analysis: $C_{26}H_{16}F_4N_3P$ Calculated: C= 65.47, H=3.38, N=8.81 %. Found: C=65.38, H=3.41, N=8.88 %. I.R. (CH_2Cl_2 cast): 3061w, 2230s, 1644s, 1614s, 1597w, 1578m, 1502s,br, 1437s, 1312w, 1226s, 1117m, 1015m, 999w, 982s, 884m, 846w, 820s, 752m, 726m, 691s, 546m, 525m, 512m, 481w. M.S.: M^+=477 (35 %). ^{1}H NMR (δ, $CDCl_3$, TMS) 9.13 ppm, d, 1H, $^3J_{PP}$=34 Hz; 8.0-7.3 ppm, m, 15H. ^{31}P NMR (δ, $CDCl_3$, H_3PO_4) 15.4 ppm, s.

B.1.iii. Reaction with sulphur to form 28.

Into a 100 mL round bottom flask was placed: 3.25 g (11.2 mmol) of *N*-diphenylphosphinobenzalimine (**1**), 0.360 g (1.41 mmol) of sulphur and 50 mL of toluene. The mixture was refluxed for 24 hours and upon cooling long fiberous crystals of sulphur precipitated from the solution. The solution was filtered under argon and the filtrate was stored for several days during which time large pale yellow blocks (1.1 g, 3.4 mmol, 30 %) crystallized. M.P.=76-79 °C. Analysis: $C_{19}H_{16}NPS$: Calculated: C=71.01, H=5.02, N=4.36 %. Found: C=70.82, H=4.94, N=4.43 %. I.R. (CH_2Cl_2): 3056w, 1611s, 1597w, 1578m, 1478w, 1451m, 1437s, 1365m, 1311m, 1217m, 1106s, 855s, 820s, 755s, 723s, 691s, 646m, 615w, 608m, 522s, 503m, 479m. M.S. M^+=321 (40 %). ^{1}H NMR (δ, $CDCl_3$, TMS) 9.43 ppm, d, 1H, $^3P_{HP}$=40 Hz; 8.1-7.5 ppm, m, 15H. ^{31}P NMR (δ, $CDCl_3$, H_3PO_4) 61.14 ppm, s.

Section C. Preparation of Metal Complexes.

C.1. Metal complexes of *N*-diphenylphosphinobenzalimine, 1.

C.1.i. Complex with $PdCl_2(PhCN)_2$, 30.

To a dichloromethane solution (25 mL) of $PdCl_2(PhCN)_2$ 284.0 mg (0.7410 mmol) was added dropwise a dichloromethane solution (25 mL) of N-diphenylphosphinobenzalimine (**1**) 428.1 mg (1.481 mmol) at -78 °C. The solution was allowed to stir for several hours and warm to room temperature. The solvent was removed *in vacuo* producing a yellow-orange oil that smelled strongly of benzonitrile. Only one product was detected by ^{31}P NMR spectroscopy. Recrystallization from hot acetonitrile produced yellow-orange crystals of $PdCl_2(Ph_2P\text{-}N{=}C(H)\text{-}Ph)_2$ (0.1176 g, 0.155 mmol, 21 %). M.P.=240-245 °C (decomposition). Analysis: $C_{38}H_{32}N_2P_2Cl_2Pd$. Calculated: C=60.38, H=4.27, N=3.71, Cl=9.38 %. Found: C=60.30, H=4.23, N=3.83, Cl=6.01 %. I.R. (CH_2Cl_2 cast) 3055w, 1624s, 1595w, 1575s, 1450w, 1436s, 1310w, 1097m, 850m, 815m, 747m, 712w, 688s, 547w, 525s, 509m. ^1H NMR (δ, CD_2Cl_2, TMS) 8.4 ppm, m, 2H; 7.8-7.3, m, 30H. ^{31}P NMR (δ, CD_2Cl_2, H_3PO_4) 72.73 ppm, s.

C.1.ii. Complex with $[Rh(CO)_2Cl]_2$, 31.

To a dichloromethane solution (25 mL) of $[Rh(CO)_2Cl]_2$ 102.7 mg (0.2641 mmol) was added dropwise a dichloromethane solution (25 mL) of *N*-diphenylphosphinobenzalimine (**1**) 307.9 mg (1.065 mmol) at 0 °C. The solution was allowed to stir for several hours and warmed to room temperature. The solvent was removed *in vacuo* producing a yellow microcrystalline powder. The product dissolved immediately in 10 mL of acetonitrile and after several hours deposited large cubic crystals of $Rh(CO)Cl(Ph_2P\text{-}N{=}C(H)Ph)_2$ (0.25 g, 0.39 mmol, 74 %). M.P.=165 °C (decomposed). Analysis: $C_{39}H_{32}N_2P_2ClRh$: Calculated: C=62.87, H=4.33, N=3.76 %.

Found: C=62.94, H=4.24, N=3.79 %. Solution M.W. (CH_2Br_2) 700 g/mol. I.R. (CH_2Cl_2) 3056w, 1980vs, 1625s, 1596w, 1576s, 1481w, 1450m, 1435s, 1310m, 1217w, 1168w, 1098m, 849m, 798s, 745s, 710w, 691s, 567m, 523s, 507m. M.S. (FAB): 681 $[Rh(Ph_2P\text{-}N{=}C(H)Ph)_2]^+$. ^1H NMR (δ, CD_2Cl_2, TMS) 8.8 ppm, vt, 2H; 7.9-7.4 ppm, m, 30H. $^1H\{^{31}P\}$ NMR 8.8 ppm, s. ^{31}P NMR (δ, CD_2Cl_2, H_3PO4) 69.73 ppm, d, $^1J_{PRh}$=130.1 Hz. ^{13}C NMR (δ, CD_2Cl_2, TMS) 186.7, dt, $^1J_{CRh}$=74.7 Hz, $^2J_{CP}$=15.1 Hz.

C.1.iii. Complex with $[Rh(COD)Cl]_2$, 32.

To a dichloromethane solution (20 mL) of $[Rh(COD)Cl]_2$ 342.9 mg (0.6955 mmol), cooled to -78 °C, was added dropwise a dichloromethane solution (40 mL) of $Ph_2P\text{-}N{=}C(H)Ph$ (**1**) (402.1 mg, 1.391 mmol). The reaction mixture was stirred for 12 hours and allowed to warm slowly to room temperature producing an orange solution. The solvent was removed *in vacuo* producing an orange microcrystalline powder. Phosphorus NMR spectroscopy demonstrated a quantitative conversion to the complex $Rh(COD)Cl(Ph_2P\text{-}N{=}C(H)Ph)$. Recrystallization from acetonitrile produced 400 mg (0.746 mmol, 54 %) of the complex as large orange crystals. M.P.=140 °C (decomposes). Analysis: $C_{27}H_{28}NPClRh$: Calculated: C=60.44, H=5.26, N=2.61, Cl=6.60 %; Found: C=60.53, H=5.26, N=2.87, Cl=6.37 %; Solution M.W. (CH_2Br_2) =515g/mol. I.R. (CH_2Cl_2 cast) 3053w, 2939w, 2915w, 2879w, 2829w, 1624s, 1596w, 1575m, 1480w, 1450m, 1434s, 1309w, 1218w, 1098m, 997w, 848m, 794m, 745s, 734m, 707m, 692s, 535s, 507s. M.S. (FAB): M^+-Cl=500 (100 %) . ^1H NMR (δ, CD_2Cl_2, TMS) 8.4 ppm, d, 1H, $^3J_{PP}$=28 Hz; 7.9-7.5 ppm, m, 15H; 5.6 ppm, s, 2H; 3.5 ppm, s, 2H; 2.4 ppm, m, 4H; 2.1 ppm, m, 4H. $^1H\{^{31}P\}$ NMR 8.4 ppm, s. ^{31}P NMR (δ, CD_2Cl_2, H_3PO_4) 73.0 ppm, d, $^1J_{PRh}$=159.7 Hz. ^{13}C NMR (δ, CD_2Cl_2, TMS) 170.3 ppm, d,

$^2J_{CP}$=8.3 Hz; 136 ppm -127 ppm, Ar; 107.0 ppm, dd, J=6.8 Hz and 5.8 Hz; 70.6 ppm, d, J=13 Hz; 33.4 ppm, s; 29.0 ppm, s.

C.2. Metal complexes of *N*-diphenylphosphino-*N'*,*N'*-bis(trimethylsilyl)-benzamidine, 2.

C.2.i. Complex with $PdCl_2(PhCN)_2$, 38.

To a dichloromethane solution (30 mL) of $PdCl_2(PhCN)_2$ (402.8 mg, 1.052 mmol) was added dropwise a dichloromethane solution (30 mL) of *N*-diphenylphosphino-*N'*,*N'*-bis(trimethylsilyl)benzamidine (**2**) (942.8 mg, 2.114 mmol) at -78 °C. The reaction mixture was stirred overnight and allowed to warm slowly to room temperature. The solvent was removed *in vacuo* producing a sticky yellow-orange solid contaminated with benzonitrile. Proton and ^{31}P NMR spectroscopy demonstrated a clean conversion to a single compound. Recrystallization from 15-20 mL of dichloromethane at -20 °C for five days produced one large crystal (2cm x 1cm x 0.3cm). The crystal broke during filtration under argon and the fragments were packaged in sealed tubes. M.P.=228-235 °C (decomposed). Analysis: $C_{44}H_{48}N_4P_2Si_2Pd{\cdot}2CH_2Cl_2$; Calculated: C=53.78, H=5.10, N=5.45, Cl=13.80 %. Found: C=53.98, H=4.98, N=5.76, Cl=11.65 %. I.R. (CH_2Cl_2 cast) 3050w, 2940w, 2880w, 1570w, 1480w, 1455s, 1445m, 1425s, 1320s, 1250m, 1240m, 1170w, 1135w, 1100m, 1070w, 1025w, 1000w, 950m, 930m, 830s, 790w, 745w, 730m, 690m, 640m, 580m, 525w, 515m, 495m. M.S. M^+=856 (100 %) . ^{1}H NMR (δ, CD_2Cl_2, TMS) 7.57-7.10, m, 30H; 0.1 ppm, s, 18H. ^{31}P NMR (δ, CD_2Cl_2, H_3PO_4) 85.5 ppm, s.

C.2.i. Complex with $[Rh(COD)Cl]_2$, 39.

To a dichloromethane solution (30 mL) of $[Rh(COD)Cl]_2$ (199.5 mg, 0.405 mmol) was added dropwise a dichloromethane solution (30 mL) of *N*-diphenylphosphino-*N′*,*N′*-bis(trimethylsilyl)benzamidine (**2**) (360.7 mg, 0.809 mmol) at -78 °C. The reaction mixture was stirred for one hour before the solvent was removed *in vacuo* producing an orange powder that was recrystallized from acetonitrile (yield=410mg, 0.62 mmol, 77 %). M.P.=65-70 °C compound discolours, 90 °C decomposes. Analysis: $C_{33}H_{45}N_2Si_2PClRh$. Calculated: C=57.01, H=6.52, N=4.03, Cl=5.10 %. Found: C=56.37, H=6.41, N=4.09, Cl=5.93 %. M.S. M^+-Me_3SiCl, 586 (38 %) . ^1H NMR (δ, CD_2Cl_2, TMS) 7.8 ppm, m, 5H; 7.4 ppm, m, 10H; 5.4 ppm, br s, 2H; 3.5 ppm, br s, 2H; 2.4 ppm, m, 4H; 2.0 ppm, m, 4H; 0.15 ppm, s, 18H. ^{31}P NMR (δ, CD_2Cl_2, H_3PO_4) 59.1 ppm, d, $^1J_{PRh}$=154.8 Hz. ^{29}Si NMR (δ, CD_2Cl_2, TMS) 7.18 ppm, s.

Section D. Less-Successful Reactions.

D.1. Reaction of 2 with $TiCl_4$.

A methylene chloride solution (25 mL) of **2** (1.38 g, 3.07 mmol) was added dropwise to a solution (CH_2Cl_2, 50 mL) of $TiCl_4(2THF)$ (1.00 g, 3.06 mmol) at 0 °C. After five hours the yellow solution had turned red and the solvent was removed *in vacuo* producing a red brown glassy solid. M.P. = 180 °C (decomposed). ^{31}P NMR (δ, $CDCl_3$, H_3PO_4) 39 peaks of significant intensity between 124 and -16 ppm.

D.2. Reaction of 2 with $CpTiCl_3$.

A methylene chloride solution (75 mL) of **2** (0.9275 g, 2.066 mmol) was added dropwise to a solution (CH_2Cl_2, 75 mL) of $CpTiCl_3$ (0.4547 g, 2.072 mmol) at -78 °C.

The temperature was maintained at -78 °C for six hours and during that time the initial orange solution turned red. The solvent was removed *in vacuo* and the solid residue was analyzed by NMR spectroscopy. ^{31}P NMR (δ, $CDCl_3$, H_3PO_4) 84.7 ppm, s (plus a dozen smaller peaks between 37 and -23 ppm).

D.3. Reaction of 2 with Cp_2TiCl_2.

A methylene chloride solution (25 mL) of **2** (1.80 g, 4.01 mmol) was added to a solution (CH_2Cl_2, 100 mL) of Cp_2TiCl_2 (1.00 g, 4.02 mmol) at room temperature. No colour change was observed upon addition. After 24 hours the solvent was removed *in vacuo* producing a sticky brown sludge. Acetonitrile (50 mL) was then added to the sludge and the resulting solution was refluxed for five hours. The solvent was again removed *in vacuo* producing a sticky brown sludge. The reaction was abandoned.

D.4. Reaction of 2 with Cp_2ZrCl_2.

A methylene chloride solution (25 mL) of **2** (1.58 g, 3.52 mmol) was added dropwise to a solution (CH_2Cl_2, 75 mL) of Cp_2ZrCl_2 (1.03 g, 3.53 mmol) at 0 °C. The solution was allowed to warm slowly overnight. No colour change was observed. No reaction occurred as monitored by ^{31}P NMR spectroscopy.

D.5. Reaction of 2 with WCl_6.

A methylene chloride solution (25 mL) of **2** (0.5968 g, 1.330 mmol) was added dropwise to a solution (CH_2Cl_2, 50 mL) of WCl_6 (0.5275 g, 1.329 mmol) at 0 °C. The solution was stirred overnight. The solvent was removed *in vacuo* producing a black powder which quickly decomposed upon exposure to air and $CDCl_3$.

D.6. Reaction of 2 with $W(CO)_6$.

An acetonitrile solution (50 mL) of **2** (1.41 g, 3.14 mmol) was added dropwise to a solution (CH_3CN, 50 mL) of $W(CO)_6$ (1.10 g, 3.13 mmol). After 4 days of heating at reflux, no reaction had occurred as determined by ^{31}P NMR spectroscopy.

D.7. Equimolar reaction of 2 with $PdCl_2(PhCN)_2$.

A methylene chloride solution (20 mL) of **2** (0.5175 g, 1.152 mmol) was added dropwise to a solution (25 mL, CH_2Cl_2) of $PdCl_2(PhCN)_2$ at -78 °C. The reaction solution was allowed to warm slowly to room temperature overnight. The solvent was removed *in vacuo* and the sticky residue was washed with hexane to remove benzonitrile. M.P. = 184°C (decomposed). Analysis: Found; C = 53.27, H = 4.34, N = 6.28, Cl = 3.61 %. ^1H NMR (δ, $CDCl_3$, TMS) 8.3 - 7.0 ppm, Integration = 3, 0.2 - -0.2 ppm, Integration = 1. ^{31}P NMR (δ, $CDCl_3$, H_3PO_4) 92.1 ppm, s; 91.5 ppm, s; 90.9 ppm, s (major peak); 89.6 ppm, s.

D.8. Reaction of 2 with $1/2[Rh(CO)_2Cl]_2$.

A methylene chloride solution (100 mL) of **2** (0.1468 g, 0.3272 mmol) was added dropwise to a solution (100 mL CH_2Cl_2) of $[Rh(CO)_2Cl]_2$ (0.0640 g, 0.165 mmol) at room temperature. The reaction mixture was stirred for 24 hours before the solvent was removed *in vacuo* and the residue was analyzed by NMR spectroscopy. ^1H NMR (δ, $CDCl_3$, TMS) 8.0 - 7.0 ppm, approx. 15 H, Ar; 0.1 ppm, approx. 9 H, Me_3Si-. ^{31}P NMR (δ, $CDCl_3$, H_3PO_4) 106.1 ppm, d, $^1J_{PRh}$ = 179.8 Hz (major peak).

2.5 References

1. D. J. Hart, K. Kanai, D. G. Thomas and T. K. Yang. *J. Org. Chem.*, **48**, 289 (1983).
2. R. T. Boeré, R. T. Oakley and R. W. Reed. *J. Organomet. Chem.*, **331**, 161 (1987).
3. A. Streitwieser Jr. and C. H. Heathcock. "Introduction to Organic Chemistry", Macmillan Publishing Co., New York, 1981.
4. C. Krüger, E. G. Rochow and U. Wannagat. *Chem. Ber.*, **96**, 2132 (1963).
5. D. P. Drolet, L. Chan and A. J. Lees. *Organometallics*, **7**, 2502 (1988).
6. W. R. Cullen and E. B. Wickenheiser. *J. Organomet. Chem.*, **370**, 141 (1989).
7. H. Brunner and G. Riepl. *Angew. Chem. Int. Ed. Eng.*, **21**, 377 (1982).
8. A. Q. Hussein and H. A. Hodali. *Synth. React Inorg. Met.-Org. Chem.*, **18**, 365 (1988).
9. A. J. Blake, A. J. Lavery, T. I. Hyde and M. Schröder. *J. C. S. Dalton Trans.*, 965 (1989).
10. C. M. Anderson, R. J. Puddephatt, G. Ferguson and A. J. Lough. *J. C. S. Chem. Commun.*, 1297 (1989).
11. a) W. Ried, M. Fulde and J. W. Bats. *Helv. Chimica Acta*, **72**, 969 (1989).

    b) R. F. Swindell, D. P. Babb, T. J. Ouellette and J. M. Shreeve. *Inorg. Chem.*, **11**, 242 (1972).

    c) A. Schmidpeter, W. Zeiss and H. Eckert. *Z. Naturforsch.*,**27b**, 769 (1972).

    d). A. Schmidpeter and W. Zeiss. *Chem. Ber.*, **104**, 1199 (1971).
12. A. R. Sanger. *Inorg. Nucl. Chem. Letters*, **9**, 351 (1973).
13. H. W. Roesky, B. Meller, M. Nolyemeyer, H. G. Schmidt, U. Scholz, and G. M. Sheldrick. *Chem. Ber.*, **121**, 1403 (1988).
14. C. Ergezinger, F. Weller and K. Dehnicke. *Z. Naturforsch*, **43b**, 1621 (1988).

15. D. Fenske, E. Hartmenn and K. Dehnicke. *Z. Naturforsch.*, **43b**, 1611 (1988).

16. S. Mair, W. Hiller, J. Strähle, C. Ergezinger and K. Dehnicke. *Z. Naturforsch.*, **43b**, 1628 (1988).

17. H. W. Roesky, U. Scholz, A. Schmidpeter, K. Karaghiosoff and W. S. Sheldrick. *Chem. Ber.*, **121**, 1681 (1988).

18. a) U. Scholz, H. W. Roesky, J. Schimkowiak and M. Noltemeyer. *Chem. Ber.*, **122**, 1067 (1989).

    b) A. W. Cordes, R. C. Haddon, R. T. Oakley, L. F. Schneemeyer, J. V. Waszczak, K. M. Young and N. M. Zimmerman. *J. Am. Chem. Soc.*, **113**, 582 (1991).

19. R. G. Cavell and R. W. Reed. Unpublished result.

20. H. W. Roesky, R. Hasselbring, J. Liebermann and M. Noltemeyer. *Z. Naturforsch.*, **45b**, 1383 (1990).

21. U. Scholz, M, Noltemeyer and H. W. Roesky. *Z. Naturforsch.*, **43b**, 937 (1988).

22. K. Bestari, A. W. Cordes, R. T. Oakley and K. M. Young. *J. Am. Chem. Soc.*, **112**, 2249 (1990).

23. C. Roques, M. R. Mazières, J. P. Majoral, M. Sanchez and J. Jaud. *Inorg. Chem.*, **28**, 3933 (1989).

24. H. R. Allcock. "Phosphorus-Nitrogen Compounds". Academic Press, New York, 1972.

25. P. E. Garrou. *Chem. Rev.*, **81**, 229 (1981).

26. C. Ergezinger, F. Weller and K. Dehnicke. *Z. Naturforsch.*, **43b**, 1119 (1988) .

27. H. W. Roesky, H. Voelker, M. Witt and M. Nolyemeyer. *Angew. Chem. Int. Ed. Eng.*, **102**, 712 (1990).

28. Approximate spectrum based on the example found in: E. D. Becker. "High Resolution NMR Theory and Chemical Applications". Academic Press, (1980).

Chapter Three

Deuterium Exchange in Bis(diphenylphosphino)methane Derivatives

3.1 Introduction

The phosphinimine phosphines, $RN{=}PPh_2\text{-}E\text{-}PPh_2$ ($R{=}Me_3Si$, Me_3Ge, C_6F_4CN, etc.)[1,2] provide hard base (N) or soft base (P) coordination to metals in both high and low oxidation states and formation of metal nitrogen bonds by Me_3SiX elimination or Me_3Si migration to terminal oxygen[1-7]. A system of compounds is accessible by employing different backbone functionalities, E. ($E{=}CH_2$, $CHCH_3$, C_2H_4, C_6H_4, etc.). Furthermore these compounds are ylids and they undergo Wittig-like reactions with aldehydes, ketones, carbon disulphide, etc.[8]. In the initial reports of the protypical compound *N*-trimethylsilyl-diphenylphosphoraniminediphenylphosphino-methane (**1**), prepared by the reaction of bisdiphenylphosphinomethane (dppm) with trimethylsilyl azide, unusual multiple resonances of **1** were displayed in the ^{31}P and ^{1}H-NMR spectra[1]. This report attributed the source of the multiple resonances to different rotational conformations of **1**. A single crystal x-ray structural determination of **1** shows only one conformation in the solid state and suggests a lack of steric congestion within the molecular framework[9]. We have now proven definitively that these multiple resonances in the ^{31}P-NMR spectra arise from facile deuterium exchange of the methylene protons of **1** with $CDCl_3$.

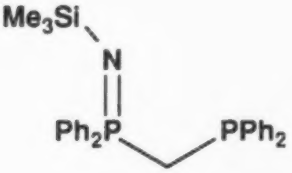

1

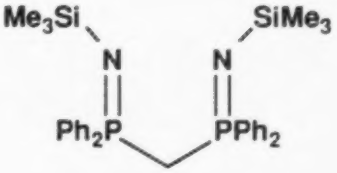

2

Deuterium exchange between solvent and substrate is often encountered especially when readily ionizable protons on alcohols, amines or water can be aided by strong base catalysis[10]. It is less common in non-aqueous media and it is frequently catalyzed by transition metals[11]. With respect to the isotope effect on ^{31}P NMR chemical shifts the following factors apply:[12] phosphorus centres with a lone pair of electrons show a much greater effect, the effect is additive (*i.e.* proportional to the number of deuterons incorporated), and the effect is usually to lower frequency (upfield). In contrast, the effect of deuterium substitution on the phosphorus-phosphorus and remaining phosphorus-proton coupling constants is usually too small to detect[13].

In the present case deuterium exchange occurs readily, presumably because of the participation of the relatively basic imine functionality. It is observable because of the enhanced isotope effect on the NMR chemical shift of the adjacent P(III) centre[12]. The related methylene bis(*N*-trimethylsilyl-diphenylphosphinimine)[14] **2** also shows a sensitivity to deuterium exchange of the methylene protons with $CDCl_3$. In this case the isotope effect on the P(V) chemical shift is an order of magnitude smaller (compared to the isotope effect on the P(III) chemical shift), making this isotopic exchange difficult to observe by ^{31}P NMR spectroscopy.

Differences in exchange rate are commensurate with differences in the basicity of the compound and at the extreme *N*-methyl-trimethylphosphinimine will violently decompose chloroform[15]. It is, however, difficult to compare rates of exchange because of the complication that the presence of trace water will catalyze the reaction[16]. The deprotonation of chloroform by a strong base in non-aqueous systems usually leads to transient dichlorocarbene formation as demonstrated by the trapping of the carbene with an olefin to produce a cyclopropane[17]. However, since the rate of deuterium exchange between chloroform and D_2O/NaOD is approximately 10^6 times faster than the rate of hydrolysis[17], we believe we have identified a situation where a basic phosphinimine nitrogen has the correct base strength to abstract deuterium from chloroform. The exchange proceeds with the aid of water catalysis, without degradation of chloroform *via* carbene formation and without observable hydrolysis of the P=N-$SiMe_3$ linkage.

3.2 Results and Discussion

The transformation of the ^{31}P NMR resonances of **1** (81 MHz in $CDCl_3$) with time is shown in Figure 3.1. The individual spectra are composed of AX patterns due to $^2J_{PP}$ (57 Hz) coupling between the P(III) and P(V) nuclei. The P(V) centre, which is downfield from the P(III) centre and well insulated by substituent groups, shows little discernable change with time (higher field strength reveals a multiplicity compatible with the behavior of the P(III) centre)[1]. The P(III) resonance pattern transforms into three doublets (total integration equal to one phosphorus with *equivalent* coupling constants), and, with time most of the intensity grows into the upfield doublet. This final signal remained constant for over eight months in a sealed NMR tube. The evolution of the signals requires one week at ambient temperature at which time the ^{1}H-NMR resonance due to the methylene protons (3.09 ppm, $CDCl_3$ solution) has all but disappeared (Figure 3.2) and a signal at 7.24 ppm ($CHCl_3$) has appeared. The trimethylsilyl carbon (^{13}C-NMR spectrum) still displays phosphorus coupling proving the $P{=}N{-}SiMe_3$ linkage intact. The methylene carbon shows a very weak first order AMX pattern (residual proton species) overlying a broad featureless hump. The lack of a signal arising from the methylene unit is contrasted by the deuterium-NMR which displayed an intense broad resonance at 2.8 ppm in toluene solution (quadripolar broadening and unresolved coupling of ^{2}H to ^{31}P(III) and ^{31}P(V)). These observations demonstrate that the multiple signals in Figure 3.1 can be assigned to the non-deuterated, mono-deuterated, and doubly deuterated methylene backbone as outlined by Equation 3.1.

Equation 3.1.

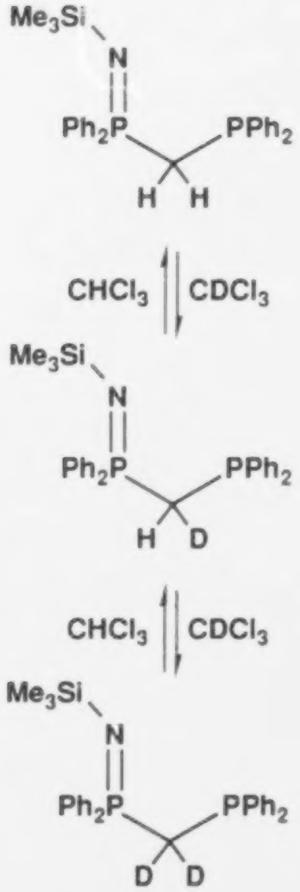

The observed changes in the P(III) chemical shift are approx. 21 Hz per deuterium while the P(V) chemical shift changes by approx. 3 Hz per deuterium substitution. The $^2J_{PP}$ coupling constants are 57.3, 56.6, and 57.3 Hz for the three isotopomers, respectively. Similarly, the phosphorus chemical shift of PH_3 changes by approx. 31 ± 1.5 Hz per deuterium substituted and the coupling constant (J_{PH}) is relatively unaffected[13]. For triphenylphosphine and triphenylphosphine oxide, replacement of all 15 protons for deuterium changes the chemical shift by 107.8 and 15 Hz, respectively[18].

In a separate experiment, 500 mg of **1** was refluxed in $CDCl_3$ for 24 hours. The solvent was then removed and the resulting oil analyzed by mass spectroscopy. The peaks for the parent ions, $M^+(H_2)$=(471) 52%, $M^+(HD)$=(472) 100%, $M^+(D_2)$=(473)

76%, clearly indicate a mixture of the three compounds shown in Equation 3.1 (addition of $CHCl_3$ reverses the process and the NMR signals evolve back to match the initial spectrum, Figure 3.3).

Mechanistically, several studies have revealed the salient factors involved in the deuterium exchange of the methylene protons of dppm derivatives with deuterochloroform. Chloroform[19] and the methylene protons of dppm[20] have large pKa values and oxidation of the phosphorus centres increases the acidity of the methylene protons[21], but it is the lability of the proton on chloroform in the presence of even trace amounts of water that provides the source of deuterium for the exchange. Furthermore, in order to replace both methylene protons by deuterium, the compound **1** must be capable of tautomerism. Phosphineamidines **3** are capable of tautomerism as are certain amine substituted Wittig reagents **4**[22]. Since the methylene protons of dppm do not undergo deuterium exchange in $CDCl_3$ solution, and since only one phosphorus centre with a double bond to nitrogen enables the exchange to occur, and since the rate of exchange appears to be proportional to the basicity of the nitrogen centre, increased nitrogen basicity must stabilize the tautomer **1'** in order to enhance the deuterium exchange[22]. In addition, β-keto phosphonium salts show significant stabilization of the enol tautomer when a second phosphonium group, capable of $p\pi$–$d\pi$ bonding, is introduced.[23] By analogy, the tautomer **1'** may also be somewhat stabilized by a $d\pi$–$p\pi$–$d\pi$ bonding interaction through the methylene backbone.

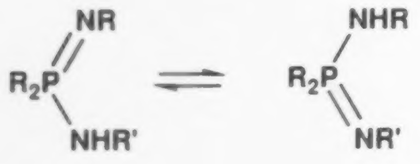

3

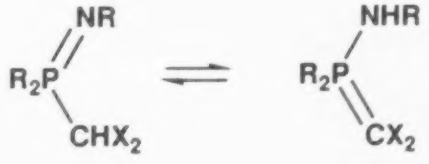

4

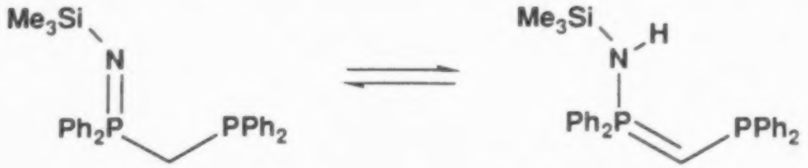

1 1'

This process does not require addition of base. The nitrogen atom supplies the necessary basicity to drive the enolization of **1** upon which the exchange is based. This basicity, combined with the acid dissociation of chloroform (catalyzed by trace moisture) provides a route for the exchange of the methylene protons of **1** for deuterium. Although there is no direct evidence for the tautomerism of **1**, the compound **2**, which can be considered as an isoelectronic analogue of acetylacetone (well known for tautomerism)[10], undergoes deuterium exchange with $CDCl_3$ even more rapidly than **1**, and the *N*-aryl derivatives of **2** (aryl = phenyl, *p*-tolyl and *p*-nitrophenyl) exchange methylene protons for deuterium in D_2O, CD_3OD and non-purified $CDCl_3$[16,24]. Furthermore, the deuterium exchange of the methylene protons of **1** with deuterobromoform (more acidic than chloroform) reaches equilibrium approximately five times faster than with deuterochloroform, reinforcing the acid-base chemistry of the mechanism. Finally, **1** does not undergo deuterium exchange with rigorously dried deuterated methylene chloride, but does with commercial deuterated methylene chloride. Additional compounds tested for the capacity to exchanging methylene protons with $CDCl_3$ are listed in Table 3.1.

Figure 3.1 Selected ^{31}P NMR spectra (81 MHz) demonstrating the evolution of the signals with time as the methylene protons are exchanged for deuterium (commercial $CDCl_3$ solution). The spectra were recorded over a 24 hour period in a sealed NMR tube and heated at approx. 45°C for 30 min. between spectra. This is not an accurate kinetic representation.

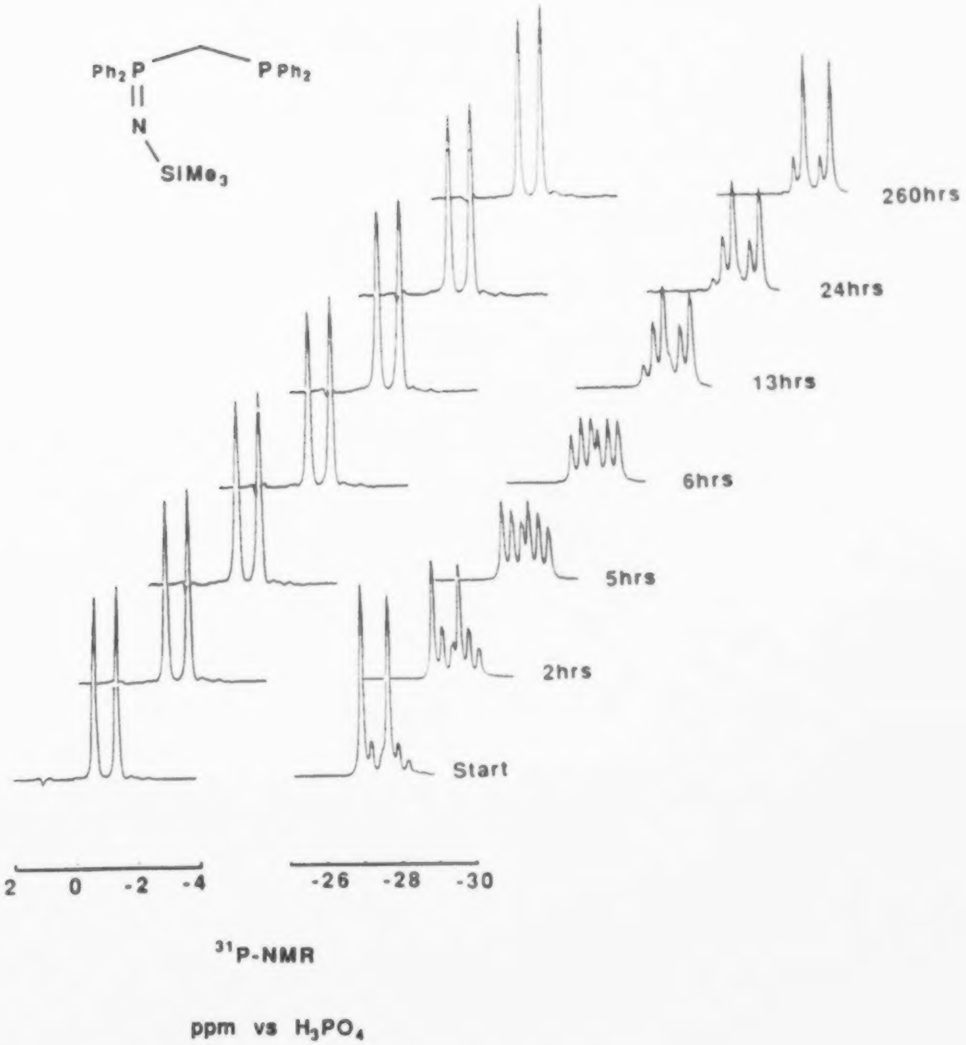

Figure 3.2 The ^{1}H NMR spectra (200 MHz) demonstrating the disappearing signals with time as the methylene protons are exchanged for deuterium ($CDBr_3$).

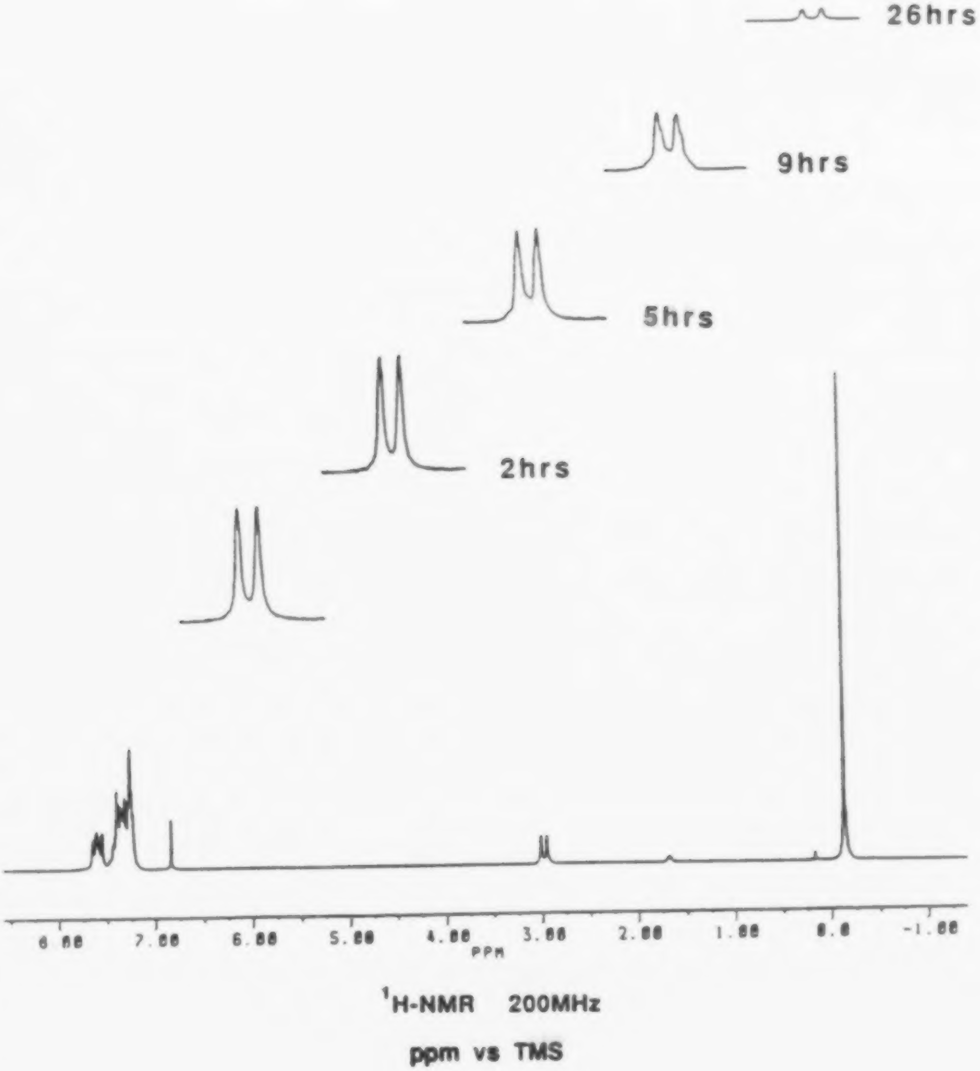

Figure 3.3 The ^{31}P NMR spectra (81 MHz) demonstrating the evolution of the P(III) signal with time as the methylene deuterons are exchange for protons ($CDCl_3/CHCl_3$).

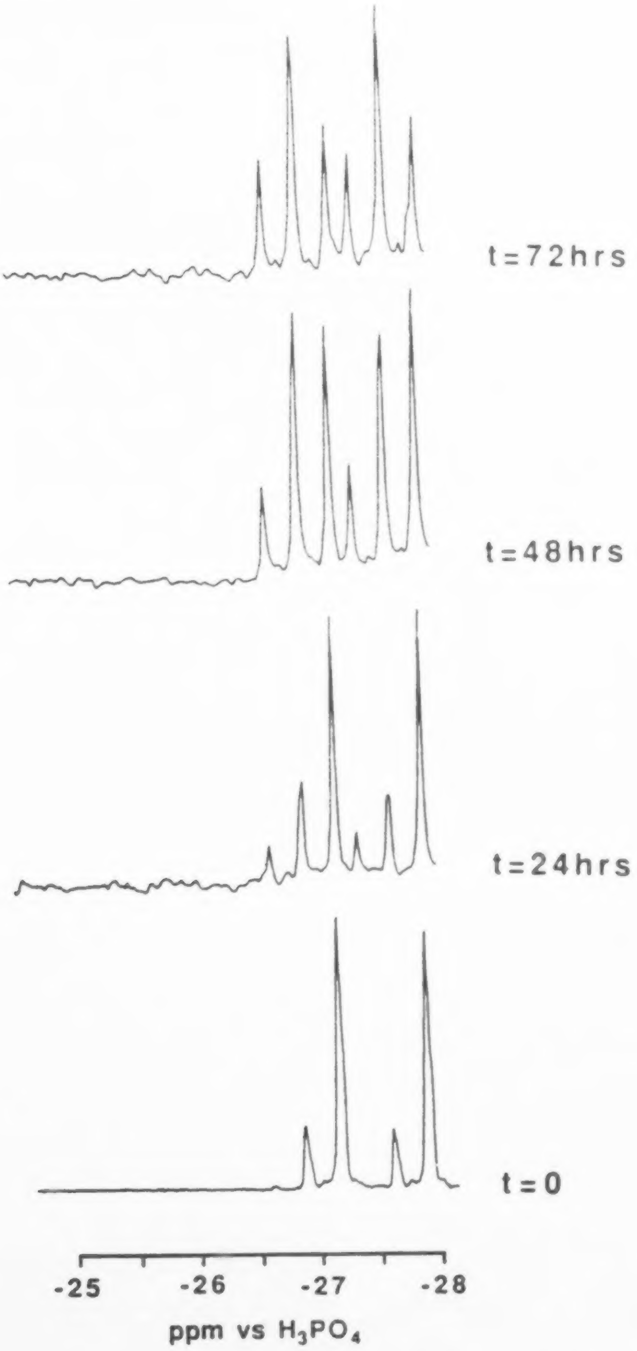

Table 3.1 Summary of compounds tested for deuterium exchange.

Compound	Solvent	Exchange	Reference
$Ph_2PCH_2PPh_2=N\text{-}SiMe_3$[!]	$CDCl_3$	Y	This work
	CD_2Cl_2	Y	" "
$Se=Ph_2PCH_2PPh_2=N\text{-}SiMe_3$[a]	$CDCl_3$	N	" "
$CH_2(PPh_2=N\text{-}SiMe_3)_2$	$CDCl_3$	Y	" "
$Ph_2PCH(Me)PPh_2=N\text{-}SiMe_3$[a]	$CDCl_3$	Y	" "
$Ph_2PCH_2PPh_2$	$CDCl_3$	N	" "
$Ph_2PCH_2PPh_2=N\text{-}C_6F_4CN$	$CDCl_3$	N	" "
$Ph_2PCH(Me)PPh_2=N\text{-}C_6F_4CN$	$CDCl_3$	N	" "
$Ph_2PCH_2PPh_2=N\text{-}CH_2Ph$[b]	$CDCl_3$	Y	" "
$Ph_2PCH(Me)PPh_2=N\text{-}CH_2Ph$[b]	$CDCl_3$	Y	" "
$Ph_2PCH_2CH_2PPh_2=N\text{-}SiMe_3$	$CDCl_3$	N	" "
$Me_3Si\text{-}N=Ph_2PCH_2CH_2PPh_2=N\text{-}SiMe_3$	$CDCl_3$	N	" "
$Ar\text{-}N=Ph_2PCH_2PPh_2=N\text{-}Ar$	$CDCl_3$	Y	16, 24
Ar = Ph, tolyl, 4-NO_2Ph	D_2O	Y	16, 24
	CD_3OD	Y	16, 24
$O=Ph_2PCH_2PPh_2=O$	$CDCl_3/D_2O$	N (decomp)	16

[!] Rate of exchange proportional to dryness of solvent. Dry CD_2Cl_2 does not exchange. $CDCl_3$ sample prepared with great care to avoid moisture and also containing hexamethyldisilazane to react with trace moisture did not exchange H/D after 4 months.

[a] Compound not isolated/unpublished result.

[b] Compound not isolated/H/D exchange finished in minutes, rate of exchange slightly greater than rate of decomposition.

3.3 Summary

This chapter describes a very important discovery. The observation that deuterochloroform will readily exchange deuterium for the methylene hydrogens of singly or doubly oxidized (with azides) dppm was not readily apparent. Furthermore, this process is catalyzed by minute traces of water due to the very fast exchange equilibrium between chloroform and water. The methylene protons and chloroform have similar pKa values and deuterium exchange readily occurs. In some cases, the exchange is complete in minutes leading to deceiving experimental results and false, but reasonable conclusions. Serendipidously, the compound **1** is an ideal model for demonstrating the deuterium isotope effects on phosphorus chemical shifts and coupling constants.

3.4 Experimental

Preparation of NMR samples.

Initially, samples were prepared with solvents dried by storage over molecular sieves and without concern for atmospheric moisture or traces of acid, alcohol and moisture (even on glass surfaces). In the extreme, in order to avoid moisture, NMR sample tubes were joined to 14/20 ground glass joints. The sample tubes were oven dried, cooled under vacuum, treated with hexamethyldisilazane and flame dried. A sample of **1** was introduced and rigorously dried solvent (distilled from hexamethyldisilazane) was transferred *in vacuo* and the tubes were flame sealed and stored in the dark.

3.5 References

1. K. V. Katti and R. G. Cavell. *Inorg. Chem.*, **28**, 413 (1989).
2. K. V. Katti, R. J. Batchelor, F. W. B. Einstein and R.G. Cavell. *Inorg. Chem.*, **29**, 808 (1990).
3. K. V. Katti and R. G. Cavell. *Organometallics*, **7**, 2236 (1988).
4. K. V. Katti and R. G. Cavell. *Organometallics*, **8**, 2147 (1989).
5. K. V. Katti and R. G. Cavell. *Inorg. Chem.*, **28**, 3033 (1989).
6. K. V. Katti and R. G. Cavell. *Phosphorus, Sulfur and Silicon*, **41**, 43 (1989).
7. K. V. Katti and R. G. Cavell. *Comments Inorg. Chem.*, **10**,53 (1990).
8. E. W. Abel and S. A. Mucklejohn. *Phosphorus and Sulfur*, **9**, 235 (1981).
9. H. Schmidbauer, G. A. Bowmaker, O. Kumberger, G. Müller and W. Wolfsberger. *Z. Naturforsch.*, **45b**, 476 (1990).
10. A. Streitweiser Jr. and C. H. Heathcock. "Introduction to Organic Chemistry" Macmillan Publishing Co., New York, 1981.
11. G. Atkinson, M. H. Fisher, D. Horley, A. T. Morse, R. S. Stuart, and E. Synnes. *Can. J. Chem.*, **43**, 1614 (1965); A. A. Al-Salem, H. D. Empsall, R. Markam, B. L. Shaw and B. Weeks. *J. C. S. Dalton*, 1972 (1979); A. B. Reitz and B. E. Maryanoff. *Synthetic Communications*. **13**, 845 (1983); B. Shaudret. *J. Organomet. Chem.*, **268**, C33 (1984); G. K. Anderson and R. J. Cross. *J. Chem. Soc., Chem. Commun.*, 1502 (1986).
12. C. J. Jameson. *Nuclear Magnetic Resonance*, **19**, 1 (1990)
13. A. K. Jameson and C. J. Jameson. *J. Mag. Res.* , **32**, 455 (1978).
14. R. Appel and I. Rupert. *Z. anorg. allg. Chem.*, **406**, 131 (1974).
15. R. T. Oakley. Ph.D. Dissertation, University of British Columbia, **1976.**
16. A. M. Aguiar, H. J. Aguiar and T. G. Archibald. *Tet. Lett.*, **27**, 3187 (1966).

17. J. Hine. "Divalent Carbon", The Ronald Press Co., p37-43 (1964); T. L. Gilcrist and C. W. Rees. "Carbenes, Nitrenes and Arynes", Nelson, p16-19 (1969); W. Kirmse. "Carbene Chemistry", Academic Press, p129-137 (1971).

18. A. R. Siedle and R. A. Newmark. *J. Am. Chem. Soc.*, **111**, 2058 (1989).

19. pK_a of $CHCl_3$=24. a) Z. Margolin and F. A. Long. *J. Am. Chem. Soc.*, **95**, 2757 (1973). B) A. C. Lin, Y. Chiang, D. B. Dahlberg and A. J. Kresge. *J. Am. Chem. Soc.*, **105**, 5380 (1983).

20. pK_a of methylene protons of dppm= approx. 30. F. G. Bordwell, W. S. Mathews and N. R. Vanier. *J. Am, Chem. Soc.*, **97**, 442 (1975).

21. Chem. Abs. **100** 174937j. M. I. Terkhova, N. G. Osipenko, N. A. Bandarenko, Yu. I. Sukhorukov, E. S. Petrov and E. N. Tsvetkov. *Zh. Obshch. Khim.*, **54**, 82 (1984).

22. Y. G. Gololobov, I. N. Zhmurova and K. F. Kasukhin. *Tetrahedron*. **37**, 437 (1981).

23. a) M. I. Kabatschnik. *Phosphorus*, **1**, 117 (1971).
b) T. A. Mastryukova, I. M. Alajeva, H. A. Suerbayev, YE. I. Matrosov and P. V. Petrovsky. *Phosphorus*, **1**, 159 (1971).

24. P. Imhoff, R. Van Asselt, C. J. Elsevier K. Vrieze, K. Goubitz, K. F. Van Malssen and C. H. Stam. *Phosphorus, Sulfur and Silicon*, **47**, 401 (1990).

Chapter Four

Oxidation of 1,2-Bis(diphenylphosphino)benzene with Azides

4.1 Introduction

Our initial investigations of the Staudinger reaction[1] with bisphosphines and the subsequent use of the reaction products as ligands for the preparation of transition metal compounds are summarized in chapter one (Schemes 1.2 and 1.3). The similar chemistry of 1,2-bis(diphenylphosphino)benzene (dppbz) is the focus of this chapter. A motivation for this study arises from the fact that the rigid phenyl ring joining the two phosphorus centres should fix the compound in a *cis* orientation and provide a system which could present some useful aspects for coordination to and reaction with transition metals. Our investigation of the mono-oxidation of dppbz was further prompted by the observation of multiple signals in the ^{31}P NMR spectrum of **1** (Chapter three, Deuterium Exchange) which were initially attributed to rotational isomerism. Furthermore the rigidity of the phenyl ring backbone should also block access to rotational isomers and absence of such isomerism would further implicate the flexible methylene backbone of **1** in the apparent isomerism. Alternatively, detection of isomers for this rigid backbone system would implicate a dynamic processinvolving the P=N-Si linkage.

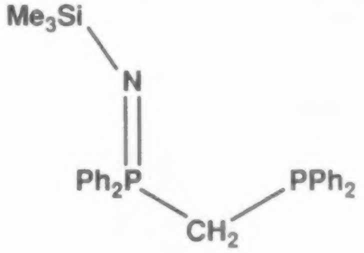

1

The first apparent result of the oxidation reaction of dppbz with trimethylsilyl azide showed that the monooxidized product had no P(III) multiple resonances in the ^{31}P NMR spectrum and that the system was rigid on the NMR timescale. The potential of a *cis* bisphosphine with a rigid backbone became further apparent with the discovery that the reaction with trimethylsilyl azide stops at the mono-oxidized product. This feature was further explored utilizing additional azides. The products of these reactions and representative rhodium complexes of the heterobifunctional products are the focus of this chapter.

1,2-Bis(diphenylphosphino)benzene.

There are a variety of synthetic methods described in the literature for the production of 1,2-bis(diphenylphosphino)benzene and related species. In most cases these syntheses suffer from low yields. The following examples illustrate the various methods for synthesizing dppbz derivatives.

McFarlane and McFarlane[2] report a 35% yield of dppbz from the reaction of *o*-difluorobenzene and sodium diphenylphosphide in liquid ammonia. Talay *et al.*[3], report that *o*-bromochlorobenzene can be converted to *o*-chlorophenyldiphenylphosphine *via* a Grignard reaction and subsequent reaction with sodium diphenylphosphide produces dppbz in 18% yield (Equation 4.1).

Equation 4.1.

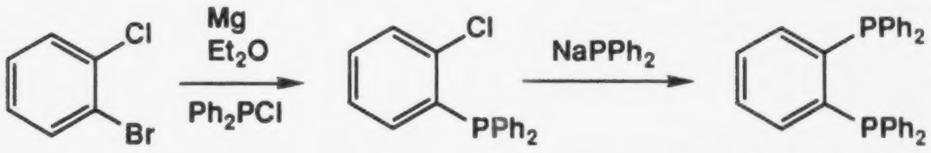

Utilizing the photolysis of $P(OMe)_3$ in the presence of *o*-dichlorobenzene, Kyba *et al.* [4] report a very versatile synthesis of dppbz derivatives with an overall yield of 37% depending upon the nature of the substituents on phosphorus (Scheme 4.1). The value of this route devolves from the variety of substituents that can be attached to the phosphorus atoms.

Scheme 4.1.

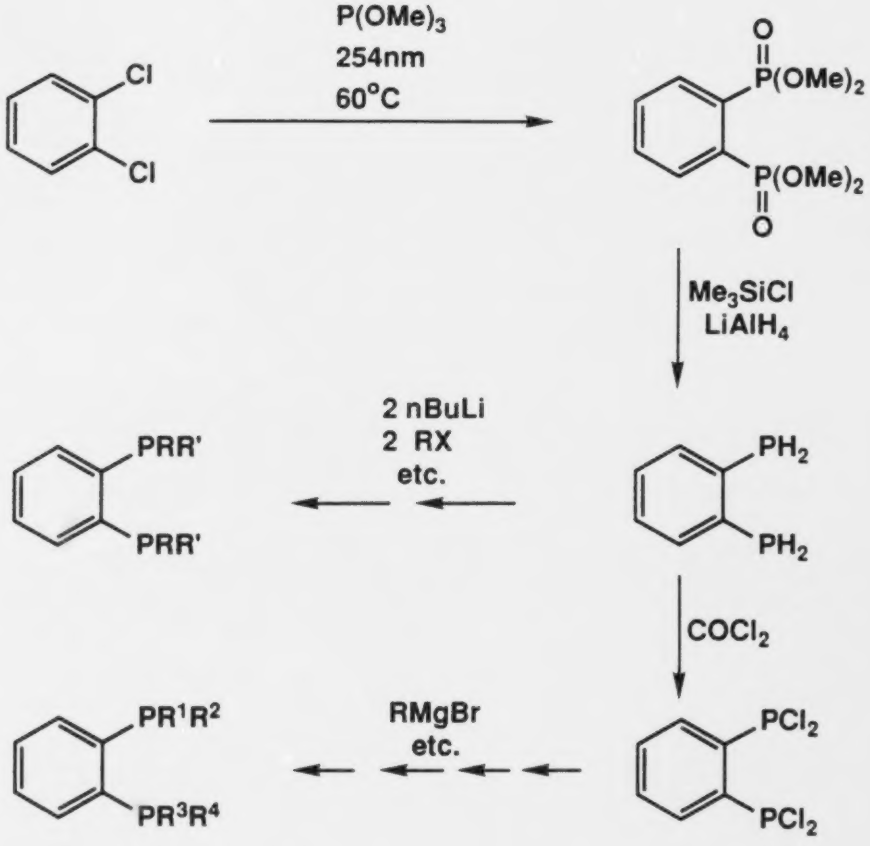
Cl
Cl
P(OMe)3
254nm
60°C
O
P(OMe)2
P(OMe)2
O
Me3SiCl
LiAlH4
PH2
PH2
2 nBuLi
2 RX
etc.
PRR'
PRR'
COCl2
PCl2
PCl2
RMgBr
etc.
PR1R2
PR3R4

Finally, Tunney and Stille[5] report the preparation of dppbz with an overall yield of 75% (Equation 4.2). In this reaction sequence, diphenyltrimethylsilylphosphine and 2-bromoiodobenzene are coupled in the presence of a palladium catalyst to produce 2-bromophenyldiphenylphosphine. Subsequent lithiation and reaction with chlorodiphenylphosphine produces dppbz. The higher yield, the milder reagents and the ease of synthesis of the starting materials makes this the synthetic method of choice.

Equation 4.2.

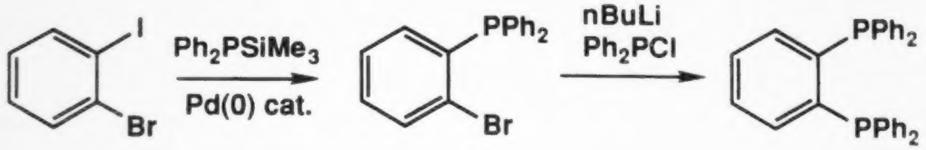

Applications of dppbz.

A variety of transition metal complexes utilizing dppbz are, of course, known. A few illustrative examples are listed below, as are a number of related heterodifunctional chelating ligands featuring a rigid benzene backbone.

Bakir *et al.*[6] report the reaction of $(nBu_4N)_2Re_2Cl_8$ with excess dppbz in refluxing nitriles (CH_3CN, EtCN, PhCN) for 18 to 100 hours produces *trans* - $ReCl_2(dppbz)_2$, **2** in approx. 40 % yields. The same reaction of the rhenium bromide salt with excess dppbz in EtCN for 17 hours affords the unusual compound **3** in 23 % yield. This purple, 18 electron species contains an imido ligand which is generated by the reduction of the nitrile. The potential application of this reaction in the catalytic conversion of nitriles to amines and *vice versa* is readily apparent[7].

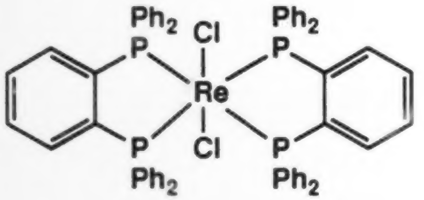

2

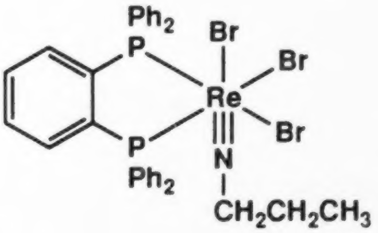

3

E. Hey[8] deprotonated 1,2-bisphosphinobenzene to produce the dilithiated dppbz derivative and subsequent reaction with zirconocene dichloride yielded the bisphosphido metallocycle **4**. This metallocycle can also be prepared by direct reaction of the phosphine with biscyclopentadienyldimethylzirconium (Scheme 4.2).

Scheme 4.2

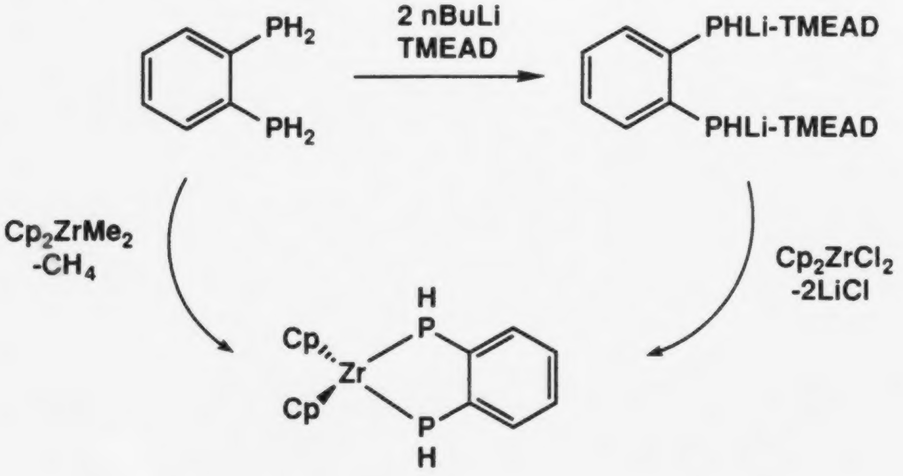

PH2
PH2
2 nBuLi
TMEAD
PHLi-TMEAD
PHLi-TMEAD
Cp2ZrMe2
-CH4
Cp2ZrCl2
-2LiCl
Cp
Cp
Zr
H
P
P
H

4

In a series of papers, Wild *et al.* [9], studied the compound **5** as a template for stereoselective synthesis of coordinated phosphines or arsines.

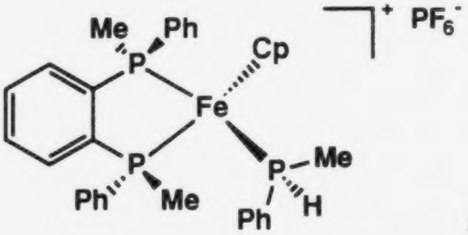

Me
Ph
P
Cp
Fe
+
PF6-
P
Ph
Me
P
Me
H
Ph

5

Deprotonation of the coordinated methylphenylphosphine at -90°C followed by either protonation or reaction with ethyliodide affords the R* or S* product phosphine complexes (respectively) in >99% diastereoisomeric excess. It is likely that at -90°C the C_2 symmetry of the dppbz ligand is capable of restricting the rotation of the coordinated phosphine resulting in a fixed template which can then direct the steroechemistry of the subsequent chemistry.

An interesting series of compounds and metal complexes have been prepared and characterized by Grobe and coworkers[10]. In these compounds chelating ligands of larger size have been prepared with a dimethylsilylene unit between the benzene backbone and the pnictogen centre (Equation 4.3).

Equation 4.3

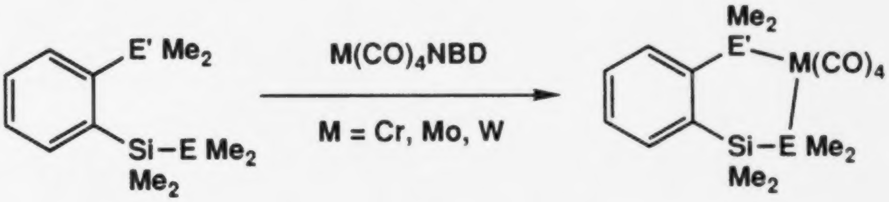

E' = P, As
E = N, P, As

Bart van Oort *et al.*[11], have prepared a very unusual and robust heterotrifunctional ligand. The neutral ligand is capable of complexing one metal centre [($Mo(CO)_4$)] in a chelating fashion and a second metal [($Mo(CO)_5$)] in a monodentate fashion. The deprotonation of the ligand nitrogen allows the chelation of both metal centres [($Mo(CO)_4$)]. Oxidation with a halide source (CCl_4, Br_2, I_2) eliminates carbon monoxide and X^- to produce **6**.

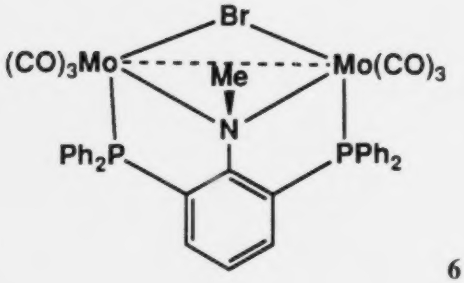

6

Other heterodifunctional ligands have been studied by Rauchfuss and coworkers[12]. In this case the oxidative addition of *o*-substituted triarylphosphines (**7** and **8**) was examined with Ir(CO)Cl$(PPh_3)_2$ and Ir(CO)Cl$(AsPh_3)_2$. For the triphenylphosphine complex the aldehyde substituted phosphine formed a stable six coordinate iridium(III) hydride species where as the other derivatives established equilibria between the iridium(I) complex and the iridium(III) hydride complex.

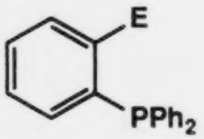

E = OH, CH_2OH, COOH,
CHO (+ $AsPPh_2$ der.)

7

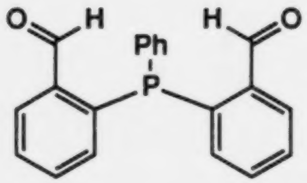

8

Of particular interest is the utilization of rigid heterodifunctional chelating ligands with a benzene backbone in asymmetric catalysis. Kreuzfeld *et al.*[13] studied the asymmetric hydrosilation of acetophenone with diphenylsilane. Utilizing a variety of chiral ligands **9** with rhodium, iridium, palladium and platinum, high chemical yields of the product alcohol were obtained. In some cases optical yields of 50% (e.e.) were also obtained.

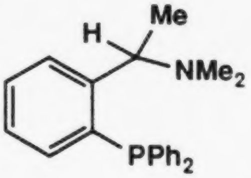

9

As a final example, structural studies on $RuCl_2(dppbz)_2$ derivatives led S. R. Hall *et al.*[14] to determine the single crystal X-ray structure of a minor reaction biproduct **10**. This is the only literature example of a metal complex of the monoxide of dppbz.

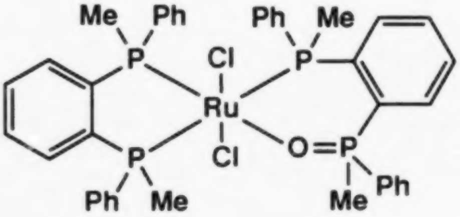

10

4.2 Results and Discussion.

Synthesis

The synthetic method of choice for the required starting material, 1,2-bis(diphenylphosphino)benzene (dppbz), is essentially that reported by Tunney and Stille[5]. Minor modifications in the synthetic procedure (especially purification steps) are detailed in the experimental section. Although the yields were lower in this work than those reported by Tunney and Stille, residues from each step were saved and recycled (when possible) in subsequent syntheses of dppbz.

One comment of caution is that diphenyltrimethylsilylphosphine, which is extremely noxious, is deceptively pyrophoric with an indeterminate induction period. The phosphine can be pipetted and weighed into an open argon filled flask, but, contact with paper or tissue will invariably cause a fire. *This might not occur for several minutes!*

Scheme 4.3

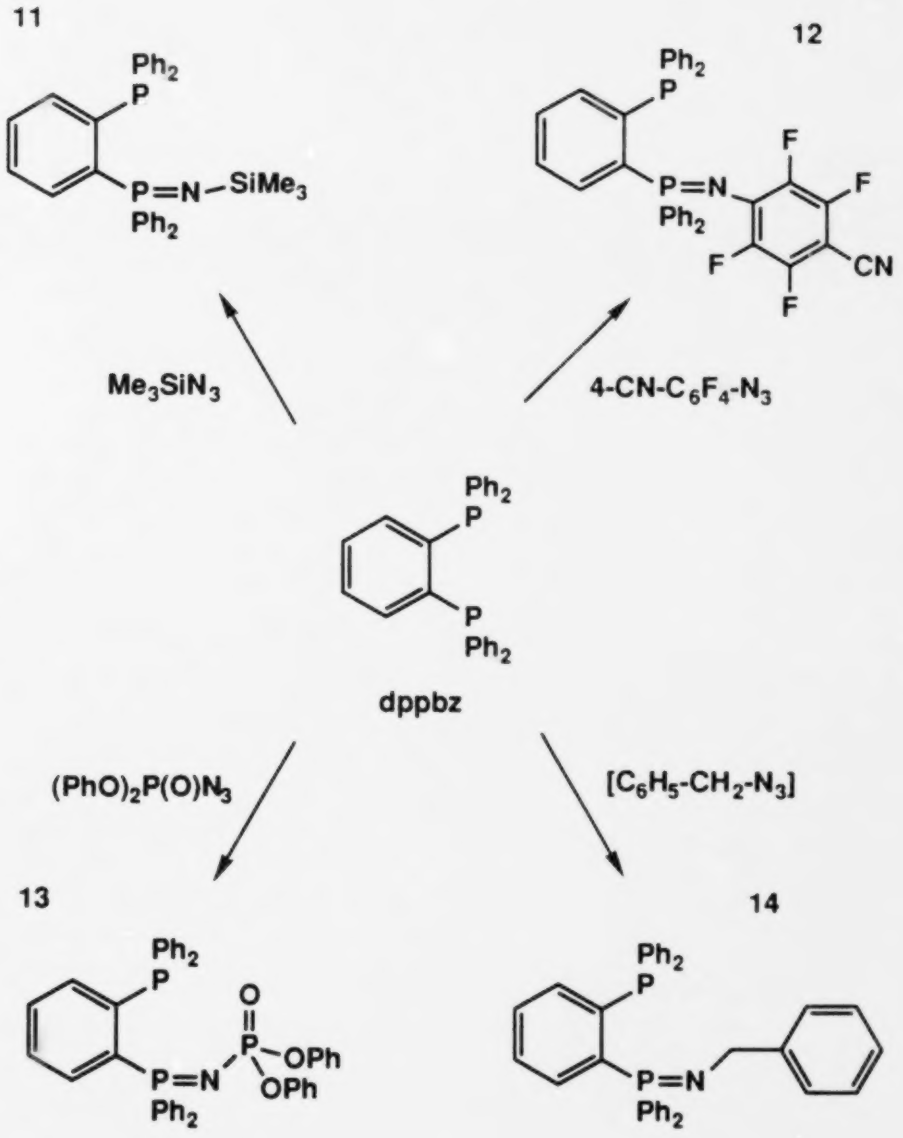
11
12
Me$_3$SiN$_3$
4-CN-C$_6$F$_4$-N$_3$
dppbz
(PhO)$_2$P(O)N$_3$
[C$_6$H$_5$-CH$_2$-N$_3$]
13
14

Reaction of dppbz with azides.

The reactions of dppbz with azides are summarized in Scheme 4.3. The preferred synthetic strategy for the reaction of bisphosphines with trimethylsilyl azide is to conduct the reaction in the absence of solvent at temperatures exceeding the melting point of the bisphosphine utilizing a very efficient reflux condenser. This method works well for dppm, however, the melting temperature of dppbz is 100°C higher than the boiling point of trimethylsilyl azide (m.p. dppbz = 179-181°C, b.p. Me_3SiN_3 = 95-97°C[15]). Under these conditions the azide is pyrolyzed before the reagents can form a homogeneous melt. Therefore, a high boiling solvent such as toluene must be used to carry out the reaction. Although high temperatures are required for reaction of trimethylsilyl azide with phosphines, in this case, the azide will also react with the solvent. In order to ensure complete reaction, careful monitoring of the extent of reaction by ^{31}P NMR spectroscopy and the addition of more azide was necessary.

Unlike the bisphosphines with flexible backbones (e.g. dppm, discussed in chapter seven) dppbz cannot be doubly oxidized with trimethylsilyl azide. Even prolonged reflux of concentrated toluene solutions of dppbz with a huge excess of azide failed to show any evidence of bis-oxidation. Presumably the failure to induce reaction at the second phosphine centre is a direct result of steric crowding due to the fixed *cis* configuration of the phosphorus centres. The bulk of the azide substituent is also significant as both H_2O_2 and S_8 will doubly oxidize dppbz. The mechanism of the reaction between a phosphine and an azide (Staudinger reaction) is still unclear, however, ^{15}N labelling experiments reveal that the alpha nitrogen is retained in the product phosphinimine linkage[16]. Whether the reaction mechanism proceeds *via* a cyclic intermediate or *via* attack of the alpha nitrogen on the phosphine (Scheme 1.4, Chapter One), steric crowding will inhibit the reaction, the second oxidation more so than the first.

Reaction of dppbz with several other azides proceeds in a straightforward fashion with reactions occuring at or below room temperature. In general, treatment of a bisphosphine with *p*-cyanotetrafluorophenyl azide at -78°C induces a colour change in the reaction solution suggesting that the reaction is occuring at low temperature, however, slow warming to room temperature and overnight reactions were standard procedure so the actual temperature at which the reaction begins is uncertain. The reaction of diphenylphosphinic azide and benzyl azide with dppbz also proceeded in a similar fashion. The products of these reactions have very different physical characteristics. While **12** is highly crystalline with limited solubility in polar solvents and insoluble in nonpolar solvents, the benzyl **14** and phosphinic **13** derivatives are highly soluble materials. Indeed, while **14** can be purified by hexane extraction followed by recrystallization from acetonitrile, the phosphinic derivative **13** produces viscous oils from most recrystallizing solvents. The best method for the isolation of the phosphinic derivative was found to be simply the use of precise stoichiometry, careful control of reaction conditions and upon completion of the reaction, removal of the solvent *in vacuo* . For the phosphinic derivative only, this method produced an amorphous powder of sufficient purity for subsequent chemistry.

Spectroscopy

Multinuclear NMR spectroscopy has been used extensively in the characterization of the products of reaction between dppbz and azides. The asymmetry of the reaction products produces an AX spin system which is easily monitored by ^{31}P NMR spectroscopy. Table 4.1 contains a summary of the ^{31}P NMR data for the 1-diphenylphosphinimine-2-diphenylphosphino-benzene derivatives. The starting material, dppbz, displays a single resonance in the ^{31}P NMR spectrum at -13.6 ppm (Lit. -14.2 ppm[5]). Oxidation of one phosphine centre produces a large chemical shift change for the P(V) centre (deshielded by 20 to 60 ppm) and leaving the chemical shift of the P(III) centre relatively unaffected.

For the *N*-trimethylsilyl derivative **11**, ^{31}P NMR spectroscopy clearly identifies the AX spin system [P(III)=-14.8 ppm, P(V)=1.2 ppm, $^{3}J_{PP}$=17.8 Hz]. Proton NMR spectroscopy identifies the presence of one trimethylsilyl group with a single line resonance at 0.04 ppm. The ^{13}C and ^{29}Si NMR spectra clearly identify the P=N-Si linkage through coupling to the phosphorus nucleus with chemical shifts of 5.6 ppm and -12.1 ppm and coupling constants $^{3}J_{CP}$=3.0 Hz and $^{2}J_{SiP}$=20.8 Hz respectively.

NMR tube reactions on **11** were carried out in order to establish the ^{31}P NMR chemical shifts of hydrolysis and oxidation products. The addition of five drops of methanol to a NMR sample of *N*-trimethylsilyl dppbzn immediately produced a new AX spectrum assigned to the protonated phosphinimine derivative **15** (P(III)=-16.3 ppm, P(V)=27.0PPm, $^{3}J_{PP}$=26.0 Hz). The reaction of **11** with a small amount of water in toluene solution for five days produced the ^{31}P NMR spectrum tentatively assigned to the mono-oxide of dppbz **16** (P(III)=-13.8 ppm, P(V)=30.1 ppm, $^{3}J_{PP}$=14.9 Hz). In addition, the 'ylidic' phosphinimine linkage undergoes Wittig-like reactions with benzaldehyde to produce **16** and *N*-trimethylsilyl-benzalimine. Further reactions of dppbz with excess H_2O_2 or sulphur produced the corresponding doubly oxidized dppbz derivatives, **17** and **18**, with ^{31}P NMR chemical shifts of 34.1 ppm and 47.5 ppm.

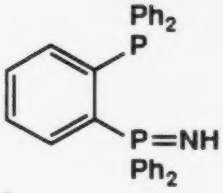

15

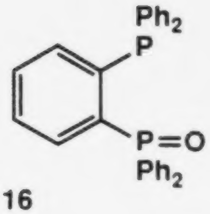

16

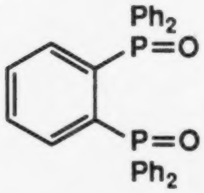

17

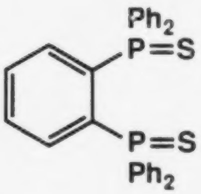

18

The reaction of dppbz with *p*-cyanotetrafluorophenyl azide proceeds cleanly to yield the mono-oxidized product **12**. This compound is clearly identified by ^{31}P NMR spectroscopy (P(III)=-15.9 ppm, P(V)=13.8 ppm, $^{3}J_{PP}$=21.0 Hz) and, in addition, small phosphorus-fluorine coupling is observed for the P(V) resonance, $^{4}J_{PF}$=4.5 Hz.

The reaction of diphenylphosphinic azide with dppbz proceed cleanly to yield a compound with three distinct phosphorus centres **13**. Phosphorus NMR spectroscopy detected the expected AMX spin system (P(III)=-15.9 ppm, P(V)=13.8 ppm, P(O)=-8.9 ppm, $^{2}J_{PP}$=36.2 Hz, $^{3}J_{PP}$=23.6 ppm). For this compound, ^{1}H and ^{13}C NMR are less informative being restricted to aromatic resonances.

The final azide investigated in this series was benzyl azide. This azide was prepared *in situ* by combining benzylbromide with amberlite ion exchange resin that had been treated with sodium azide[17]. A five fold excess of the ion exchange resin (approx. 2.55 mmol azide/g) with benzylbromide, in a minimum of methylene chloride, was stirred for 24 hours. The resin was filtered, washed with methylene chloride, and the resulting solution added directly to a methylene chloride solution of dppbz. The oily residue from this reaction was extracted with hexane and the hexane soluble material was recrystallized from acetonitrile to yield **14**. (P(III)=-13.9 ppm, P(V)=10.3 ppm, $^3J_{PP}$=15.0 Hz). For this derivative, the benzyl protons are clearly identified by ^{1}H NMR spectroscopy (4.5 ppm, $^3J_{PP}$=17 Hz).

The above examples **11**, **12**, **13**, and **14**, as characterized by multinuclear NMR spectroscopy, clearly demonstrate the utility of rigid ligand backbone in these reactions. The production of mono-oxidized dppbz derivatives proceeds cleanly, in good yields, without the complicating production of further reaction products. The rigid backbone between the phosphorus centres fixes the conformation of the bisphosphine and the phosphorus centres are sterically crowded leading to cleaner reactions with azides.

Table 4.1 ^{31}P NMR spectroscopy data for the ligands.

ligand	**$^{31}P(III)$ ppm**	**$^{31}P(V)$ ppm**	**$^{3}J_{PP}$ Hz**
dppbz	-13.6		
11	-14.8	1.2	17.8
12[a]	-15.9	13.8	21.0
13[b]	-15.9	13.8	23.6
14	-13.9	10.3	15.0
15[c]	-16.3	27.0	26.0
16[c]	-13.8	30.1	14.9
17[c]		34.1	
18[c]		47.5	

[a] $^{4}J_{PF}$=4.5 Hz, [b] Phosphinic δ=-8.9 ppm, $^{2}J_{PP}$=36.2 Hz, [c] not isolated.

X-ray Crystallography of 11.

An X-ray structural analysis of **11** was done by Dr. B. D. Santarsiero of the University of Alberta Structure Determination Laboratory[18] and was prompted by the scarcity of structural information on P=N-Si linkages and the unique nature of this compound to resist double oxidation by azides. The experimental details (Table A.3) are tabulated in the appendix. The ORTEP representation is shown in Figure 4.1. The rigid backbone, P1-C1-C2-P2, is essentially planar (maximum displacement from plane 0.04Å), and the phosphorus-nitrogen double bond forms a dihedral angle of 60^0 from this plane. The lone pair of electrons on the phosphorus and nitrogen atoms extend in an overlapping fashion into the open mouth of the ligand and suggest a promising chelating ability. Furthermore, the bulk of the $SiMe_3$ group and the disposition of the electron pairs on phosphorus and nitrogen indicate reasons for the resistance of **11** to undergo further oxidation with a second mole of azide. The rigid backbone of **11** prevents the relief of steric congestion through bond rotation, and thus the formation of a second phosphazide intermediate is strongly inhibited even under strenuous conditions. The P=N and N-Si bond lengths, 1.529(5)Å and 1.672(5)Å, are similar to those found for $Me_3P{=}N{-}SiMe_3$[19], 1.542(5)Å and 1.705(5)Å, and $Ph_2PCH_2P(Ph_2){=}N{-}SiMe_3$[20], 1.529(3)Å and 1.668(3)Å. The P=N-Si bond angles are large, *c.f.* 152.7(3)° for **11**, 150.2(2)° for $Ph_2PCH_2P(Ph_2){=}N{-}SiMe_3$ and 144.6(1.1)° for $Me_3P{=}N{-}SiMe_3$. Indeed the P=N-Si angle in these molecules is more closely reminescent of the near linear N-trimethylsilyl-imido-metal systems (*e.g.*, $Cl_3V{=}N{-}SiMe_3$, <V=N-Si=177.5(1)°)[21] rather than the P=N-C systems in which the nitrogen atom adopts the more classical sp^2 hybridized geometry (*e.g.*, $Ph_2FP{=}NMe$, <P=N-C =119°)[22]. Upon coordination, there is a decrease in the P=N-Si angle (to 127.0(2)°) in $[Ph_3P{=}N(SiMe_3)CuCl_2]$ and a lengthening of the P=N and N-Si bonds (to 1.598(3)Å and 1.751(3)Å)[23]. These results demonstrate the contribution of the nitrogen lone pair electrons to the stabilization of the large P=N-Si angle.

Theoretical calculations by Wheeler *et al.* for phosphazene systems[24], and our own *ab initio* studies on the models $H_3P=N-SiH_3$ and $H_3P-N-PH_3^+$, reveal pairs of orthogonal, high-lying occupied molecular orbitals localized on nitrogen with significant d-orbital contributions from phosphorus and silicon[25]. One of these orbitals represents the phosphorus-nitrogen double bond, and the other orbital represents the diffusion of the nitrogen lone pair of electrons into the more electropositive phosphorus and silicon centres. This produces strong, yet hydrolytically unstable, bonding in the P=N-Si linkage.

This view of the bonding in the P=N-Si unit is in agreement with the photoelectron spectroscopic studies of $Ph_3P=N-SiMe_3$ and $Me_3P=N-SiMe_3$[26]. These two compounds display only one low ionization potential in the photoelectron spectrum corresponding to the two highest occupied molecular orbitals. In contrast, similar compounds with P=N-C or P=N-H linkages show two ionization potentials, one which can be attributed to the nitrogen lone pair of electrons and one which can be attributed to the P=N π bond.

Figure 4.1 The ORTEP representation of **11**. Structure courtesy of Dr. B. D. Santarsiero, Structure Determination Laboratory, University of Alberta. (Unit cell coordinates, bond lengths and angles are tabulated in the appendix: Tables A.4, A.5, A.6)

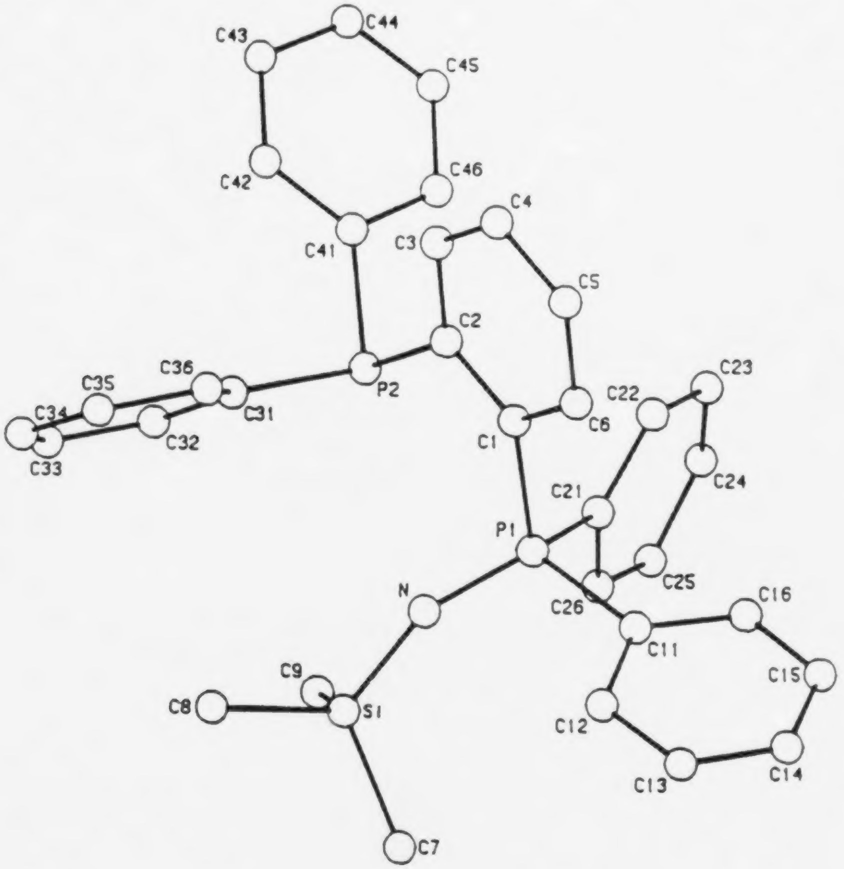
C43
C44
C45
C46
C42
C4
C41
C3
C5
C2
C36
C35
P2
C23
C22
C34
C31
C6
C32
C1
C33
C21
C24
P1
C25
N
C26
C16
C11
C9
C15
C8
SI
C12
C13
C14
C7

Complexes with $[Rh(CO)_2Cl]_2$

Synthesis

In order to establish the chelating ability of the ligands, representative rhodium complexes were prepared from $[Rh(CO)_2Cl]_2$. This is an ideal reagent for this purpose for several reasons. The rhodium nucleus posesses a spin of 1/2 allowing decisive interpretation of multinuclear NMR spectra to quickly identify reaction products through highly characteristic coupling constants. Complexation reactions proceed in a straight forward manner with the only biproduct being carbon monoxide gas. This allows the isolation of essentially analytically pure metal complexes in quantitative yield simply by removing the reaction solvent. All complexation reactions were found to proceed cleanly as monitored by ^{31}P NMR spectroscopy.

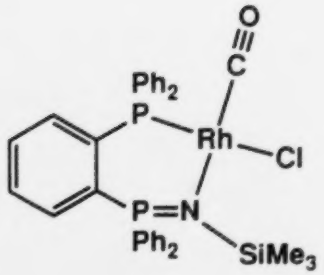
O
C
Ph2
P
Rh
Cl
P=N
Ph2
SiMe3

19

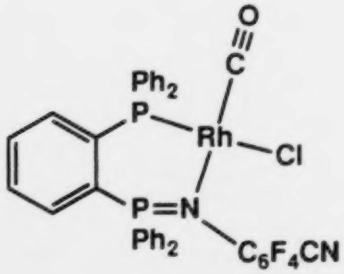
O
C
Ph2
P
Rh
Cl
P=N
Ph2
C6F4CN

20

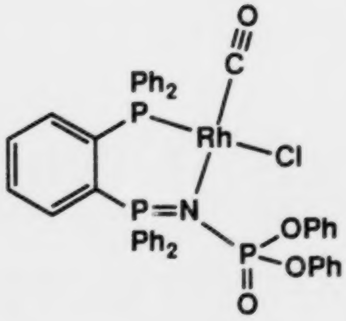
O
C
Ph2
P
Rh
Cl
P=N
Ph2
P
OPh
OPh
O

21

Spectroscopy

Complexation of **11**, **12** and **13** with $[Rh(CO)_2Cl]_2$ produces the corresponding complexes **19** ($SiMe_3$), **20** (4-CN-C_6F_4) and **21** [$P(=O)(OPh)_2$]. The ^{31}P NMR and selected infrared spectroscopy data for these compounds are listed in Table 4.2.

The ^{31}P NMR spectrum of **19** is shown in Figure 4.2. The large coordination effect on the P(III) chemical shift (+55 ppm) and the large $^1J_{PRh}$ coupling constant associated with that signal (175.2 Hz) clearly identifies the coordinated P(III) resonance. Likewise, the smaller change in the P(V) chemical shift (+19 ppm) and the presence of a small $^2J_{PRh}$ coupling constant (1.9 Hz) demonstrates chelate formation. Proton (-0.29 ppm), ^{13}C (5.6 ppm, $^3J_{CP}$=5.6 Hz) and ^{29}Si (6.6 ppm, $^2J_{SiP}$=5 Hz) NMR spectroscopy all demonstrate that the P=N-Si linkage is intact. Infrared spectroscopy recorded an intense absorption at 1980 cm^{-1} attributed to a single carbonyl on the rhodium centre, and in the mass spectrum an intense signal was detected at mass number 671 (87.5%), assigned to loss of carbon monoxide from the parent ion.

In a similar fashion, the complex **20** displays the same characteristic multinuclear NMR signals. The P(III) chemical shift and coupling constants (36.5 ppm, $^1J_{PRh}$=169.6 Hz, $^3J_{PP}$=27.9 Hz) are very similar, however, the broad P(V) signal is not as well resolved (27.8 ppm) masking additional structural information from long range fluorine and rhodium coupling constants. The poor solubility of this complex resulted in limited detection of aromatic ^{13}C NMR signals and ^{19}F NMR spectroscopy revealed two poorly resolved complex multiplets. Infrared spectroscopy detected the strong carbonyl absorption at 1986 cm^{-1} for **20**, similar to **19** (1980 cm^{-1}), suggesting similar stereochemistry for the rhodium centre.

The final rhodium complex of the diphenylphosphinic derivative **21** also displays characteristic spectroscopic features as the previous two examples, but, the incorporation of an additional phosphorus centre produces a more complicated ^{31}P NMR spectrum. The deshielded P(III) resonance is clearly identified by the large rhodium coupling constant (50 ppm, $^1J_{PRh}$=170.6 Hz, $^3J_{PP}$=20.1 Hz). The middle P(V) centre (40.5 ppm) appears as an overlapping doublet of doublets due to similar coupling to the terminal phosphinic group (7.3 ppm, $^2J_{PP}$=18.5 Hz). The greater solubility of the complex enabled the detection of the rhodium carbonyl (I.R.:ν(CO)=1986 cm^{-1}) in the ^{13}C NMR spectrum (185.9 ppm, $^1J_{CRh}$=78.5 Hz, $^2J_{CP}$=16.2 Hz). The coupling constants are in the expected range[27] for a carbonyl is cis to the P(III) centre on rhodium and the similar infrared stretching frequency for the carbonyl suggests the same steroechemistry prevails for all three complexes.

Figure 4.2 The ^{31}P NMR spectrum of **19** (161 MHz, CD_2Cl_2).

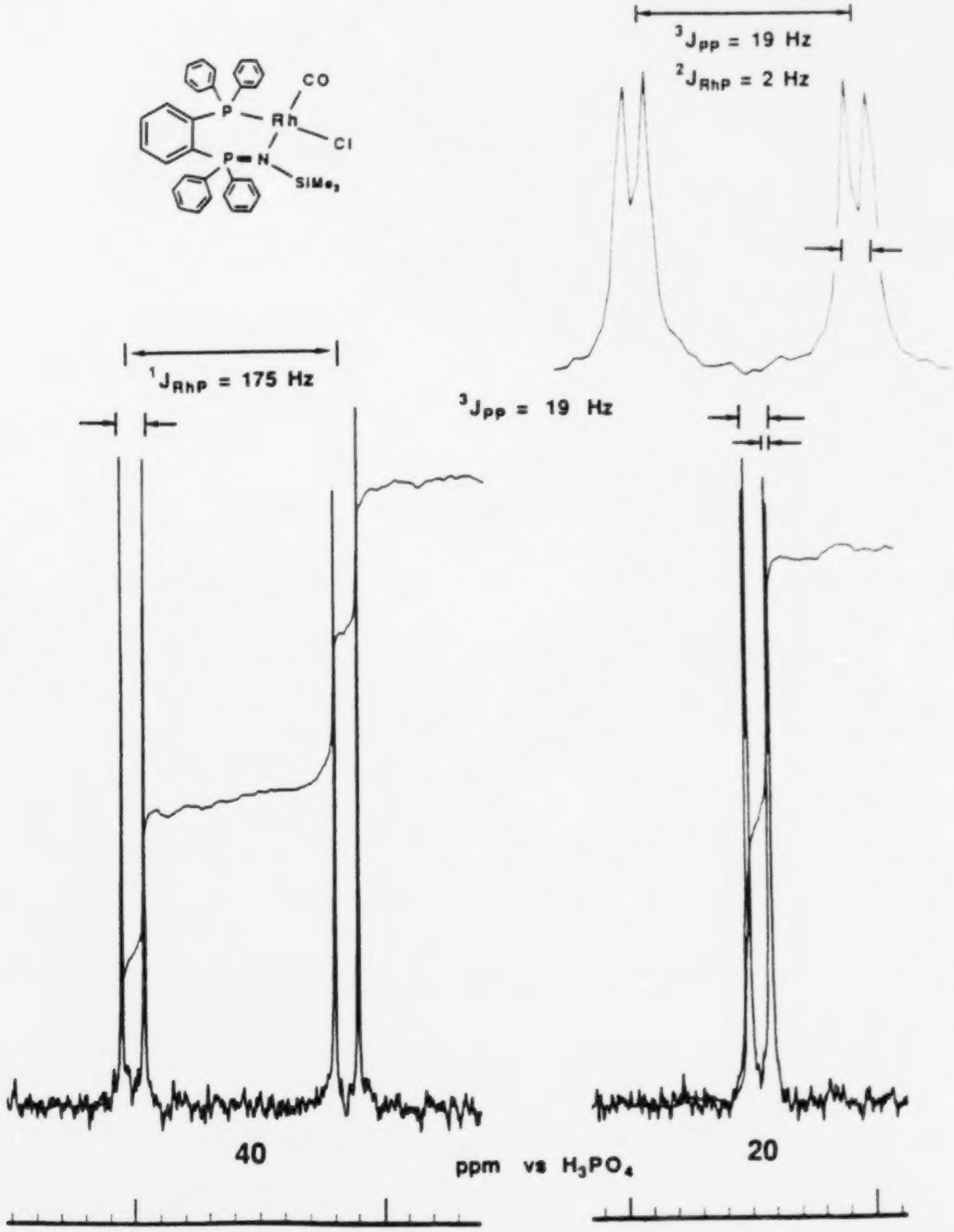

Table 4.2. Selected ^{31}P NMR and I.R. data[a] for the rhodium complexes.

Complex	**δ P(III)** ppm	**$^1J_{PRh}$** Hz	**$^3J_{PP}$** Hz	**δ P(V)[b]** ppm	**ν(CO)** cm^{-1}
19	40.45 dd	175.2	19.1	20.2 dd[a]	1980
20	36.52 dd	169.6	27.9	27.8 d	1986
21[c]	50.0 dd	170.6	20.1	40.5 't'	1986

[a] dd = doublet of doublets, d = doublet, 't' = triplet (overlapping doublet of doublets)

[b] $^2J_{PRh}$ = 1.9 Hz

[c] P(O)(OPh)$_2$ δ 7.3 ppm, $^2J_{PP}$ = 18.5 Hz

X-ray Crystallography of 19.

An X-ray structural analysis of **19** was done by Dr. B. D. Santarsiero of the University of Alberta Structure Determination Laboratory[28].

The stereochemistry of the rhodium centre in complex **19** and the effect of coordination upon the P=N-Si linkage was clearly established by a single crystal X-ray structure determination. The experimental details (Table A.7) are tabulated in the appendix. The ORTEP representation is shown in Figure 4.3. The rhodium centre is square planar with the carbonyl ligand *cis* to the P(III) centre as anticipated from ^{13}C NMR spectroscopy on the N-diphenyl-phosphinic derivative.

The overall structure of the ligand is unchanged with the exception of the P=N-Si unit. The P1-C1-C2-P2 backbone is planar (maximum deviation 0.15Å). The P=N-Si linkage forms a plane with a dihedral angle of 58.8° above the P1-C1-C2-P2 plane and the plane defined by the four atoms joined to the rhodium centre defines a dihedral angle of 43.5° below the P1-C1-C2-P2 plane. The six membered heteroatom ring formed from these planar units is highly distorted (see Figure 4.3).

A comparison of bond lengths about the rhodium centre and the carbonyl infrared stretching frequencies is summarized in Table 4.3. Although the compounds listed in the table are not all chelate complexes of the same ring size as **19**, the bond lengths are reasonable except for the rhodium-carbonyl linkage. The Rh-C bond is longer by approx. 0.1Å and C-O bond is shorter by 0.1Å suggesting that there is an unusual difference in this compound compared to the others (**22**-**27**) listed in Table 4.3.

Figure 4.3 The ORTEP representation of **19** (two views). Structure courtesy of Dr. B. D. Santarsiero, Structure Determination Laboratory, University of Alberta. (Unit cell coordinates, Bond lengths and angles are tabulated in the appendix: Tables A.8, A.9, A.10)

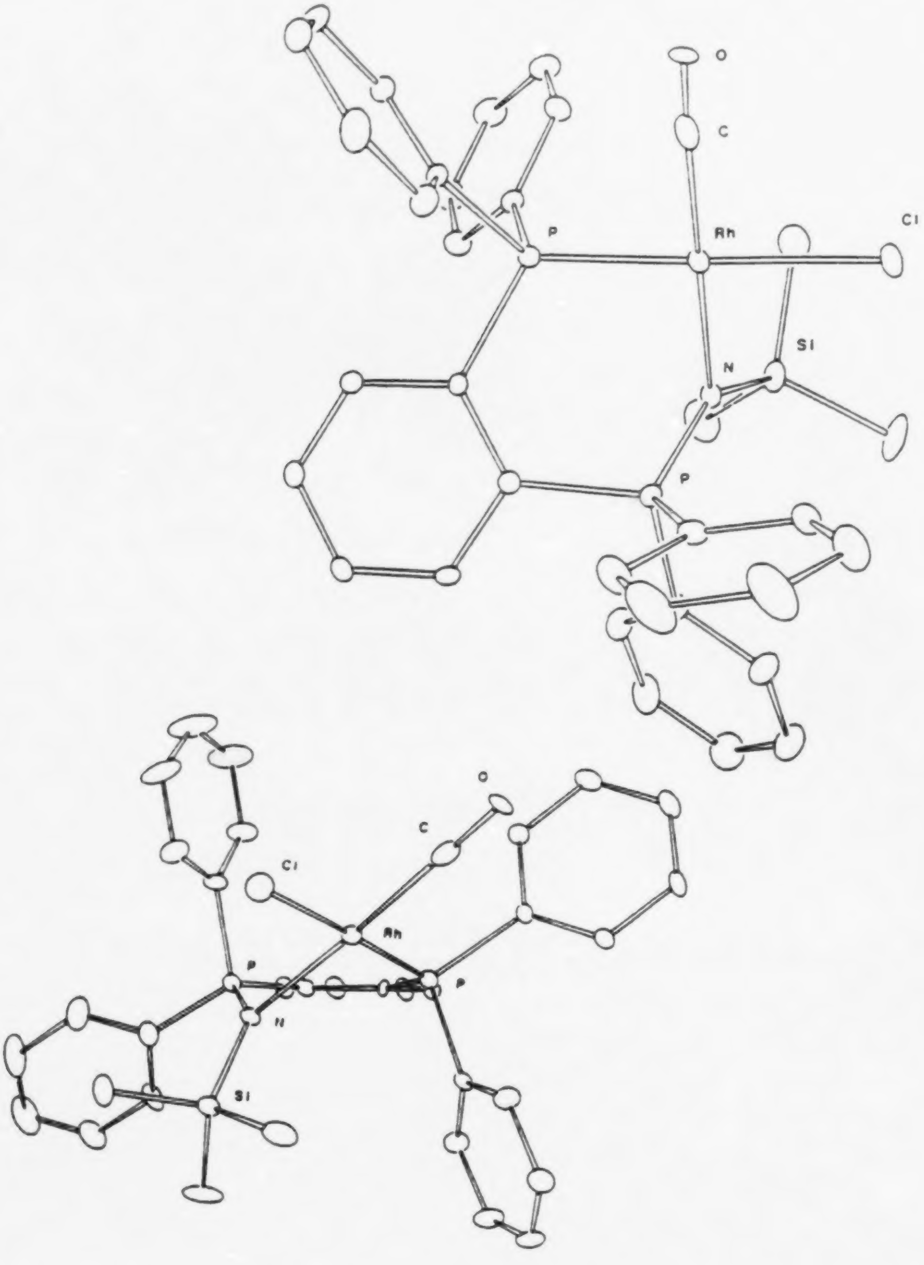

A closer examination of Figure 4.3 reveals the source of the bond length anomaly. The ellipsoid representing the carbonyl carbon is elongated and oriented along the rhodium-carbonyl linkage. The structure is disordered.

A disordered structure of this type is not uncommon. Indeed, a disorder of exactly this type led to the mistaken belief in 'bond-stretch-isomers'[29]. Bond stretch isomerism was the term coined to explain the long molybdenum-oxygen bond length [1.803(11)Å] observed for the 'green' form of *cis-mer*-$MoOCl_2(PR_3)_3$[30]. The 'blue' form of *cis-mer*-$MoOCl_2(PR_3)_3$ possesses a Mo=O bond length of 1.676(7)Å[31]. The mistake which arose was caused by the co-crystallization of the yellow paramagnetic impurity, *mer* -$MoCl_3(PR_3)_3$, *that was isostructural in all features except for one substituent* [32]. This resulted in a final fully refined structure in which the oxygen atom was actually a composite of two different atoms (chlorine and oxygen) but refined as an average of the two. Indeed, a Mo=O bond length of 1.789(3)Å was observed for the molecular composition $Mo(PMe_2Ph)_3O_{0.97}Cl_{2.03}$ [32]. In the case of compound **19**, a spectroscopically invisible amount of the *trans* carbonyl-P(III) complex would exchange the carbonyl and chloride ligands without altering the rest of the ligand. Even a small percentage of the other isomer can make a significant change in the Rh-C bond length simply due to the greater X-ray diffracting power of chlorine (17 electrons) over carbon (6 electrons).

The most striking feature of the structure is the P=N-Si bond angle of 131.9(5)°. This angle has decreased 21° from 152.7(3)° in the free ligand simply upon coordination of the nitrogen lone pair of electrons to the rhodium centre. The P=N and N-Si bond lengths are noticeably longer in the complex and this observation parallels the behavior of $Ph_3P=N-SiMe_3$ upon complexation to CuCl[23]. The changing bond lengths and angles further support the view that the bonding in the uncomplexed P=N-Si linkage reflects delocalized bond contraction and strengthening through the diffusion of the lone pair of electrons on nitrogen into the empty d-orbitals on phosphorus and silicon.

Table 4.3 Structural data for rhodium Complexes.

Complex	**Bond lengths Å**				
	Rh-P	**Rh-Cl**	**Rh-C**	**C-O**	**Rh-N**
19	2.203(2)	2.402(2)	1.918(11)	1.068(11)	2.146(6)
22[a]	2.156(1)	2.384(1)	1.815(3)	1.141(5)	2.199(2)
23[b]	2.261(2)		1.786(9)	1.155(11)	2.098(9)
24[c]	2.322	2.381(2)	1.800(2)	1.150(7)	
25[d]	2.230(3)	2.410	1.78(1)	1.12(1)	
26[e]	2.326	2.371(2)	1.810(7)	1.144(8)	
27[f]	2.232(1)		1.809(6)	1.145	

I.R. data: Carbonyl stretching frequency, cm^{-1}

19	**22**[a]	**25**[d]	**26**[e]
1980	1991	1986	1980

[a-f] Reference 33, a-f.

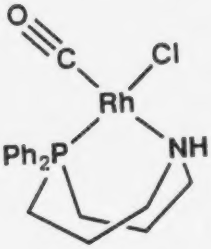

O
C
Cl
Rh
Ph$_2$P
NH

22

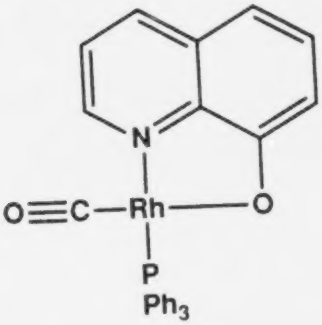

N
O≡C—Rh
O
P
Ph$_3$

23

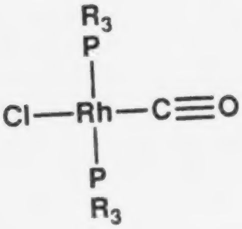

R$_3$
P
Cl—Rh—C≡O
P
R$_3$

24 R=4-FC$_6$H$_4$

26 R=Ph

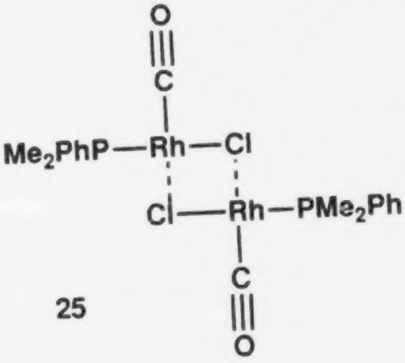

O
C
Me$_2$PhP—Rh—Cl
Cl—Rh—PMe$_2$Ph
C
O

25

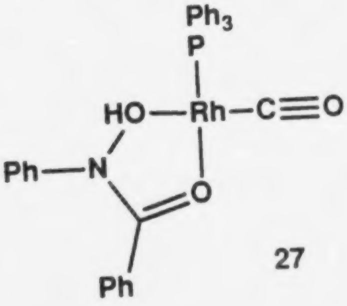

Ph$_3$
P
HO—Rh—C≡O
Ph—N
O
Ph

27

4.3 Summary

The work described in this chapter clearly demonstrates that selective mono-oxidation of a bisphosphine can be achieved through steric control. The utilization of a bisphosphine with a rigid backbone prevents the relief of steric congestion by forcing the phosphorus centres to maintain a *cis* conformation. For 1,2-bis(diphenylphosphino)benzene, the oxidation of one phosphorus centre by an azide proceeds smoothly but the second oxidation is prevented. Structural (compound **11**) and theoretical examination of the P=N-Si linkage reveals shorter bond lengths and a larger bond angle are to be expected compared to a P=N-C linkage. These characteristics have been attributed to additional bonding interactions between the atoms generated by the ability of the lone pair of electrons on the nitrogen centre to diffuse into the available d-orbitals on phosphorus and silicon. These mono-oxidized bisphosphine compounds form stable rhodium-carbonyl-chloride complexes. Spectroscopic and structural examination of these complexes reveal square planar rhodium(I) complexes with the carbonyl ligand cis to the co-ordinating P(III) centre. There is evidence from compound **19** that a small percentage of the trans-carbonyl-P(III) complex co-crystallized with the primary structural form. This responsible isomer was invisible to spectroscopic detection, but, X-ray crystallography reveals a subtle disorder in the rhodium-carbonyl bond lengths and this disorder demonstrates the minute presence of the trans-carbonyl-P(III) complex in the single crystal studied.

4.4 Experimental.

General techniques, reagents, solvents and instrumentation are listed in the appendix.

Section A. Total synthesis of 1,2-bis(diphenylphosphino)benzene (dppbz).

A1. Preparation of bromoiodobenzene[5].

Into an Erlenmeyer flask was placed 25 g (145 mmol) of 2-bromoaniline, 250 mL of water and 60 mL of concentrated H_2SO_4. After cooling to 0 ^oC, 10.0 g (145 mmol) of $NaNO_2$ in 40 mL of water was added dropwise. The solution was stirred for one hour. This solution was then carefully added to an aqueous solution (100 mL) of KI (30 g, 180 mmol). This solution was stirred and heated to 70 ^oC and then allowed to cool slowly for several hours. Extraction of the aqueous solution with $CHCl_3$ (100 mL, 3X) was followed by washing the $CHCl_3$ solution with 50 mL each of: 10% NaOH, 1M Na_2SO_3, 10% HCl, H_2O, saturated $NaHCO_3$ and saturated NaCl. The $CHCl_3$ solution was then dried over Na_2SO_4 and the $CHCl_3$ was removed with a rotary evaporator producing a brown-red liquid (32.78g, 116 mmol). Vacuum distillation 65-68 ^oC (0.6mm Hg) produced 23.05g (81 mmol, 56 %) of pure C_6H_4BrI as a pale red liquid. Analysis: Calculated: C=25.34, H=1.40 %; Found: C=25.47, H=1.43 %.

A2. Preparation of diphenyltrimethylsilylphosphine[5].

Into a 1000 mL three neck 24/40 round bottom flask was placed 50 g (191 mmol) of triphenylphosphine and 500 mL of freshly distilled THF. To this was added 7g (1 mol) of sliced and quartered lithium rod. This solution was stirred at room temperature for eight hours and then filtered through a large C-frit filter stick to remove unreacted lithium. Next, 60 mL of trimethylsilyl chloride (473 mmol) was added dropwise to the red solution (excess to destroy phenyl-lithium). After stirring overnight, the solvent was removed *in vacuo* and the remaining liquids were decanted into a small flask for vacuum distillation. Double distillation produced 40g (155 mmol, 81 %) of Ph_2PSiMe_3 as a clear, colourless liquid, b.p. 110-115 °C, 0.02mm Hg; Lit.[5] 119-120°C, 0.2mm Hg. ^{31}P NMR -55.9 ppm; Lit.[5]=-56.2 ppm.

A3. Preparation of 2-bromophenyldiphenylphosphine[5].

Into a 500 mL 24/40 round bottom flask was placed: 20.08 g (70.9 mmol) of 2-bromoiodobenzene and 18.5 g (71.7 mmol) of Ph_2PSiMe_3. The liquids were degassed by repeated exposure to vacuum and introduction of an argon atmosphere. Dry toluene (250 mL) was then added and the solution was repeatedly degassed . Next $PdCl_2(PhCN)_2$ (250 mg, 0.65 mmol, catalyst) was added to the reaction mixture and the solution immediately turned bright red. The solution was again degassed briefly and then heated to 80-90 °C using an oil bath. After 19 hours the red colour had disappeared, however, ^{31}P NMR spectroscopy revealed that the reaction was incomplete and 50 mg (0.13 mmol) of additional catalyst was added. After 3 days, the solution was cooled to room temperature and all of the volatiles were removed *in vacuo* . The tan-coloured solid was extracted with two 200 mL portions of boiling ethanol (dried over Na_2SO_4) which upon cooling to room temperature produced 14.5 g (47.6 mmol, 67 %) of 2-bromophenyl-diphenylphosphine. M.P.=105-108 °C, Lit.[5]=112-114°C. ^{31}P NMR =-4.0 ppm, Lit.[5]=-4.4 ppm.

A4. Preparation of 1,2-bis(diphenylphosphino)benzene [5] (dppbz).

Into a 250 mL side arm round bottom flask was placed 2.40 g (7.04 mmol) of 2-bromophenyldiphenylphosphine and 100 mL of dry THF. The solution was then cooled to -78 °C and 5 mL of 1.6M nBuLi was added dropwise. The solution was then stirred for one hour before the slow addition of 1.60 g (7.27 mmol) of chlorodiphenylphosphine in 20 mL of THF. The solution was stirred overnight and allowed to warm to room temperature slowly. The solvent was removed using a rotary evaporator to produce a thick oil which was dissolved in 50 mL of hot 50/50 ethanol/toluene. Gravity filtration through a fluted filter paper and slow cooling to room temperature to produce 2.00g (4.48 mmol, 64 %) of small white crystals of $C_6H_4(PPh_2)_2$. mp=176-179 °C, Lit.[5]= 179-181°C. ^{31}P NMR = -12.8 ppm, Lit.[5]=-14.2 ppm.

Section B. Reaction of dppbz with azides.

B1. Reaction with trimethylsilyl azide: formation of 11.

Into a 250 mL 24/40 round bottom flask was placed 9.86g (22.1 mmol) of dppbz, 3.03g (26.3 mmol) of trimethylsilyl azide and 100 mL of dry toluene. The flask was fitted with a water cooled reflux condensor and the solution was refluxed vigorously. The progress of the reaction was monitored by ^{31}P NMR spectroscopy and more azide was added periodically. After five days of heating the cooled solution was filtered under argon to remove some fluffy precipitate, and the flask was placed in the freezer (-20 °C) overnight. Filtration of the cold solution under argon produced 6.80g (12.8 mmol, 58 %) of pure **11** as small white crystals. M.P.=165-169 °C. Analysis: $C_{33}H_{33}P_2NSi$. Calculated: C=74.27, H=6.23, N=2.62 %. Found: C=74.28, H=6.36, N=2.65 %. I.R. (CH_2Cl_2 cast): 3053s, 2949s, 1580m, 1568w, 1550w, 1481s, 1435vs, 1305br vs, 1265w, 1239m, 1177w, 1110s, 1067w, 1022m, 995w, 906w, 859vs, 828vs, 744vs, 712s, 695vs, 650w, 580w, 540vs, 513m, 495w. M.S.: M^+=533 (2%), 456 (100%). ^1H NMR (δ, $CDCl_3$, TMS) 7.6-7.2 ppm, m, 24H; 0.04 ppm, s, 9H. ^{31}P NMR (δ, $CDCl_3$, H_3PO_4) 1.23 ppm, d; -14.77 ppm, d, $^3J_{PP}$=17.8 Hz. ^{13}C NMR (δ, $CDCl_3$, TMS) 139-127 ppm, Ar; 5.58 ppm, $^3J_{CP}$=3.0 Hz. ^{29}Si NMR (δ, $CDCl_3$, TMS) -12.06 ppm, $^2J_{SiP}$=20.7 Hz.

B2. Reaction with 4-cyanotetrafluorophenyl azide: formation of 12.

To a chloroform solution (30 mL) of dppbz (1.81g, 4.05 mmol) at 0 °C was added dropwise 0.95g (4.40 mmol) of 4-CN-C_6F_4-N_3 in 20 mL of chloroform. The reaction was complete in one hour as determined by ^{31}P NMR spectroscopy. The reaction mixture was stirred overnight and then the solvent was removed *in vacuo* . Recrystallization from acetonitrile produced 2.20g (3.47 mmol, 86 %) of fine, off-white crystals of **12**. M.P.=211-213°C. Analysis: $C_{37}H_{24}F_4P_2N_2$. Calculated: C=70.04, H=3.81, N=4.41 %. Found: C=69.84, H=4.02, N=4.26 %. I.R. (CH_2Cl_2 cast): 3055w, 2225w, 1647m, 1502s, 1433m, 1230m, 1103w, 1050s br, 980s, 739w, 734m, 715m, 690s, 528vs, 511w, 505w, 492m. M.S.: M$^+$=634 (23%), 557 (100%). ^{1}H NMR (δ, $CDCl_3$, TMS) 8.0-7.0 ppm, Ar. ^{31}P NMR (δ, $CDCl_3$, H_3PO_4) 11.88 ppm, dt, $^3J_{PP}$=21.0 Hz, $^4J_{PF}$=4.54 Hz; -14.84 ppm, d, $^3J_{PP}$=20.8 Hz. ^{19}F NMR (δ, $CDCl_3$, C_6F_6) -139.4 ppm, m; -151.7 ppm, m.

B3. Reaction with diphenylphosphinic azide: formation of 13.

Into a 100 mL 24/40 round bottom flask was placed: 3.00g (6.72 mmol) of dppbz, 1.85g (6.72 mmol) of diphenylphosphinic azide, and 50 mL of dry toluene. The reaction mixture was stirred and heated gently overnight. Removal of the solvent *in vacuo*, followed by repeated addition of CH_2Cl_2 to the resulting oil and removal of the solvent *in vacuo* eventually produced an off-white, hydroscopic, amorphous powder. M.P.=56 °C. Analysis: $C_{42}H_{34}O_3P_3N$. Calculated: C=72.73, H=4.94, N=2.02 %. Found: C=72.43, H=5.22, N=1.95 %. I.R. (CH_2Cl_2 cast): 3075w, 2970w, 1594m, 1489s, 1435m, 1304m br, 1244m, 1203br vs, 1162w, 1114m, 1026w, 913s, 746s, 718w, 691s, 536s, 497m. M.S.: M$^+$=693 (1%), 616 (5%). ^{1}H NMR (δ, $CDCl_3$, TMS) 7.8-6.7 ppm, Ar. ^{31}P NMR (δ, $CDCl_3$, H_3PO_4) 13.8 ppm, dd, $^3J_{PP}$=23.6 Hz; -8.9 ppm, d, $^2J_{PP}$=36.2 Hz; -15.9 ppm, d, $^3J_{PP}$=23.6 Hz.

B4. Reaction with benzyl azide: formation of 14.

Into a Schlenk tube was placed: 5g (20 mmol azide) of Amberlite anion exchange resin (chloride replaced by azide)[17], 1.00g (5.85 mmol) of benzylbromide and enough CH_2Cl_2 to saturate the resin (20 mL). This mixture was stirred for eight hours at room temperature. The solution was then filtered under argon and the resin was washed with two 10 mL portions of CH_2Cl_2. (***CAUTION!!*** THIS IS POTENTIALLY VERY DANGEROUS!! EXPOSURE OF THE AZIDE TO A GLASS FRIT COULD CAUSE DETONATION OF THE AZIDE) The CH_2Cl_2 solution containing the azide was then added dropwise to a CH_2Cl_2 solution (20 mL) of dppbz (2.33g, 5.22 mmol) at 0 °C. The reaction mixture was allowed to warm slowly overnight and removal of the solvent *in vacuo* produced an oil. Dissolving the oil in a minimum of CH_2Cl_2 and the addition of 100 mL of dry hexane produced an oil. The solvent was decanted from the oil and both fractions were analyzed by ^{31}P NMR spectroscopy. The solvent fraction contained **14** exclusively, but the oil contained a large variety of unknown phosphorus containing compounds. The solvent fraction was recrystallized from acetonitrile to yield approximately 1g (30 %) of pure **14.** M.P.=129-131 °C. Analysis: $C_{37}H_{31}P_2N$. Calculated: C=80.57, H=5.66, N=2.54 %. Found: C=80.19, H=5.68, N=2.98 %. Calculated with 0.2 moles of acetonitrile: C=80.24, H=5.69, N=3.00 %. I.R. (CH_2Cl_2 cast): 3050w, 2800w, 2120 (CH_3CN), 1585w, 1490w, 1480m, 1437s, 1280m br, 1182m, 1108s, 1026m, 998w, 724s br, 694vs, 548m, 530m. M.S.: M^+-77=474 (100%). ^1H NMR (δ, $CDCl_3$, TMS) 7.8-6.9 ppm, Ar, 29H; 4.5 ppm, d, $^3J_{HP}$=16.97 Hz; (1.97 ppm CH_3CN). ^{31}P NMR (δ, $CDCl_3$, H_3PO_4) 10.3 ppm, d, $^3J_{PP}$=15.0 Hz; -13.9 ppm, d, $^3J_{PP}$=15.5 Hz. ^{13}C NMR (δ, $CDCl_3$, TMS) 138-125 ppm, Ar; 49.75 ppm, s.

Section C. Complexes with $[Rh(CO)_2Cl]_2$.

C1. The complex of 11 (19).

A CH_2Cl_2 solution (30 mL) of **11** (0.2884 g, 0.5411 mmol) was added dropwise to a CH_2Cl_2 solution (80 mL) of $[Rh(CO)_2Cl]_2$ (0.1029 g, 0.2645 mmol) at room temperature. After one hour the initial red solution had turned yellow-orange and the solvent was removed *in vacuo* . Phosphorus NMR spectroscopy of the resulting yellow microcrystalline powder revealed a clean conversion to the complex **19**. Recrystallization from 25 mL of hot acetonitrile produced large clear orange blocks of **19** (59 mg, 0.84 mmol, 16 %). M.P.=255 °C (discoloured), 264 °C (decomposed-degassed vigorously). Analysis: $C_{34}H_{33}P_2NSiRhOCl$. Calculated: C=58.34, H=4.75, N=2.00 %. Found: C=57.72, H=4.77, N=2.18 %. I.R. (CH_2Cl_2 cast): 3050w, 2940w, 2890w, 1980vs, 1580w br, 1435m, 1240w, 1139m, 1126s, 1107w, 1093m, 835s, 769m, 750w, 743w, 727m, 693s, 581m, 555s, 542m, 507m. M.S.: M^+-CO=671 (87.5%). ^1H NMR (δ, $CDCl_3$, TMS) 7.7-7.2 ppm, Ar, 24H; -0.29, s, 9H. ^{31}P NMR (δ, $CDCl_3$, H_3PO_4) 40.45, dd, $^1J_{PRh}$=175.2 Hz, $^3J_{PP}$=19.1 Hz; 20.16, dd, $^3J_{PP}$=19.2 ppm, $^2J_{PRh}$=1.86 Hz. ^{13}C NMR (δ, $CDCl_3$, TMS) carbonyl not observed, 137-127 ppm, Ar; 5.60 ppm, $^3J_{CP}$=4.16 Hz. ^{29}Si NMR (δ, $CDCl_3$, TMS) 6.6 ppm, d, $^2J_{SiP}$=5.08 Hz.

C2. The complex of 12 (20).

A CH_2Cl_2 solution (20 mL) of **12** (0.1616g, 0.255 mmol) was added dropwise to a CH_2Cl_2 solution (30 mL) of $[Rh(CO)_2Cl]_2$ (0.0496g, 0.127 mmol) at room temperature. The next day the initial red solution had turned yellow-orange and the solvent was removed *in vacuo*. Phosphorus NMR spectroscopy of the resulting yellow microcrystalline powder revealed quantitative formation of the complex **20**. Recrystallization from 50 mL of hot acetonitrile produced small yellow cubes (100mg, 0.14 mmol, 55 %) of **20**. M.P.=312°C decomposed. Analysis: $C_{38}H_{24}F_4P_2N_2OClRh$. Calculated: C=56.99, H=3.02, N=3.50 %. Found: C=56.50, H=2.85, N=3.50 %. I.R.

(CH_2Cl_2 cast): 2930w, 2240w, 1986vs, 1643m, 1493s, 1484s, 1435m, 1184m, 1113m, 997w, 981m, 892w, 741m, 729m, 581m, 529m. M.S.: M^{+}-35=675 (1%), M^{+}-35-28=737 (4%), M^{+}-35-28-77=660 (8%), M=28 (100%). ^1H NMR (δ, $CDCl_3$, TMS) 7.8-7.2 ppm, m, Ar. ^{31}P NMR (δ, $CDCl_3$, H_3PO_4) 36.52 ppm, dd, $^1J_{PRh}$=169.6 Hz, $^3J_{PP}$=27.86 Hz; 27.84, d, broad. ^{19}F NMR (δ, $CDCl_3$, C_6F_6) -137.5, m; -142.5, m.

C3. The complex of 13 (21).

A CH_2Cl_2 solution (50 mL) of **13** (0.1493g, 0.215 mmol) was added dropwise to a CH_2Cl_2 solution (50 mL) of $[Rh(CO)_2Cl]_2$ (0.0419g, 0.216 mmol) at -78 °C. The solution was allowed to warm slowly to room temperature and the solvent was removed *in vacuo* . Phosphorus NMR spectroscopy of the resulting yellow microcrystalline powder revealed clean formation of the complex **21**. M.P.=116 °C (decomposes). Analysis: $C_{43}H_{34}P_3O_4NClRh$. Calculated: C=60.05, H=3.98, N=7.63 %. Found: C=57.82, H=3.97, N=7.75 %. I.R. (CH_2Cl_2 cast): 3057w, 1986vs, 1590m, 1489s, 1436m, 1261m br, 1195m, 1120s, 1097m, 10265w, 930s, 810m, 746m, 690s, 553m, 513m. ^1H NMR (δ, $CDCl_3$, TMS) 8.0-7.0 ppm, Ar. ^{31}P NMR (δ, $CDCl_3$, H_3PO_4) 50.0 ppm, dd, $^1J_{PRh}$=170.6 Hz, $^3J_{PP}$=20.1 Hz; 40.5 ppm, overlapping dd; 7.3 ppm, d, $^2J_{PP}$18.49 Hz. ^{13}C NMR (δ, $CDCl_3$, TMS) 185.9 ppm, dd, $^1J_{CRh}$=78.5 Hz, $^2J_{CP}$=16.1 Hz; 151 ppm, d, J=7.0 Hz, 137-120 ppm, Ar.

4.5 References

1. H. Staudinger and J. Meyer. *Helv. Chim. Acta.*, **2**, 635 (1919).

2. H. C. E. McFarlane and W. McFarlane. *Polyhedron.*, **2**, 303 (1983).

3. R. Talay and D. Rehder. *Z. Naturforsch.*, **36b**, 451 (1981).

4. a) E. P. Kyba, S. T. Liu and R. L. Harris. *Organometallics*, **2**, 1877 (1983).

   b) E. P. Kyba, M. C. Kerby and S. P. Rines. *Organometallics*, **5**, 1189 (1986).

5. S. E. Tunney and J. K. Stille. *J. Org. Chem.*, **52**, 748 (1987).

6. M. Bakir, F. A. Cotton, M. M. Cudahy, C. Q. Simpson, T. J. Smith, E. F. Vogel and R. A. Walton. *Inorg. Chem.*, **27**, 2608 (1988).

7. M. Bakir, P. E. Fanwick and R. A. Walton. *Inorg. Chem.*, **27**, 2016 (1988).

8. E. Hey. *J. Organomet. Chem.*, **378**, 375 (1989).

9. a) G. Salem and S. B. Wild. *J. C. S. Chem. Commun.*, 1378 (1987).

   b) G. Salem and S. B. Wild. *J. Organomet. Chem.*, **370**, 33 (1989).

   c) G. T. Crisp, G. Salem, F. S. Stephens and S. B. Wild. *J. C. S. Chem. Commun.*, 600 (1987).

10. P. Aslanidis and J. Grobe. *J. Organomet. Chem.*, **249**, 103 (1983).

11. A. Bart van Oort, P. H. M. Budzelaar, J. H. G. Frijns and A. G. Orpen. *J. Organomet. Chem.*, **396**, 33 (1990).

12. E. F. Landvatter and T. B. Rauchfuss. *Organometallics*, **1**, 506 (1982).

13. A. Kinting, H. J. Kreuzfeld and H. P. Abicht. *J. Organomet. Chem.*, **370**, 343 (1989).

14. S. R. Hall, B. W. Skelton and A. H. White. *Aust. J. Chem.*, **36**, 267 (1983).

15. S. W. Washburne and W. R. Peterson Jr. *J. Organomet. Chem.*, **33**, 153 (1971).

16. Yu. G. Gololobov, I. N. Zhmurova and L. F. Kasukhin. *Tetrahedron*, **37**, 437 (1981).

17. A. Hassner and M. Stern. *Angew. Chem. Int. Ed. Engl.*, **25**, 478 (1986).

18. Reference number SDL:RGC9001.

19. E. E. Astrup, A. M. Bouzga and K. A. O. Starzweski. *J. Mol. Str.*, **51**, 51 (1979).

20. H. Schmidbaur, G. A. Bowmaker, O. Kumberger, G. Müller and W. Wolfsberger. *Z. Naturforsch.*, **45b**, 476 (1990).

21. E. Schweda, K. D. Scherfise and K. Dehnicke. *Z. anorg. allg. Chem.*, **528**, 117 (1985).

22. G. W. Adamson and J. C. J. Bart. *Chemical Communications*, 1036 (1969).

23. D. Fenske, E. Böhm, K, Dehnicke and J. Strähle. *Z. Naturforsch.*, **43b**, 1 (1988).

24. R. A. Wheeler, R. Hoffmann and J. Strähle. *J. Am. Chem. Soc.*, **108**, 5381 (1986).

25. See Chapter one, reference 17.

26. K. A. O. Starzewski and H. T. Dieck. *Inorg. Chem.* , **18**, 3307 (1979).

27. J. A. Jenkins. Ph. D. Dissertation, University of Alberta, Edmonton, Alberta, Canada, 1991.

28. Reference number SDL:RGC8908.

29. a) Y. Jean, A. Lledos, J. K. Burdett and R. Hoffmann. *J. Am. Chem. Soc.*, **110**, 4506 (1988).

    b) Y. Jean, A. Lledos, J. K. Burdett and R. Hoffmann. *J. C. S. Chem. Commun.*, 140 (1988).

30. B. L. Haymore, W. A. Goddard III, and J. N. Allison. *Proc. Int. Conf. Coord. Chem.*, 23rd, 535 (1984).

31. J. M. Mayer. *Inorg. Chem.*, **27**, 3899 (1988).

32. K. Yoon, G. Parkin and A. L. Rheingold. *J. Am. Chem. Soc.*, **113**, 1437 (1991).

33. a) D. Bondoux, B. F. Mentzen and I. Tkatchenko. *Inorg. Chem.*, ***20***, 839 (1981).

    b) J. G. Liepoldt, S. S. Basson and C. R. Dennis. *Inorganica Chimica Acta.*, **50**, 121 (1981).

    c) A. Monge, E. Gutièrrez-Puebla, J. V. Herase and E. Pinilla. *Acta. Cryst.*, **C39**, 446 (1983).

d) J. J. Bonnet, Y. Jeannin, P. Kalck, A. Maisonnat and R. Poilblanc. *Inorg. Chem.*, **14**, 743 (1975).

e) A. Ceriotti, G. Ciani and A. Sironi. *J. Organomet. Chem.*, **247**, 345 (1983).

f) J. G. Leipoldt and E. C. Grobler. *Inorganica Chimica Acta.*, **60**, 141 (1982).

Chapter Five

The Selectivity of Oxidation of *cis* and *trans* Bis(diphenylphosphino)ethylene with *p*-Cyanotetrafluorophenyl Azide

5.1 Introduction

In the previous chapter, the oxidation of 1,2-bis(diphenylphosphino)benzene (dppbz) with azides was found to proceed to the mono-oxidized product, but the oxidation of both phosphorus centres was inhibited. There appear to be two factors in the prevention of the oxidation of the second phosphine. The first is that the rigid backbone has locked the two diphenylphosphine groups into a *cis* orientation which sterically crowds the functionalities thus preventing a second azide from reacting successfully. The second factor follows from the first; since sulphur or hydrogen peroxide will oxidize both phosphorus centres, it is clear that the bulk of the substituent on the imine which results from the first oxidation also contributes to the protection of the remaining phosphine group once the first oxidation has been achieved.

There is, however, the possibility that 'electronic cooperativity' exists between the two phosphorus centres. In order to test whether electronic communication (between the phosphorus centres *after* mono-oxidation) influences the reactivity of the second phosphorus centre, or whether simple steric crowding of the remaining phosphine group is most likely responsible for the cessation of oxidation by azide after the first step, the following experiments were performed. The two bisphosphines, *cis*-1,2-bis(diphenylphosphino)ethylene **1** and *trans*-1,2-bis(diphenylphosphino)ethylene **2**, were synthesized[1] and allowed to react with one mole of an azide. The azide chosen was 4-cyanotetrafluorophenyl azide[2]. This azide is highly reactive, therefore the observed differences in the reactivity of the *cis* and *trans* compounds can be attributed to the phosphines. If both phosphines are cleanly converted to the corresponding mono-oxidized products, **3** and **4**, then the phosphinimine group has sufficiently decreased the basicity of the remaining phosphine centre in **4** and directed the reaction . But, if the *trans* isomer **2** does not react cleanly to produce **4**, then the selectivity of the mono-oxidation can be largely attributed to the enhanced steric crowding of the phosphine groups in **1** and dppbz.

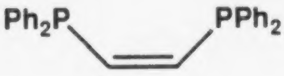

1

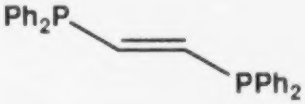

2

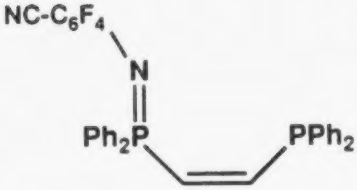
NC-C$_6$F$_4$
N
Ph$_2$P
PPh$_2$

3

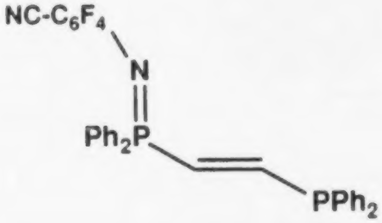
NC-C$_6$F$_4$
N
Ph$_2$P
PPh$_2$

4

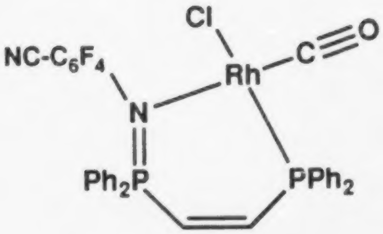
Cl
C≡O
NC-C$_6$F$_4$
Rh
N
Ph$_2$P
PPh$_2$

5

5.1 Results and Discussion

The phosphines **1** and **2** were allowed to react with 4-cyanotetrafluorophenyl azide under identical conditions. For both reactions, the quantities of reagents, the dilution, and the temperature were as similar as possible. A portion of each reaction mixture was removed and analyzed by ^{1}H and ^{31}P NMR spectroscopy. The phosphorus NMR spectra are shown in Figures 5.1 and 5.2.

The examination of Figures 5.1 and 5.2 reveals that **1** reacts smoothly with the azide to produce **3**, but **2** does not react cleanly to produce **4** exclusively. Indeed, **2**, **4**, and the doubly oxidized product are detected by ^{31}P NMR as shown in Figure 5.2. The ^{31}P NMR data for **3** (P(III) -23.7 ppm, $^{3}J_{PP}$=12.5 Hz, $^{4}J_{PF}$=5.5Hz; P(V)2.06 ppm, $^{3}J_{PP}$=12.5 Hz, $^{7}J_{PF}$=6.7 Hz) and for **4** (P(III) -4.42 ppm, $^{3}J_{PP}$=15.3 Hz; P(V) 7.84 ppm, $^{4}J_{PF}$=5.2 Hz) is essentially as expected. The P(III) chemical shifts of **3** and **4** change slightly from **1** and **2** (-23.04 ppm and -7.47 ppm) compared to the chemical shift changes experienced by the remote P(V) centre. The $^{3}J_{PP}$ coupling constants in **3** and **4** have similar magnitudes with the *trans* coupling in **4** being slightly larger (by approx. 3 Hz) (vicinyl $^{3}J_{HH}$ couplings ; *trans* > *cis*)[3]. A curious feature, a $^{7}J_{P(V)F}$ coupling of 6.7 Hz, is observed for **3**. In the absence of structural evidence it can only be speculated that there is a close phosphorus(III)-fluorine contant responsible for this unusual coupling. The absence of a similar coupling in **4** suggests that the coupling arises *via* a 'through space' interaction and not through a 'seven-bond' interaction.

Overall, for the bisphosphines **1** and **2**, the above results demonstrate that the selectivity of oxidation is determined by the steric crowding of the phosphorus centres due to the rigid *cis* ethylene backbone. Analogously, the selectivity of oxidation found in the previous chapter for dppbz can also be attributed to the steric bulk inhibiting the oxidation of the second phosphorus centre.

Figure 5.1 The ^{31}P NMR spectrum (81 MHz) of the reaction solution of **3** ($CDCl_3$).

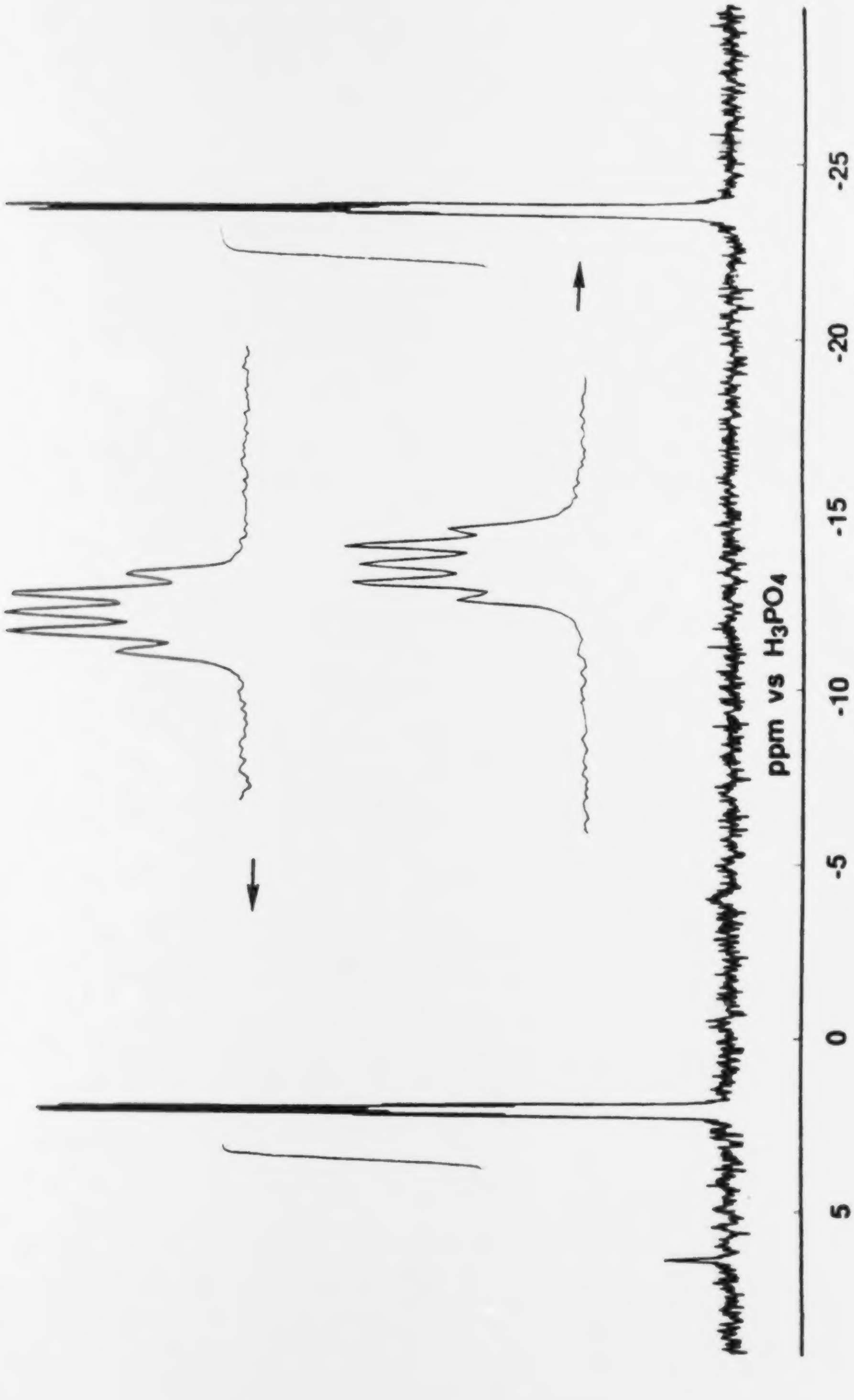

Figure 5.2 The ^{31}P NMR spectrum (81 MHz) of the reaction solution of **4** ($CDCl_3$).

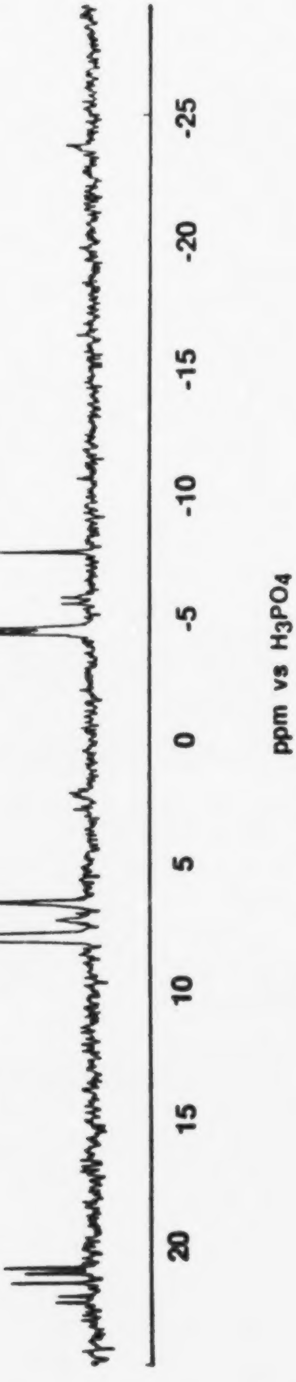

In a fashion parallel to the dppbz based ligands, the compound **3** reacts cleanly with $[Rh(CO)_2Cl]_2$ to form the complex **5**. The ^{13}C NMR data for the carbonyl ligand (δ=186.8 ppm, $^1J_{CRh}$=72.5 Hz, $^2J_{CP}$=19.6 Hz) and the I.R. stretching frequency for the carbonyl ligand of 1996 cm^{-1} are similar to those found for the dppbz derivatives in Chapter four and indicate that the complex is square planar about rhodium with the carbonyl ligand *cis* to the P(III) centre of the chelating ligand. The ^{31}P NMR data (P(III) 29.73 ppm, $^1J_{PRh}$=171.0 Hz, $^3J_{PP}$=37.4 Hz; P(V) 15.24 ppm, $^3J_{PP}$=37.6 Hz) also demonstrates similar chemical shift changes found upon complexation for the dppbz based derivatives. In contrast to the dppbz derivatives, the $^3J_{PP}$ coupling constant has increased dramaticly from 12.5 to 37.5 Hz upon complexation to rhodium. Since the vicinal proton resonances are masked by the aromatic resonances in the ^1H NMR spectrum, there is little evidence to indicate the source of this larger coupling constant. The I.R. spectra of **3** and **5** indicate that the ethylene carbon-carbon double bond is unaffected with stretching frequencies of 1644 and 1643 cm^{-1} respectively. In the absence of data on the corresponding derivative of bis(diphenylphosphino)ethane and structural information on **5**, this coupling anomaly remains a mystery.

5.3 Summary

Through the use of the *cis* and *trans* isomers of bis(diphenylphosphino)ethylene, the nature of the selectivity of the Staudinger reaction has been explored. The *cis* isomer can be reacted cleanly with an azide to yield the mono-oxidized product , but the *trans* isomer cannot. The lack of selectivity shown for the *trans* isomer further demonstrates that the oxidation of the first phosphine centre has little influence on the basicity and hence the reactivity of the second phosphorus centre. The primary cause of selective oxidation in the *cis* isomer (and in the analogous dppbz derivatives) must be the steric crowding of the phosphorus centres. Once the first oxidation has been achieved the additional substituent on the P(V) centre adds to the steric protection of the remaining phosphine.

5.4 Experimental

General techniques, reagents, solvents and instrumentation are listed in the appendix. The phosphines **1** and **2**[1] and the azide[2] were prepared as reported in the literature.

The reaction of 1 with 4-NC-C_6F_4-N_3.

To a cold (-78°C) methylene chloride solution (approx. 75 mL) of **1** (1.05 g, 2.65 mmol) was added dropwise 0.58 g (2.7 mmol) of 4-NC-C_6F_4-N_3 in approx. 25 mL of methylene chloride. Upon completion of the addition, the dry-ice/acetone cooling bath was removed and the reaction mixture was allowed to warm to room temperature and stirred overnight. A 5 mL aliquot was removed and the ^1H and ^{31}P NMR spectra were recorded. The solvent was removed *in vacuo* and the residue was recrystallized from 30 mL of hot acetonitrile producing 1.05 g (1.80 mmol, 68 %)) of **3** as pale yellow crystals. M.P.=111-114 °C. Analysis: $C_{33}H_{22}F_4N_2P_2$; Calculated: C=67.81, H=3.79, N=4.79 % ; Found: C=66.78, H=4.03, N=4.91 %. I.R. (CH_2Cl_2 cast): 3050w, 2229m,

1644s, 1502vs, 1436s, 1222s, 1112m, 1011m, 999m, 981s, 742m, 720s, 708m, 694s, 563m. M.S. M^+=584 (14 %), 507 (100 %). ^{1}H NMR (δ, $CDCl_3$,TMS) 7.9-7.1 ppm, m, Ar. ^{31}P NMR (d, $CDCl_3$, H_3PO_4) 0.16 ppm, -25.65 ppm, $^3J_{PP}$=12.5 Hz, $^4J_{PF}$=5.5 Hz, $^7J_{PF}$=6.5 Hz.

The reaction of 2 with 4-NC-C_6F_4-N_3.

To a cold (-78 °C) methylene chloride solution (approx. 75 mL) of **2** (1.05 g, 2.65 mmol) was added dropwise 0.60 g (2.8 mmol) of 4-NC-C_6F_4-N_3 in approx. 25 mL of methylene chloride. Upon completion of the addition, the dry-ice/acetone cooling bath was removed and the reaction mixture was allowed to warm to room temperature and stirred overnight. A 10 mL aliquot was removed and the ^{1}H and ^{31}P NMR spectra were recorded. See Figure 5.2. The coupling constants reported in the text were extracted from the spectrum recorded at 161.9 MHz.

Complexation of 3 with $[Rh(CO)_2Cl]_2$ (5).

A 10 mL solution of **3** (0.1159 g, 0.198 mmol) was added dropwise at room temperature to a 15 mL solution of $[Rh(CO)_2Cl]_2$ (0.0390 g, 0.100 mmol). The mixture was stirred for one hour before the solvent was removed *in vacuo* and the resultant yellow-orange solution analyzed by ^{31}P NMR spectroscopy. Slow recrystallization from methylene chloride/ diethyl ether produced a few crystals of **5**. M.P.=160 °C (decomposed). Analysis: $C_{34}H_{22}F_4N_2P_2RhOCl$; Calculated: C=54.38, H=2.95, N=3.73 % ; Found: C=53.65, H=2.71, N=3.73 %. I.R. (CH_2Cl_2 cast): 3060w, 2980w, 2241m, 1989vs, 1643s, 1493s, 1485s, 1435m, 1181m, 1113m, 1099m, 1003m, 998m, 982m, 895m, 739m, 730m, 716m, 693m, 674w, 627w, 588m, 559w, 509w. ^{1}H NMR (δ, CD_2Cl_2, TMS) 7.9-7.2 ppm, m, Ar. ^{31}P NMR (d, CD_2Cl_2, H_3PO_4) P(III) 29.73 ppm,

$^1J_{PRh}$=171.0 Hz, $^3J_{PP}$=37.4 Hz; P(V) 15.24 ppm, $^3J_{PP}$=37.6 Hz. ^{13}C NMR (d, CD_2Cl_2, TMS) carbonyl ligand 186.8 ppm, $^1J_{CRh}$=72.5 Hz, $^2J_{CP}$=19.6 Hz.

5.5 References

1. A. M. Aguiar and D. Daigle. *J. Am. Chem. Soc.*, **86**, 2299 (1964).
2. J. F. W. Keana and S. X. Cai. *J. Fluorine Chem.*, **43**, 151 (1989).
3. E. D. Becker. "High Resolution NMR Theory and Chemical Applications" Academic Press, 1980.

Chapter Six

When Phosphorus Spins Collide: The Unusual Temperature Dependence of Coupling in an ABMX Spin System.

6.1 Introduction

Our investigations into the chemistry of the Staudinger reaction[1] of azides with bisphosphines have developed a family of interesting compounds which are also useful heterodifunctional ligands[2]. These ligands, featuring soft phosphine and hard nitrogen centres, display the ability to complex a variety of transition metals encompassing a wide range of oxidation states[2-8]. Furthermore, modification of the functional group on nitrogen enables the basicity of the lone pair of electrons on nitrogen to be altered in a conscious fashion[9]. In addition, these ligands possess two distinctly different phosphorus atoms, formally P(III) and P(V), and hence ^{31}P-NMR spectroscopic chemical shifts and coupling constants reveal decisively the connectivity (monodentate *vs* chelating) of the metal complexes.

For the ligands, the P(V) resonance is typically deshielded 10 to 50 ppm[4] from the P(III) resonance, however, upon metal complexation both signals are further deshielded. Depending upon the initial difference in the phosphorus chemical shifts, and, the relative deshielding of the P(III) and P(V) centres by the metal centre, the assignment of the ^{31}P-NMR signals for the complexes can be ambiguous in the absence of additional coupling. The utilization of metals with isotopes possessing a spin of one-half and functional groups on nitrogen containing fluorine or phosphorus allows for the unambiguous assignment of the NMR spectra and establishes the connectivity of the complex.

This chapter describes the preparation of the complex **1** and its characterization by multinuclear NMR spectroscopy. Due to the relative shielding of the phosphorus chemical shifts described above, the difference in the phosphorus chemical shifts for **1** is small resulting in unusual observed spectra.

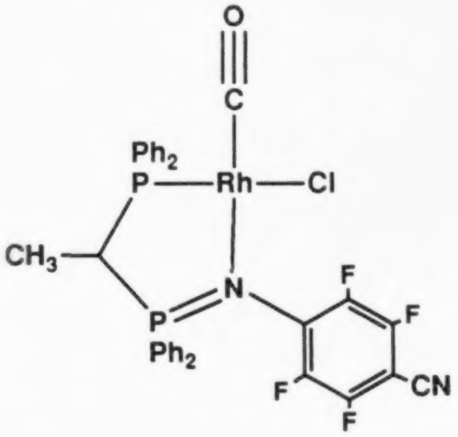

1

6.2 Results and Discussion

Synthesis

Reaction of 1,1-bis(diphenylphosphino)ethane[10] with 4-cyanotetrafluorophenyl azide[11] at -78 °C in methylene chloride and subsequent slow warming to room temperature yield cleanly the mono-oxidized bisphosphine, 1-(N-4-cyanotetrafluorophenyl-diphenylphosphinimine-1-diphenylphosphino)ethane **2** ($[\alpha]_D=0$). Combination of **2** with $[Rh(CO)_2Cl]_2$ in methylene chloride yields quantitatively the complex **1**. The complex is insoluble in aromatic solvents, poorly soluble in chloroform and moderately soluble in methylene chloride, tetrachloroethane and acetonitrile. The multinuclear-NMR data are listed in Table 6.1 and the significant coupling constants are listed in Table 6.2.

Table 6.1 Multinuclear NMR data for **1** at +55°C (CD_2Cl_2/CD_3CN).

Nucleus (Z)		δ ppm	J_{RhZ} Hz	J_{PZ} Hz	**sub-spin system**[a]
^{31}P	P(III)	47.4	161.4	40.5	ABM
	P(V)	46.1	<4	40.2	ABMYY'
^{13}C	Carbonyl	187.6	75	18	ABMX
^{19}F		-137.4	<4	<4	
		-137.6	<4	<4	
		-142.3	<1	<1	
		-142.8	<1	<1	ABXY[b]

[a] X=^{13}C, M=Rh, A=P(III), B=P(V), Y=F

[b] fluorine only, 25°C.

Table 6.2 Matrix of the significant coupling constants for **1**.

	P(III)	**P(V)**	**Rh**	**^{13}C**
P(III)		**40**	**161**	**18**
P(V)			**<4**	**<1**
Rh				**75**

Spectroscopy

The 81 MHz ^{31}P-NMR spectrum of **1** was unexpectedly complex with a multiplet centred at 46.5 ppm (ambient temperature, CD_2Cl_2 solution). Variable temperature studies utilizing CD_2Cl_2, CD_3CN or solvent mixtures of the former solvents with tetrachloroethane and toluene (+55°C to -115°C) revealed that an unusual temperature dependence of the phosphorus chemical shifts was involved. In addition the chemical shifts are also sensitive to concentration[12]. The variable temperature ^{31}P NMR spectra of **1** recorded from 30° to -60°C in CD_2Cl_2 solution are shown in Figure 6.1. The large $^1J_{RhP}$ coupling for the P(III) centre (161Hz) and the complex J_{RhP} and J_{FP} couplings for the P(V) centre identify these resonances decisively. At the high temperature limit the ^{31}P-spectrum is almost first order in appearance (ABMYY') with the P(III) resonance downfield from the P(V) resonance by 220Hz. As the temperature is lowered, the difference in the chemical shifts of the phosphorus centres decreases and the spectral line intensities change with increasing second order character. Eventually the phosphorus resonances collide (isochronous) at -25°C.(or at T=-18°C in d^8-toluene/CD_3CN or at -5°C in CD_2Cl_2/CD_3CN), yielding an AA'MYY' spin system. As the temperature continues to decrease the shifts diverge again to cause the spectrum to revert to increased first order behavior. The simulation of this behavior is shown in Figure 6.2.

In an attempt to probe the source of the unusual NMR behavior observed for phosphorus the complex, **1** was isotopically labelled with ^{13}CO by stirring a methylene chloride solution of **1** under an atmosphere of ^{13}CO in a small flask. The resulting variable temperature spectra (^{13}C-NMR), and their simulation, are shown in Figures 6.3 and 6.4. At the high and low temperature limits the spectra in the carbonyl region appear to be first order AMX spin system (doublet of doublets, A=P(III), M=Rh and X=^{13}C). But the phosphorus centres are strongly coupled and a more realistic assignment is as an ABMX spin system (B=P(V)) where the coupling $J_{CP(V)}$ is not resolved. Also, when the phosphorus centres are isochronous the spectra appear as an AMX spin system. Again, parallel to the ^{31}P-NMR, the observed spectral transformations occur as the difference in the ^{31}P chemical shifts decrease. At the point where the P(V) resonance "collides" with the upfield doublet of the P(III) resonance,

i.e. $((\nu_{P(III)}-\nu_{P(V)}) - 1/2(J_{P(III)Rh}-J_{P(V)Rh}))=0$ [13],

the ^{13}C-NMR spectra shows a doublet and a triplet for the carbonyl respectively. At lower temperature when the P(V) resonance "collides" with the downfield doublet of the P(III) resonance,

i.e. $((\nu_{P(III)}-\nu_{P(V)}) + 1/2(J_{P(III)Rh}-J_{P(V)Rh}))=0$ [13],

the ^{13}C-NMR spectra shows a triplet and a doublet (respectively) in the carbonyl region (Figure 6.5).

The ^{19}F-NMR spectra reveal an ABXY spin system (fluorine only) at T=25°, 0° and -40°C. Some temperature variation in the chemical shifts is observed, but, the asymmetry of the fluorine spin system demonstrates that the 4-cyano-tetrafluorophenyl group is not free to rotate and maintains a fixed orientation with respect to the molecular framework of **1**. Furthermore, the ^{1}H-NMR spectra of **1** show no discernable change with temperature (T=25°, 0° and -40°C). Since the size of J_{PH} coupling constants generally display a large angular dependence[13], this further indicates that the five-membered ring of **1** maintains a fixed orientation in solution with respect to the 4-cyanotetrafluorophenyl group and that the molecule **1** posesses a rigid structure.

In spite of this apparent rigidity of the molecule, in the ^{31}P-NMR spectra the P(III) signal broadens into the base line at low temperature (T= approx. -50°C d^8-toluene/CD_3CN or T=-80°C CD_2Cl_2/CD_3CN) and then reappears at -110°C (CD_2Cl_2/CD_3CN) *with the same coupling constants before and after the event*. With no spectroscopic evidence to indicate a structural change accompanying this event (the ^{13}C-NMR spectra (CD_2Cl_2/CD_3CN) are unaffected through this temperature range), this collapse and reimergence of the P(III) signal is most likely due to a thermally induced decoupling which operates to collapse the signal as the temperature controlled T_1(Rh) passes through its minimum value. Most of the different relaxation components required to minimize T_1(Rh) (*i.e.* dipolar, quadrupolar, scalar, chemical shift anisotropy, etc.[13]) are contained within the complex spin system of compound **1** , however the details of this process have not yet been pursued.

Figure 6.1 Variable temperature ^{31}P NMR spectra of **1** in CD_2Cl_2 solution (161 MHz) measured from 30° to -60°C.

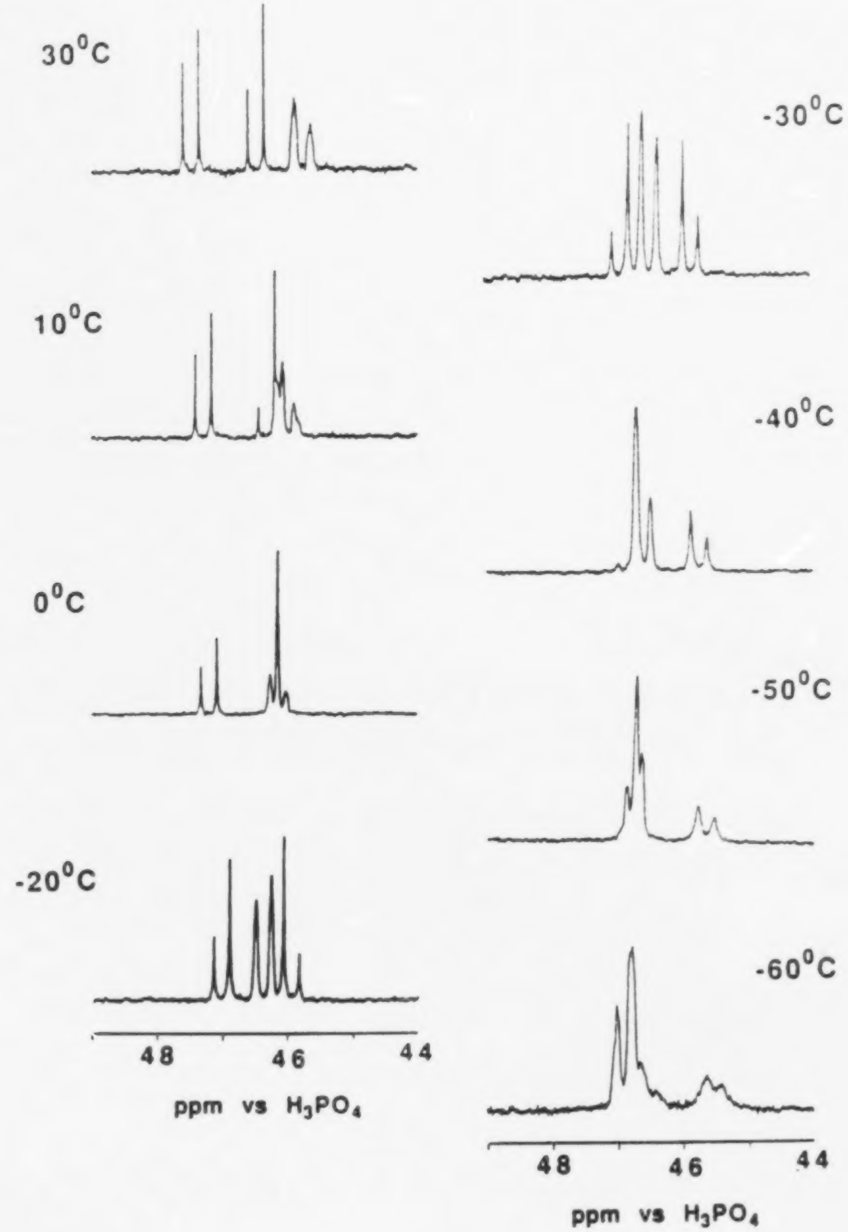

Figure 6.2 Simulation of the variable temperature ^{31}P NMR spectra demonstrating the effect of changing phosphorus chemical shifts on the ^{31}P NMR spectral features.

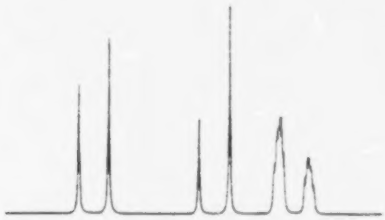

$\Delta\delta$(P(III) - P(v)) = 180 Hz

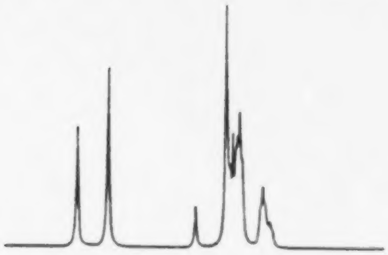

$\Delta\delta$(P(III) - P(v)) = 120 Hz

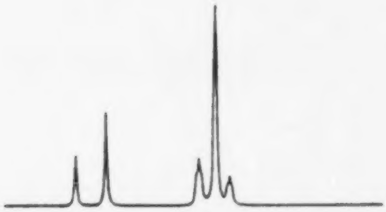

$\Delta\delta$(P(III) - P(v)) = 80 Hz

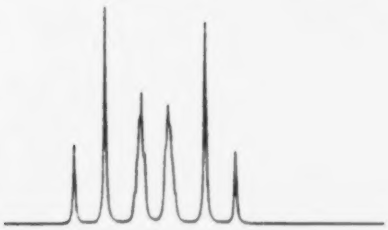

$\Delta\delta$(P(III) - P(v)) = 0 Hz

Figure 6.3 Variable temperature ^{13}C NMR spectra of **1** in CD_2Cl_2/CD_3CN solution (100.6 MHz).

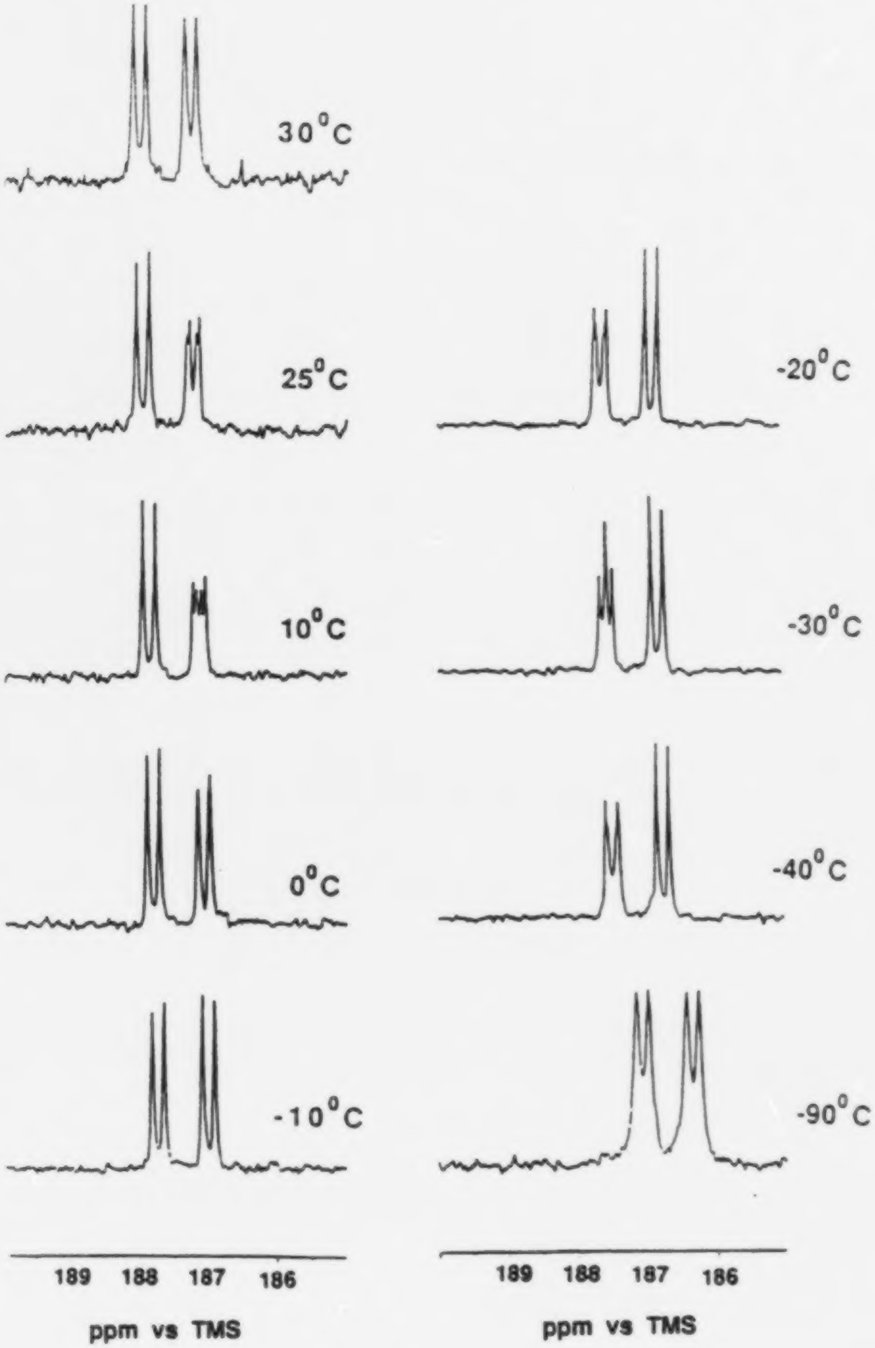

Figure 6.4 Simulation of the variable temperature ^{13}C NMR spectra demonstrating the effect of changing phosphorus chemical shifts on the ^{13}C NMR spectral features.

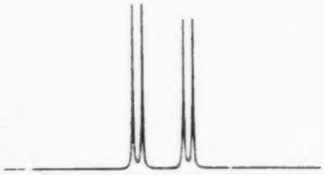

$\Delta\delta$(P(iii) - P(v)) = 200 Hz

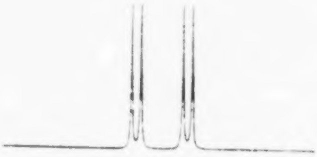

$\Delta\delta$(P(iii) - P(v)) = 0 Hz

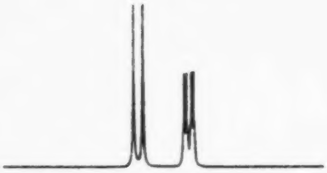

$\Delta\delta$(P(iii) - P(v)) = 100 Hz

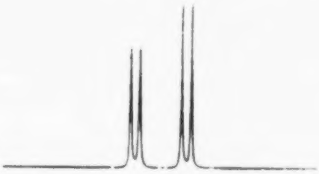

$\Delta\delta$(P(iii) - P(v)) = -25 Hz

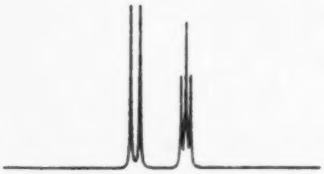

$\Delta\delta$(P(iii) - P(v)) = 80 Hz

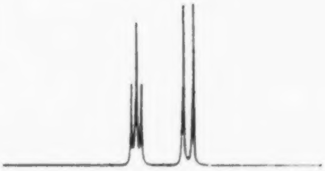

$\Delta\delta$(P(iii) - P(v)) = -80 Hz

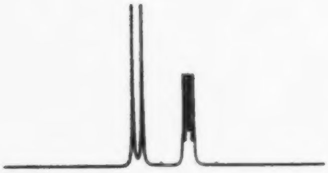

$\Delta\delta$(P(iii) - P(v)) = 65 Hz

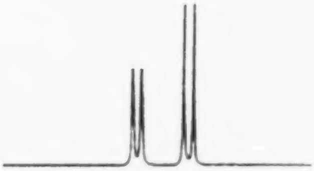

$\Delta\delta$(P(iii) - P(v)) = -125 Hz

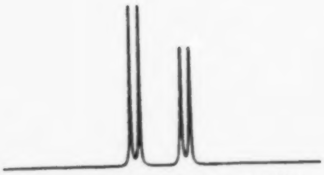

$\Delta\delta$(P(iii) - P(v)) = 25 Hz

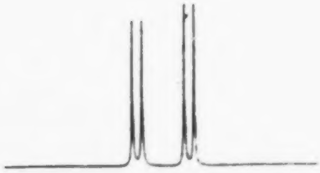

$\Delta\delta$(P(iii) - P(v)) = -200 Hz

Figure 6.5 The ^{31}P (161 MHz) and ^{13}C NMR (50.3 MHz) spectra at the point at which the difference between the phosphorus chemical shifts is approximately one-half of the large phosphorus-rhodium coupling constant.

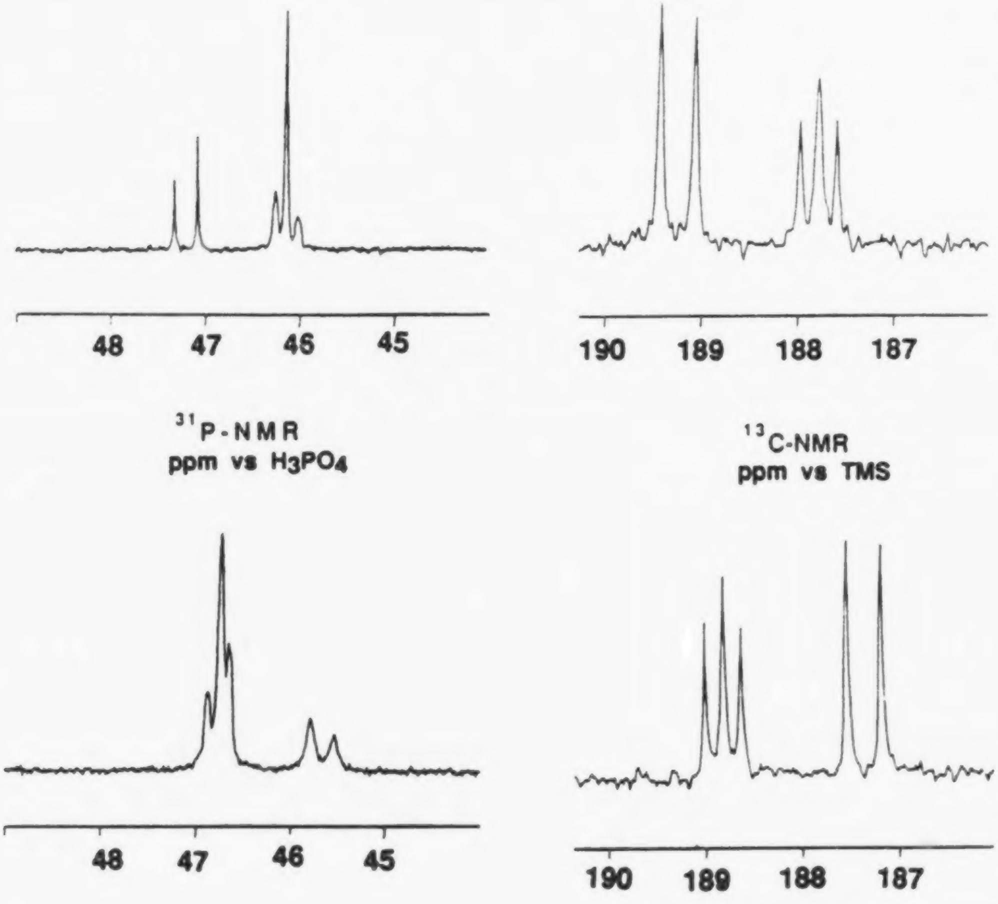

Spectral simulations

The simulations of the ^{31}P-NMR and ^{13}C-NMR spectra (Figures 6.2 and 6.4) were carried out utilizing the coupling constants listed in Table 6.2. The smaller, unresolved coupling constants are approximate values while the larger coupling constants were extracted from the multinuclear NMR data. Utilizing the equations of Pople and Schaeffer[15] describing $ABMX_n$ (n=1-x) spin systems, the complex spectra for the ^{31}P and ^{13}C-NMR can readily be understood.

For the ^{31}P-NMR spectra there are two instances when an apparent loss of coupling information is indicated by the spectra in Figure 6.5. This occurs when the doublet of multiplets for the P(V) centre overlaps either the upfield or the downfield doublet of the P(III) centre. Concentrating on the AB portion of the spin system, the equations describing these transitions contain terms that depend upon the frequency of the phosphorus chemical shifts. The consequence of this is that when the difference in the chemical shifts of the two phosphorus centres equals one-half of the difference in their respective J_{PRh} coupling constants, the frequency of the transitions all depend upon $(J_{PP})^2$, the square of the phosphorus-phosphorus coupling constant and hence the apparent simplification of the ^{31}P NMR spectra. For the complex **1**, with P(III) transitions at higher frequency than the P(V) transitions at the high temperature limit and $^1J_{P(III)Rh} >> ^2J_{P(V)Rh}$, the convention dictates that the $^1J_{P(III)Rh}$ coupling constant must be positive.

The ^{13}C-NMR spectral behavior is analogous to the ^{31}P-NMR spectra except there is an additional first order coupling constant. For the observed transitions, half are independent of the phosphorus chemical shifts *but* the other half are dependent on the ^{31}P NMR chemical shifts. The equations describing the ^{13}C NMR spectra are listed in Figure 6.6. Similar to the ^{31}P-NMR spectra, when the combined sums and differences of the coupling constants equals the difference of the phosphorus chemical shifts, one side of the overlapping doublet of doublets becomes a ('virtual') triplet. This occurs twice, once when $\nu_{P(III)}$-$\nu_{P(V)}$ is positive (high temperature) and once when the difference is negative (low temperature). The occurence of the triplet in the ^{13}C-NMR spectra matches the apparent simplification of the ^{31}P-NMR spectra (Figure 6.5) and at these points the coupling constant information can be extracted. The transitions unaffected by the changing phosphorus chemical shifts in the ^{13}C NMR spectra are simply the first order splittings and the coupling constants can be measured directly from these lines.

Figure 6.6 Equations describing the ^{13}C NMR spectral behaviour[15].

x=^{13}C, m=Rh, a=P(III), b=P(V).

a) TRANSITIONS INDEPENDENT OF PHOSPHORUS CHEMICAL SHIFTS:

$$\boldsymbol{V_x \pm 1/2J_{mx} \pm 1/2(J_{ax} + J_{bx})}$$

b) TRANSITIONS THAT DEPEND UPON PHOSPHORUS CHEMICAL SHIFTS.

$$\boldsymbol{V_x + 1/2J_{mx} \pm C_{r,x+1} \pm C_{r,x}}$$

where:

$$C_{r,x+1} = 1/2\{[(V_a - V_b) + 1/2(J_{am} - J_{bm}) - 1/2(J_{ax} - J_{bx})]^2 + J_{ab}^2\}^{1/2}$$

$$C_{rx} = 1/2\{[(V_a - V_b) + 1/2(J_{am} - J_{bm}) + 1/2(J_{ax} - J_{bx})]^2 + J_{ab}^2\}^{1/2}$$

and

$$\boldsymbol{Vx - 1/2J_{mx} \pm C_{r,x+1} \pm C_{r,x}}$$

where:

$$C_{r,x+1} = 1/2\{[(V_a - V_b) - 1/2(J_{am} - J_{bm}) - 1/2(J_{ax} - J_{bx})]^2 + J_{ab}^2\}^{1/2}$$

$$C_{rx} = 1/2\{[(V_a - V_b) - 1/2(J_{am} - J_{bm}) + 1/2(J_{ax} - J_{bx})]^2 + J_{ab}^2\}^{1/2}$$

So, when Phosphorus Spins Collide:

$$\boldsymbol{V_x + 1/2J_{mx} \pm C_{r,x+1} \pm C_{r,x}}$$

simplifies to become: A TRIPLET !

1 $\boldsymbol{V_x + 1/2J_{mx} + C_{r,x+1} + C_{r,x}}$

2 $\boldsymbol{V_x + 1/2J_{mx}}$

1 $\boldsymbol{V_x + 1/2J_{mx} - C_{r,x+1} - C_{r,x}}$

6.3 Summary

The ^{13}C NMR coupling constants ($^{1}J_{CRh}$=75 Hz, $^{2}J_{CP}$=18 Hz) indicated that the complex **1** is square planar with the carbonyl ligand on rhodium *cis* to the P(III) centre[15]. The complex has a rigid structure and variable temperature multinuclear NMR experiments (^{1}H, ^{13}C, ^{19}F, ^{31}P) demonstrate that the structure is unchanged with temperature. The complex spectra observed for ^{13}C and ^{31}P NMR variable temperature studies are the direct result of the phosphorus centres possessing opposite chemical shift temperature dependence. This unusual chemical shift temperature dependence results in apparent gain and loss of coupling information with temperature. These features arise due to the small phosphorus chemical shift differences and relatively large coupling constants.

6.4 Experimental

General techniques, reagents, solvents and instrumentation are listed in the appendix.

Preparation of the ligand 1-(*N*-4-cyanotetrafluorophenyl-diphenylphosphinimine-1-diphenylphosphino)ethane, 2.

Into a 250 mL side-arm round bottom flask was placed 3.28 g (8.24 mmol) of 1,1-bis(diphenylphosphino)ethane[10] and 50 mL of dry CH_2Cl_2. The solution was cooled to -78°C and 1.77 g (8.19 mmol) of 4-cyanotetrafluorophenyl azide[11] in 30 mL of CH_2Cl_2 was added dropwise. The reaction solution immediately developed a yellow colour. The solution was allowed to stir and warm slowly to room temperature overnight. Removal of the solvent *in vacuo* followed by recrystallization from acetonitrile produced 3.55 g (6.05 mmol) of large white blocks of **2**. M.P.=178-180°C. Analysis: $C_{33}H_{24}F_4N_2P_2$; Calculated: C=67.58, H=4.12, N=4.78 %; Found: C=67.24, H=4.27, N=4.78 %. I.R. (CH_2Cl_2 cast, cm^{-1}) 3080w, 2230s, 1645s, 1510vs br, 1435s, 1325w, 1310w, 1300w, 1290w, 1265w, 1220s, 1185w, 1160w, 1110s, 1010m, 980s, 865m, 740s, 695s, 575m, 525s, 505m. M.S. M^+=586 (3%). ^1H NMR (δ, $CDCl_3$, TMS) 7.50 ppm, m, 20H; 3.75ppm, doublet of sextets, 1H; 1.20 ppm, m, 3H. ^{31}P NMR (δ, $CDCl_3$, H_3PO_4) 21.9 ppm, dt, $^2J_{PP}$=67.8Hz, $^4J_{PF}$=4.2Hz.; -14.8 ppm, d, $^2J_{PP}$=68.0 ppm. ^{19}F NMR (δ, $CDCl_3$, C_6F_6) -139.3 ppm, m; -152.0 ppm, m.

Preparation of the complex 1.

Into a 150 mL side arm round bottom flask was placed 0.0748 g (0.192 mmol) of $[Rh(CO)_2Cl]_2$ in 25 mL of CH_2Cl_2. 0.2229 g of **2** (0.3804 mmol) in 50 mL of CH_2Cl_2 was added dropwise at room temperature. After 3 hours the solvent was removed *in vacuo* producing a yellow microcrystalline powder. The yield was quantitative by ^1H NMR. M.P.=242°C (decomposes). Analysis: $C_{34}H_{24}F_4N_2P_2ClRhO$: Calculated: C=54.24, H=3.21, N=3.72 %; Found: C=54.35, H=3.37, N=3.78 %. I.R. (CH_2Cl_2 cast,

cm^{-1}) 3056w, 2239w, 1981vs, 1644m, 1492s, 1487s, 1454w, 1435s, 1185m, 1112m, 1099m, 997m, 986m, 885w, 741m, 724m, 692m, 640w, 626w, 578w, 550m. M.S. M^+-28=724 (0.1%), 28 (100%). Multinuclear NMR: See text.

6.5 References

1. H. Staudinger and J. Meyer. *Helv. Chim. Acta.*, **2**, 635 (1919).
2. K. V. Katti and R. G. Cavell. *Inorg. Chem.*, **28**, 413 (1989).
3. K. V. Katti, R. J. Batchelor, F. W. B. Einstein and R.G. Cavell. *Inorg. Chem.*, **29**, 808 (1990).
4. K. V. Katti and R. G. Cavell. *Organometallics*, **7**, 2236 (1988).
5. K. V. Katti and R. G. Cavell. *Organometallics*, **8**, 2147 (1989).
6. K. V. Katti and R. G. Cavell. *Inorg. Chem.*, **28**, 3033 (1989).
7. K. V. Katti and R. G. Cavell. *Phosphorus, Sulfur and Silicon*. **41**, 43 (1989).
8. K. V. Katti and R. G. Cavell. *Comments Inorg. Chem.* **10**,53 (1990).
9. See Chapter one: 1.2 Structure and bonding.
10. C. L. Lee, Y. P. Yang S. J. Rettig, B. R. James, D. A. Nelson and M. A. Lilga. *Organometallics*, **5**, 2220(1986).
11. J. F. W. Keana and S. X. Cai. *J. Fluorine Chem.*, **43**, 151 (1989).
12. For examples of concentration dependence see:
    a) R. J. Abraham and H. J. Bernstein. *Can. J. Chem.*, **39**, 216 (1961).
    b) T. Schaefer. *Can. J. Chem.*, **40**, 1678 (1962).
13. E. D. Becker. "High Resolution NMR Theory and Chemical Applications", Academic Press, 1980.
14. J. A. Pople and T. Schaeffer. *Mol. Phys.*, **3**, 547 (1960).
15. See Chapters four and five for similar values of coupling constants in *cis*-phosphine-carbonyl-rhodium (I) complexes, also: J. A. Jenkins, Ph.D. Dissertation, University of Alberta, Edmonton, Alberta, Canada, 1991.

Chapter Seven

The Control of Oxidation: A Discussion.

The selective oxidation of one phosphorus centre of a bisphosphine, with an azide, to produce compounds of the general formula **1** becomes increasingly difficult as the number of methylene units, n, increases. Typically, the products of oxidation include the desired mono-oxidized compound **1** and the doubly oxidized material as well as the starting bisphosphine. For example the reaction of bis(diphenylphosphino)methane (dppm) with trimethylsilyl azide invariably produces a mixture of compounds, but the major component (50-70% by ^{31}P NMR spectroscopy) is the desired compound **1** (n=1, E=N-$SiMe_3$) (Figure 7.1). Careful fractional crystallization of the mixture results in 40% yields of analytically pure **1** in the first crop. Further recovery of **1** is usually futile. When a deficit of azide is used unreacted dppm can be recrystallized from the filtrate. Alternatively, the phosphines in the filtrate can be converted into the doubly oxidized material with more azide.

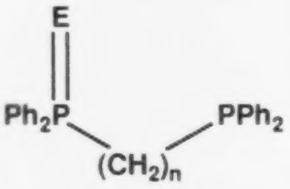

1

In general, there are a number of difficulties associated with the mixture of compounds. When n=2 (dppe) and E=N-$SiMe_3$, **1** has very similar chemical and physical properties to the corresponding bisphosphine and doubly oxidized bisphosphine. For example, the melting points and solubilities are almost identical and recrystallization attempts usually succeed in precipitating all three compounds. Separation can only be achieved through a tedious extraction process as the mono-oxidized compound is slightly less soluble in acetonitrile or hexane at room temperature. Spectroscopic examination reveals overlapping ^{1}H and ^{31}P NMR (Figure 7.2) chemical shifts and ultimately an equal ratio of **A** and **C** will produce an elemental analysis identical to that of pure **1**! In addition, isolated yields are reduced (only 10 to 20 %) and it can be expected that the above difficulties will apply for **1** derivatives with n>2. Only

Figure 7.1 A ^{31}P NMR spectrum (81 MHz) of the reaction mixture of trimethylsilylazide with bis(diphenylphosphino)methane (dppm) demonstrating the three compounds. A=dppm B=$Ph_2PCH_2P(Ph_2)$=N-$SiMe_3$ C=Me_3Si-N=$(Ph_2)PCH_2P(Ph_2)$=N-$SiMe_3$

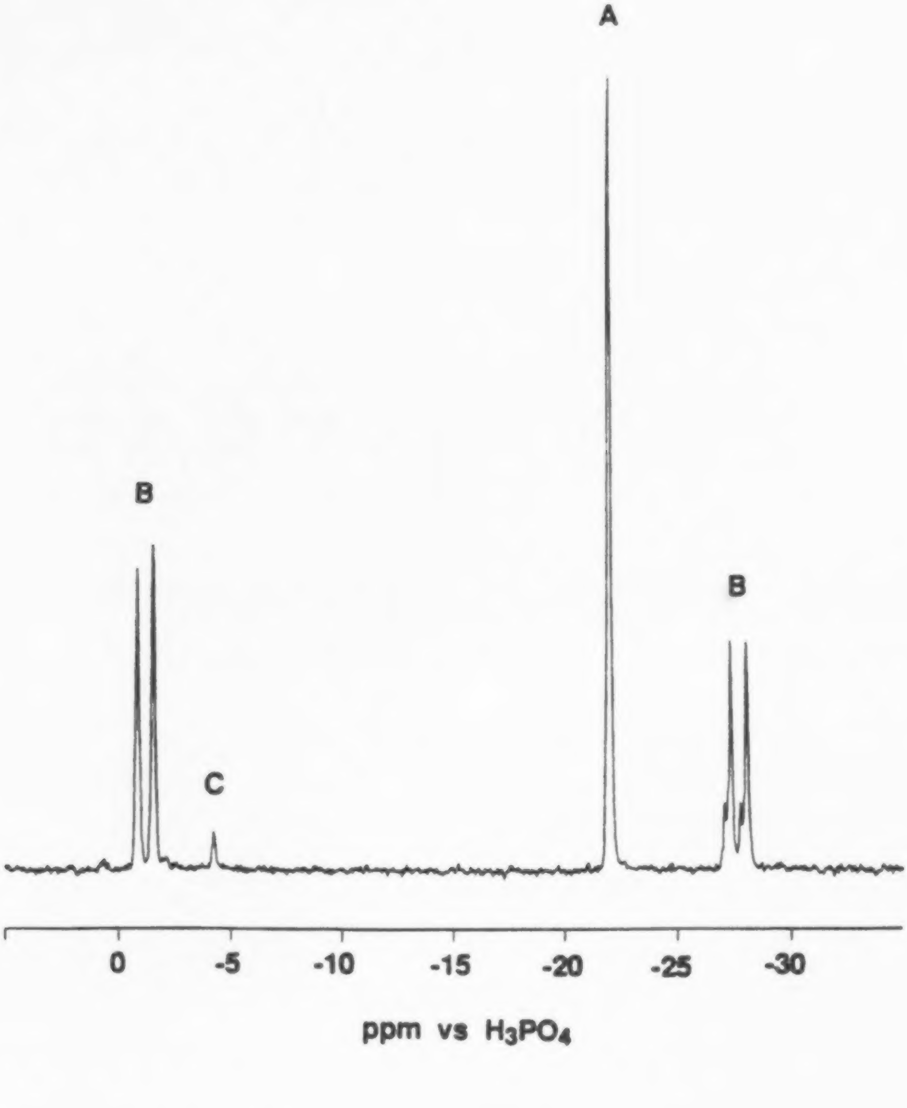

Figure 7.2 A ^{31}P NMR spectrum (81 MHz) of the reaction mixture of trimethylsilylazide with bis(diphenylphosphino)ethane (dppe) demonstrating the three compounds (Note the overlapping signals).

A=dppe B=$Ph_2PCH_2CH_2P(Ph_2)$=N-$SiMe_3$

C=Me_3Si-N=(Ph_2)$PCH_2CH_2P(Ph_2)$=N-$SiMe_3$

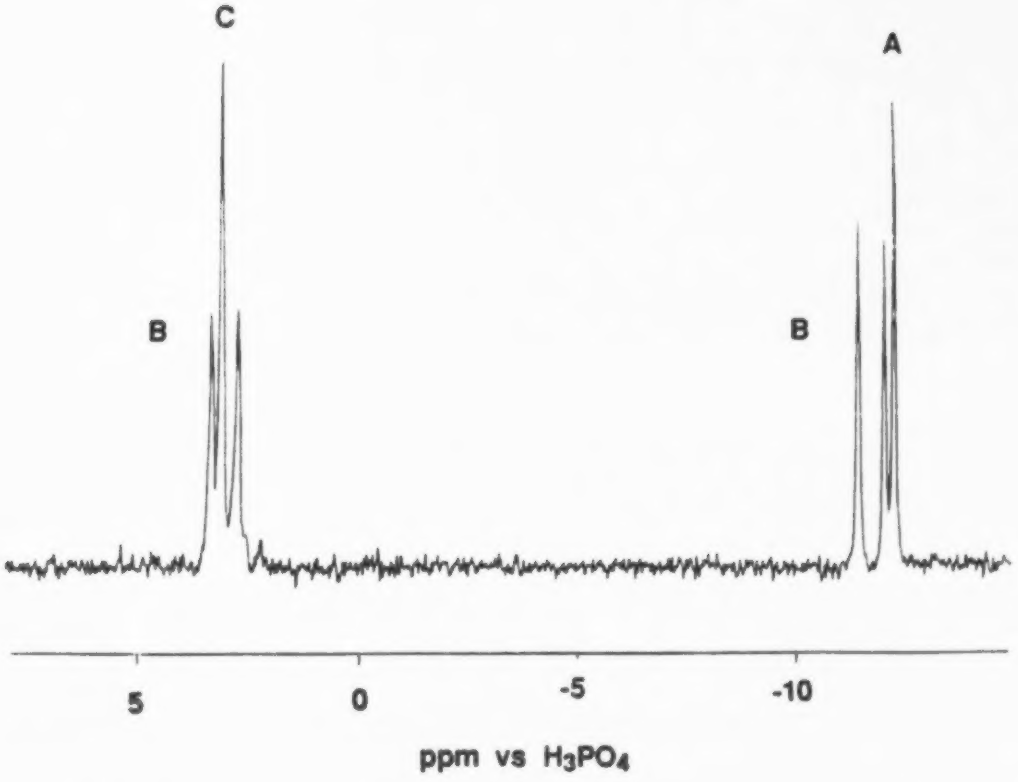

when n=1 do compounds of the general formula **1** display clearly separated ^{31}P and ^{1}H NMR resonances from dppm and the doubly oxidized bisphosphine.

The feature of a bisphosphine which enables successful single oxidation to occur is simple. The oxidation of the first phosphorus centre must somehow alter the accessability of the second phosphorus centre. In Chapters Four and Five it was clearly demonstrated that fixing the two phosphorus centres into a *cis* configuration with a rigid linkage such as a phenyl ring or an ethlyene unit inhibited the oxidation of the second phosphorus centre with a second mole of azide. For those two examples, steric control of the oxidation was possible, but when a flexible alkane links the two phosphorus centres the steric control disappears through bond rotation about the backbone of the bisphosphine.

The distribution of products shown in Figures 7.1 and 7.2, however, demonstrate that dppm seems to display a greater selectivity for mono-oxidation with azides than dppe. An examination of the solid state structures of dppm[1] and dppe[2] is shown in Scheme 7.1. In addition, bis(diphenylphosphino)butane displays structural features similar to dppe except, of course, for the additional number of methylene units between the phosphorus centres[3]. In general, the two phosphorus atoms and the connecting methylene carbons lie in the same plane. For dppm, the presence of only one methylene unit between the phosphorus centres could still restrict access to the phosphorus lone pairs due to steric crowding by the phenyl groups. A modified Newman projection between the two phosphorus atoms (omitting the methylene units) shows that the phosphorus lone pairs have a gauche conformation[1]. Furthermore, the structure of dppm mono-oxidized with trimethylsilyl azide[4] and the mono-selenide[5] have the same gauche conformation. When two methylene units are present between the phosphorus centres (dppe), the diphenylphosphine groups have an anti arrangement in the solid state and the phosphorus lone pairs are not as well protected. The modified Newman projection shows the phosphorus lone pairs to have a dihedral angle approaching 180° [2]. These structural features and the lower yields of **1** (n=2, E=SiMe$_3$) suggests that for dppm there is greater restricted rotation about the methylene backbone and less relief of steric congestion facilitating mono-oxidation.

Scheme 7.1

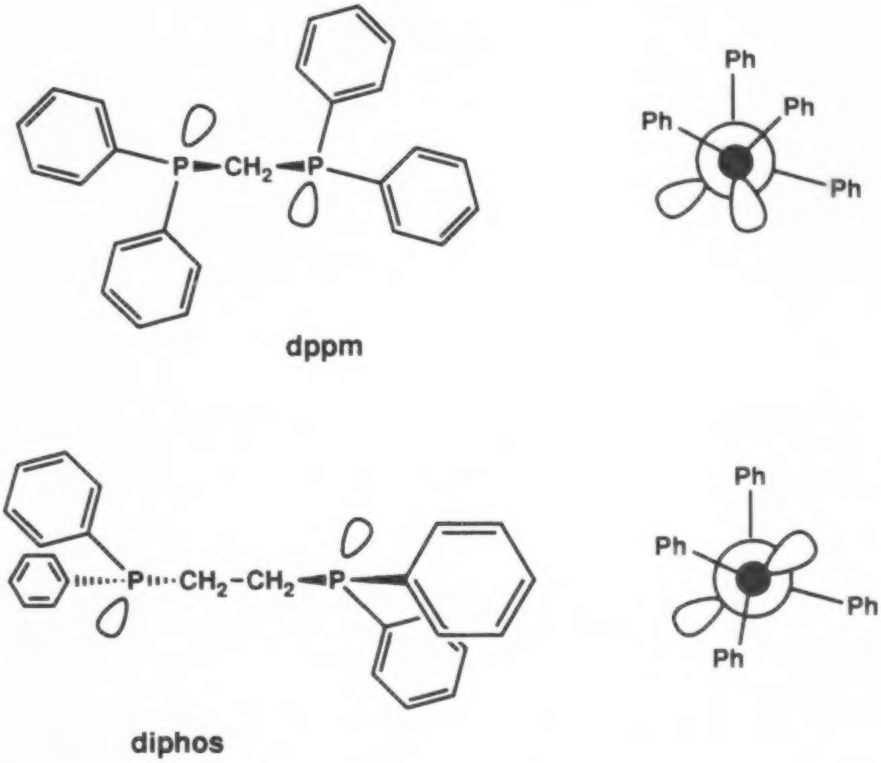
P
CH$_2$
P
Ph
Ph
Ph
Ph
dppm
P
CH$_2$–CH$_2$
P
Ph
Ph
Ph
Ph
diphos

A curious feature of dppm is that reaction with the disulphide of dppm at high temperature in the absence of solvent produces $Ph_2PCH_2P(Ph_2)=S$ (Equation 7.1) cleanly[6]. In this situation, steric bulk cannot protect the second phosphorus centre from oxidation by the relatively small sulphur atom, therefore an additional influence must be present. The same reaction of dppe with the disulphide of dppe does not proceed in the same fashion, but instead an equilibrium is established[6] (Equation 7.2).

Equation 7.1

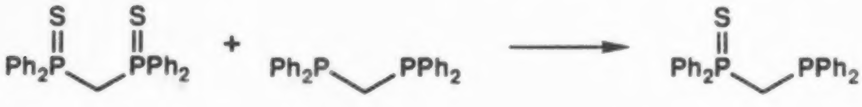

Equation 7.2

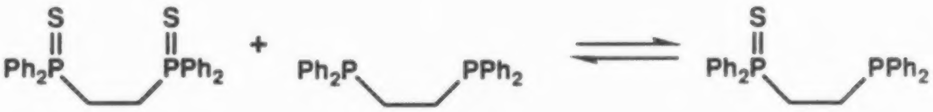

These results suggest that for dppm, oxidation of one phosphorus centre reduces the basicity of the other phosphorus centre two bonds away. When the phosphorus groups are separated by three bonds this effect is small or absent[6]. The ^{31}P NMR data for a series of bisphosphines mono-oxidized with azides is listed in Table 7.1. Considering that oxidation of a phosphine will produce a more electron deficient P(V) centre and hence alter the chemical shift, an operative inductive effect will be indicated by a chemical shift change for the remaining P(III) centre. Indeed, when the phosphorus centres are separated by two bonds the P(III) centre chemical shifts move upfield by 5 to 8 ppm. When the phosphorus centres are separated by three bonds the effect on the chemical shift is much smaller. These results demonstrate that for dppm there is 'some' communication between the two phosphorus groups, but this effect, combined with possible steric constraints on the oxidation of the second phosphorus group, is too small to allow selective mono-oxidation with trimethylsilyl azide to dominate.

The conclusion of this discussion is simply stated. When the phosphorus centres in a symmetric bis-phosphine are too far apart, the reaction with azides will not be selective for the mono-oxidized product.

Table 7.1 ^{31}P NMR chemical shifts and coupling constants.

Bisphosphine$^{(ref.)}$	**P(III) ppm**	**P(V) ppm**	**J_{PP} Hz**
$Ph_2PCH_2PPh_2$[6,b]	-22		
$Ph_2PCH_2PPh_2{=}S$[6]	-27.3	39.2	73
$Ph_2PCH_2PPh_2{=}N\text{-}SiMe_3$[7,a]	-27.4	-1.1	57.0
$Ph_2PCH_2PPh_2{=}N\text{-}C_6F_4\text{-}CN$[7,a]	-30.0	12.9	53.8
$Ph_2PCH(Me)PPh_2$[8]	-6.6		
$Ph_2PCH(Me)PPh_2{=}N\text{-}SiMe_3$[a]	-11.6	5.7	70.0
$Ph_2PCH(Me)PPh_2{=}N\text{-}C_6F_4\text{-}CN$[a]	-14.0	22.0	68.0
$Ph_2PCH_2CH_2PPh_2$[b]	-12.3		
$Ph_2PCH_2CH_2PPh_2{=}N\text{-}SiMe_3$[7,a]	-11.8	3.3	48.7
$Ph_2PCH_2CH_2PPh_2{=}N\text{-}C_6F_4\text{-}CN$[9]	-12.9	16.7	47.5
$Ph_2PC_6H_4PPh_2$[10]	-13.8		
$Ph_2PC_6H_4PPh_2{=}N\text{-}SiMe_3$[a]	-14.5	1.3	18.0
$Ph_2PC_6H_4PPh_2{=}N\text{-}C_6F_4\text{-}CN$[a]	-14.8	11.9	20.8

[a] This work. [b] Experimental observation.

References.

1. H. Schmidbaur, G. Reber, A. Schier, F. E. Wagner and G. Müller. *Inorganica Chimica Acta*, **147**, 143 (1988).
2. C. Pelizzi and G. Pelizzi. *Acta Cryst.*, **B35**, 1785 (1979).
3. A. V. Rivera, D. Gómez, C. E. Rodulfo de Gil and T. Suárez. *Acta Cryst.*, **C44**, 277 (1988).
4. H. Schmidbaur, G. A. Bowmaker, O. Kumberger, G. Müller and W. Wolfsberger. Z. *Naturforsch*, ***45b***, 476 (1990).
5. R. Colton, B. F. Hoskins and P. Panagiotidou. *Aust. J. Cehm.*, **40**, 1909 (1987).
6. D. H. Brown, R. J. Cross and R. Keat. *J. C. S. Dalton*, 871 (1980).
7. K. V. Katti, R. J. Batchelor, F. W. B. Einstein and R. G. Cavell. *Inorg. Chem.*, **29**, 808 (1990).
8. C. L. Lee, Y. P. Yang, S. J. Rettig, B. R. James, D. A. Nelson and M. A. Lilga. *Organometallics*, **5**,2220 (1986).
9. R. G. Cavell, P. Collins and R. W. Reed. Unpublished result.
10. S. E. Tunney and J. J. Stille. *J. Org. Chem.*, **52**, 748 (1987).

Chapter Eight

Conclusions

Conclusions

The conclusions have already been stated at the end of each chapter in the Summary sections, however, a number of valuable lessons have been learned from this work. In Chapters two, three, and six, unusual multinuclear NMR features have been observed and exploration of these features has provided valuable structural and chemical information. This suggests that, in general, second order NMR spectra should be given careful consideration in order to establish the presence of additional information before the spectra are dismissed as complex. Recently, an excellent example of an AA'X spin system transforming into an ABX spin system was given little attention by the authors[1]. In Chapters four and five, the exploration of the Staudinger reaction with rigid *cis* bisphosphines has clarified some of the requirements for efficient mono-oxidation with an azide. In Chapter seven a general discussion was presented in order to bring the overall requirements of the mono-oxidation of bisphosphines into perspective. Simply stated, the selectivity of the Staudinger reaction for mono-oxidation decreases with the separation of the phosphorus centres in bisphosphines.

The deuterium exchange process reported in Chapter three brings an additional view point into the discussion of the basicity of the phosphinimine nitrogen. When strongly electron withdrawing substituents are present, the exchange does not proceed (in unpurified $CDCl_3$), but when deuterium exchange does occur, the phosphinimine nitrogen has a greater Lewis basicity. In addition, decomposition of the phosphinimine unit suggests a nitrogen centre with even greater basicity. The observed trend in the substituents for these compounds seems to be: CH_3[1]$>PhCH_2>Me_3Si>$fluoroaromatic.

Finally, a variety of rhodium (I) complexes have been prepared and characterized by multinuclear NMR spectroscopy. One of these has also been characterized by X-ray crystallography. These complexes are square planar about rhodium with the carbonyl ligand *cis* to the coordinated phosphine. There is very little ^{13}C NMR spectroscopic data available for the carbonyl group in the literature for complexes of this type[1] and so a compilation of chemical shifts and coupling constants is presented in Table 8.1.

Table 8.1 The carbonyl carbon ^{13}C NMR data for rhodium complexes possessing *cis* carbonyl and phosphine ligands.

Complex	^{13}C ppm	$^{1}J_{CRh}$ Hz	$^{2}J_{CP}$ Hz
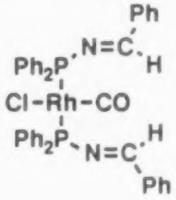	186.7	74.7	15.1
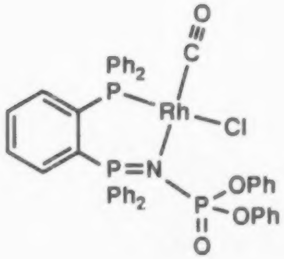	185.9	78.5	16.1
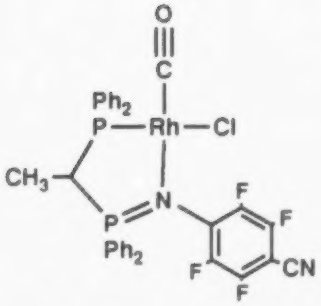	187.6	75	18
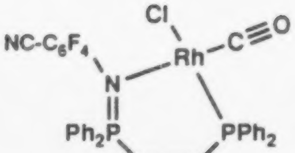	186.8	72.5	19.6

References

1. L. Stepan Van Der Sluys, K. A. Kubat-Martin, G. J. Kubas and K. G. Caulton. *Inorg. Chem.*, **30**, 306 (1991).
2. R. T. Oakley. Ph. D. Dissertation, University of British Columbia, Vancouver, British Columbia, Canada (1976).
3. J. A. Jenkins. Ph. D. Dissertation, University of Alberta, Edmonton, Alberta, Canada (1991).

Appendix

General Procedures.

Unless otherwise noted in the experimental sections, all of the synthetic work in this thesis was carried out using standard Schlenk techniques. All solvents were distilled prior to their use and all reactions were carried out under an argon atmosphere.

Table A.1. Solvents and Drying agents.

Acetonitrile	P_4O_{10} then CaH_2
Benzene	Na or Na/benzophenone
Carbon tetrachloride	P_4O_{10}
Chloroform	P_4O_{10}
Dichloromethane	P_4O_{10} or CaH_2
Diethyl Ether	$LiAlH_4$
Hexane	$LiAlH_4$
Tetrahydrofuran	Na or K or Na/benzophenone
Toluene	Na

Table A.2. Instrumentation.

A. NMR	Nuclei	Frequency
Bruker WP200	^{1}H	200.133
	^{13}C	50.323
	^{31}P	81.015
Bruker AM300	^{1}H	300.13
	^{13}C	75.469
Bruker WH400	^{1}H	400.135
	^{13}C	100.614
	^{19}F	376.503
	^{29}Si	79.495
	^{31}P	161.978

B. Other Instrumentation:

a) Infrared spectra were recorded as CH_2Cl_2 casts on KBr cells on a Nicolet FTIR spectrometer.

b) Low resolution EI mass spectra were recorded on a AEI MS12 magnetic sector mess spectrometer at 70 ev (sometimes 16 eV).

c) Chemical analyses were performed by the University of Alberta, Chemistry department, Microanalytical Laboratory.

d) Melting points were obtained on a MEL-TEMP melting point apparatus and were uncorrected.

Crystallography

The complete structure determination and refinement of $C_{33}H_{33}NP_2Si$ was carried out by Dr. B. D. Santarsiero, Structure Determination Laboratory, University of Alberta, reference file number: SDL:RGC9001. (Chapter four, compound **11**, Figure 4.1, page 88)

Table A3. Crystallographic Experimental Details: $C_{33}H_{33}NP_2Si$.

A. Crystal Data

$C_{33}H_{33}NP_2Si$; FW = 533.67

Crystal dimensions: 0.38 x 0.38 x 0.57 mm

Monoclinic space group $P2_1/c$

$a = 11.093$ (5), $b = 14.898$ (5), $c = 18.811$ (2) Å

$\beta = 102.76$ (2)$^{\circ}$

$V = 3031$ Å^3; $Z = 4$; $D_c = 1.169$ g cm^{-1}; $u = 1.99$ cm^{-1}

B. Data Collection and Refinement Conditions

Radiation:	Mo K_{α} ($\lambda = 0.71073$ Å)
Monochromator:	incident beam, graphite crystal
Take-off angle:	3.00°
Detector aperture:	2.40 mm horiz. x 4.0 mm vert.
Crystal-to-detector distance:	205 mm
Scan type:	θ-2θ
Scan rate:	1.0 - 2.5° min^{-1}
Scan width:	$0.800 + 3.34\tan\theta$
Data collection 2θ limit:	56°

Data collection index range:	-h, -k, ±l
Number of Reflections:	7542 total, averaged: 2941 with $I > 2.50\sigma_I$
Observations: variables ratio:	2941: 334
Agreement factors R_1, R_2, GOF:	0.068, 0.074, 1.92
Corrections applied:	empirical absorption correction

$$R_1 = \Sigma\| F_o| - |F_c\| / \Sigma|F_o| \qquad R_2 = (\Sigma w(|F_o| - |F_c|)^2 / \Sigma w F_o^2)^{1/2}$$

Table A.4 Table of Atomic Coordinates (x 10^{-4}) and Equivalent Isotropic Gaussian Parameters (Å, x 10^{-3})

Atom	x	y	z	U{eq}.
P1	2116(1)	1121(1)	4172.5(8)	45.0(4)
P2	818(1)	1090(1)	2448.3(8)	43.7(4)
Si	3990(2)	2379(1)	3655(1)	70.5(7)
N	3079(4)	1538(3)	3803(2)	53(2)
C1	1533(4)	68(3)	3729(3)	42(2)
C2	956(4)	48(3)	2993(3)	42(2)
C3	525(5)	-767(3)	2679(3)	58(2)
C4	649(6)	-1552(4)	3077(3)	72(3)
C5	1216(6)	-1525(4)	3804(4)	77(3)
C6	1656(5)	-724(4)	4130(3)	62(2)
C7	5003(7)	2780(6)	4499(4)	174(4)
C8	4976(5)	2015(5)	3037(3)	90(3)
C9	3044(7)	3343(5)	3188(5)	141(4)
C11	2715(5)	863(4)	5125(3)	54(2)
C12	3961(6)	704(5)	5359(4)	84(3)
C13	4472(7)	484(6)	6087(4)	124(4)
C14	3728(6)	444(5)	6582(4)	94(3)
C15	2504(6)	609(4)	6360(3)	72(3)

C16	1979(5)	818(4)	5646(3)	60(2)
C21	726(4)	1763(3)	4174(3)	44(2)
C22	-421(5)	1367(4)	4089(3)	61(2)
C23	-1460(5)	1874(5)	4113(3)	73(3)
C24	-1358(6)	2783(4)	4220(4)	81(3)
C25	-216(6)	3184(4)	4318(4)	92(3)
C26	826(5)	2670(4)	4301(3)	68(2)
C31	1986(4)	924(4)	1910(3)	48(2)
C32	2153(5)	1643(4)	1467(3)	67(2)
C33	2999(5)	1599(5)	1043(3)	90(3)
C34	3708(5)	830(5)	1059(3)	90(3)
C35	3586(6)	131(5)	1514(3)	86(3)
C36	2713(5)	180(4)	1937(3)	68(2)
C41	-600(5)	867(3)	1778(3)	46(2)
C42	-673(5)	560(4)	1080(3)	62(2)
C43	-1797(5)	433(4)	595(3)	75(3)
C44	-2864(5)	632(5)	826(4)	85(3)
C45	-2821(6)	943(5)	1515(4)	89(3)
C46	-1692(5)	1049(4)	1985(3)	66(2)

The equivalent isotropic Gaussian parameter U{eq} is $1/3\sum r_i^2$ (i=1 to 3), where r_i are the root-mean-square amplitudes of the AGDP's (anisotropic Gaussian displacement parameters).

Table A.5 Table of Selected Interatomic Bond Lengths (in Å)

Si	N	1.672 (5)	N	P1	1.529 (5)
Si	C7	1.831 (8)	Si	C8	1.845 (7)
Si	C9	1.879 (7)			
P1	C11	1.809 (5)	P1	C21	1.814 (5)
P2	C31	1.829 (6)	P2	C41	1.816 (5)
P1	C1	1.827 (5)	P2	C2	1.847 (5)
C1	C2	1.391 (7)	C1	C6	1.391 (7)
C2	C3	1.388 (7)	C3	C4	1.380 (8)
C4	C5	1.373 (9)	C5	C6	1.380 (8)
C11	C12	1.375 (8)	C11	C16	1.409 (9)
C12	C13	1.401 (9)	C13	C14	1.375 (11)
C14	C15	1.351 (9)	C15	C16	1.376 (8)
C21	C22	1.380 (7)	C21	C26	1.372 (8)
C22	C23	1.387 (8)	C23	C24	1.370 (9)
C24	C25	1.375 (9)	C25	C26	1.392 (9)
C31	C32	1.394 (8)	C31	C36	1.366 (8)
C32	C33	1.360 (9)	C33	C34	1.387 (10)
C34	C35	1.374 (10)	C35	C36	1.383 (9)
C41	C42	1.376 (8)	C41	C46	1.379 (8)
C42	C43	1.385 (8)	C43	C44	1.379 (9)
C44	C45	1.367 (10)	C45	C46	1.373 (8)

Table A.6 Table of Selected Interatomic Angles (in degrees)

C1	C2	C3	118.8 (5)
C1	C6	C5	120.6 (5)
C1	P1	C11	106.5 (2)
C1	P1	C21	103.8 (2)
C2	C1	C6	119.3 (5)
C2	C3	C4	121.8 (5)
C2	P2	C31	102.2 (2)
C2	P2	C41	100.7 (2)
C3	C4	C5	119.0 (5)
C4	C5	C6	120.5 (6)
C7	Si	C8	107.9 (3)
C7	Si	C9	109.2 (4)
C8	Si	C9	106.1 (4)
C11	C12	C13	120.9 (7)
C11	C16	C15	120.3 (5)
C11	P1	C21	103.7 (3)
C12	C11	C16	117.7 (5)
C12	C13	C14	119.9 (7)
C13	C14	C15	119.7 (6)
C14	C15	C16	121.5 (6)
C21	C22	C23	121.0 (5)
C21	C26	C25	120.6 (5)
C22	C21	C26	118.6 (5)
C22	C23	C24	120.0 (6)
C23	C24	C25	119.5 (6)
C24	C25	C26	120.2 (6)
C31	C32	C33	120.9 (6)
C31	C36	C35	120.3 (6)
C31	P2	C41	101.6 (2)
C32	C31	C36	119.3 (5)
C32	C33	C34	119.3 (7)
C33	C34	C35	120.4 (6)

C34	C35	C36	119.7 (6)
C41	C42	C43	121.9 (6)
C41	C46	C45	121.9 (6)
C42	C41	C46	117.7 (5)
C42	C43	C44	118.2 (6)
C43	C44	C45	121.3 (5)
C44	C45	C46	119.0 (6)
N	P1	C1	110.7 (3)
N	P1	C11	113.3 (2)
N	P1	C21	117.8 (2)
N	Si	C7	112.2 (3)
N	Si	C8	110.4 (3)
N	Si	C9	110.8 (3)
P1	C1	C2	120.8 (4)
P1	C1	C6	119.9 (4)
P1	C11	C12	118.5 (5)
P1	C11	C16	123.8 (4)
P1	C21	C22	122.4 (4)
P1	C21	C26	118.9 (4)
P2	C2	C1	119.8 (4)
P2	C2	C3	121.3 (4)
P2	C31	C32	115.6 (4)
P2	C31	C36	125.0 (5)
P2	C41	C42	125.7 (4)
P2	C41	C46	116.6 (4)
Si	N	P1	152.7 (3)

The complete structure determination and refinement of $C_{34}H_{33}ClNOP_2RhSi$ was carried out by Dr. B. D. Santarsiero, Structure Determination Laboratory, University of Alberta, reference file number: SDL:RGC8908. (Chapter four, compound **19**, Figure 4.3, page 96)

Table A7. Crystallographic Experimental Details: $C_{34}H_{33}ClNOP_2RhSi$.

A. Crystal Data

$C_{34}H_{33}ClNOP_2RhSi$; FW = 700.03

Crystal dimensions: 0.32 x 0.44 x 0.66 mm

Monoclinic space group $P2_1/c$

$a = 13.793\ (3)$, $b = 12.622\ (11)$, $c = 20.436\ (6)$ Å

$\beta = 105.93\ (2)^\circ$

$V = 3421.2$ Å^3; $Z = 4$; $D_c = 1.359$ g cm^{-1}; $\mu = 7.214$ cm^{-1}

B. Data Collection and Refinement Conditions

Radiation:	Mo K_α ($\lambda = 0.71073$ Å)
Monochromator:	incident beam, graphite crystal
Take-off angle:	3.00°
Detector aperture:	2.40 mm horiz. x 4.0 mm vert.
Crystal-to-detector distance:	205 mm
Scan type:	θ-2θ
Scan rate:	2.0 - 4.0° min^{-1}
Scan width:	$0.900 + 0.347\tan\theta$
Data collection 2θ limit:	56°
Data collection index range:	-h, -k, ±l

Number of Reflections:	8589 total, averaged; 3537 with $I > 2\sigma_I$
Observations: variables ratio:	3537: 370
Agreement factors R_1, R_2, GOF:	0.064, 0.061, 1.45
Corrections applied:	empirical absorption correction

$R_1 = \sum| |F_o| - |F_c| | \; / \; \sum|F_o|$ $R_2 = (\sum w(|F_o| - |F_c|)^2 / \sum wF_o^2)^{1/2}$

Table A.8 Table of Atomic Coordinates (x 10^{-4}) and Equivalent Isotropic Gaussian Parameters (x 10^{-3})

Atom	x	y	z	U{eq}
Cl	1620(2)	2529(2)	-780(1)	69.3(10)
N	2418(4)	3149(6)	839(3)	41(2)
P1	1845(2)	2738(2)	1363(1)	40.2(8)
P2	3815(2)	1260(2)	1186(1)	38.0(7)
Rh	2729.3(5)	1844.7(6)	253.2(3)	38.7(2)
Si	2820(2)	4390(2)	684(1)	60(1)
C	2971(6)	662(8)	-270(4)	63(4)
O	3086(5)	18(6)	-579(3)	39(3)
C1	2588(5)	1907(7)	2037(3)	40(3)
C2	3414(5)	1307(7)	1971(3)	35(3)
C3	3918(6)	661(7)	2508(4)	47(3)
C4	3616(6)	598(7)	3096(4)	54(3)
C5	2812(6)	1149(8)	3159(4)	53(3)
C6	2294(6)	1815(8)	2645(3)	50(3)
C7	3730(7)	4282(9)	165(5)	90(5)
C8	1741(8)	5188(9)	204(6)	124(6
C9	3502(8)	5069(9)	1488(5)	113(6)
C11	769(6)	1964(8)	945(4)	47(3)

C12	485(7)	1044(9)	1236(4)	77(4)
C13	-337(8)	458(12)	893(5)	134(6)
C14	-859(9)	768(12)	268(5)	149(6)
C15	-618(7)	1669(11)	-35(5)	113(6)
C16	205(6)	2249(9)	305(4)	69(4)
C21	1396(7)	3813(8)	1783(4)	60(4)
C22	494(8)	4288(10)	1476(5)	98(5)
C23	179(9)	5195(11)	1749(6)	135(6)
C24	786(10)	5603(10)	2333(5)	132(6)
C25	1672(9)	5146(9)	2638(5)	100(6)
C26	1984(8)	4261(8)	2374(4)	77(4)
C31	4165(6)	-133(7)	1171(4)	39(3)
C32	5137(6)	-475(7)	1252(4)	49(3)
C33	5345(7)	-1530(7)	1194(4)	62(4)
C34	4600(7)	-2259(8)	1052(4)	68(4)
C35	3623(7)	-1936(8)	976(5)	76(4)
C36	3412(6)	-880(8)	1043(4)	57(4)
C41	5015(5)	1944(7)	1394(4)	41(3)
C42	5509(6)	2331(8)	2028(4)	60(4)
C43	6463(7)	2804(9)	2139(5)	79(5)
C44	6915(7)	2890(8)	1641(5)	78(4)
C45	6436(7)	2518(8)	1002(5)	71(4)
C46	5492(6)	2040(8)	875(4)	57(4)

The equivalent isotropic Gaussian parameter U{eq} is $1/3\Sigma r_i^2$ (i=1 to 3), where r_i are the root-mean-square amplitudes of the AGDP's (anisotropic Gaussian displacement parameters).

Table A.9 Table of Selected Interatomic Lengths (in Å)

Rh	Cl	2.402 (2)
Rh	P2	2.203 (2)
Rh	N	2.146 (6)
Rh	C	1.918 (11)
C	O	1.068 (11)
P1	C1	1.809 (7)
P1	N	1.584 (5)
P1	C11	1.786 (8)
P1	C21	1.802 (9)
P2	C2	1.836 (7)
P2	C31	1.825 (8)
P2	C41	1.811 (7)
C1	C2	1.406 (9)
C1	C6	1.413 (8)
C2	C3	1.390 (9)
C3	C4	1.377 (9)
C4	C5	1.346 (10)
C5	C6	1.382 (10)
N	Si	1.720 (7)
Si	C7	1.857 (9)
Si	C8	1.841 (9)
Si	C9	1.862 (9)
C11	C12	1.409 (11)
C11	C16	1.375 (10)
C12	C13	1.374 (12)
C13	C14	1.342 (14)
C14	C15	1.379 (16)
C15	C16	1.369 (12)
C21	C22	1.369 (11)
C21	C26	1.379 (11)
C22	C23	1.393 (14)
C23	C24	1.358 (16)

C24	C25	1.340 (14)
C25	C26	1.360 (13)
C31	C32	1.375 (10)
C31	C36	1.374 (10)
C32	C33	1.375 (11)
C33	C34	1.351 (11)
C34	C35	1.375 (12)
C35	C36	1.379 (12)
C41	C42	1.377 (9)
C41	C46	1.399 (9)
C42	C43	1.406 (11)
C43	C44	1.336 (11)
C44	C45	1.374 (11)
C45	C46	1.393 (10)

Table A.10 Table of Selected Interatomic Angles (in degrees).

C	Rh	N	178.3 (3)
C	Rh	P2	92.3 (2)
Cl	Rh	C	87.5 (2)
Cl	Rh	N	92.2 (2)
Cl	Rh	P2	176.9 (1)
P2	Rh	N	88.1 (2)
N	P1	C11	111.0 (4)
N	P1	C21	112.1 (4)
N	Si	C7	109.9 (4)
N	Si	C8	110.0 (4)
N	Si	C9	111.5 (4)
P1	N	Si	131.9 (5)
P1	C1	C2	122.9 (6)
P1	C1	C6	118.5 (6)
P1	C11	C12	122.7 (5)
P1	C11	C16	119.5 (7)
P1	C21	C22	120.0 (7)
P1	C21	C26	122.0 (7)
P2	C2	C1	123.3 (5)
P2	C2	C3	117.8 (6)
P2	C31	C32	123.6 (7)
P2	C31	C36	118.4 (6)
P2	C41	C42	125.1 (7)
P2	C41	C46	116.9 (5)
Rh	C	O	177.7 (7)
Rh	N	P1	109.9 (4)
Rh	N	Si	118.2 (4)
Rh	P2	C2	116.7 (2)
Rh	P2	C31	115.4 (2)
Rh	P2	C41	113.8 (3)
C1	C2	C3	118.8 (7)
C1	C6	C5	120.3 (8)

C1	P1	C11	105.6 (4)
C1	P1	C21	105.7 (4)
C1	P1	N	115.0 (4)
C2	C1	C6	118.4 (7)
C2	C3	C4	121.2 (8)
C2	P2	C31	100.9 (4)
C2	P2	C41	104.7 (3)
C3	C4	C5	120.5 (7)
C4	C5	C6	120.6 (8)
C7	Si	C8	108.1 (5)
C7	Si	C9	106.3 (5)
C8	Si	C9	110.9 (5)
C11	C12	C13	121.0 (8)
C11	C16	C15	121.2 (10)
C11	P1	C21	106.9 (4)
C12	C11	C16	117.8 (8)
C12	C13	C14	118.7 (12)
C13	C14	C15	122.4 (11)
C14	C15	C16	118.8 (10)
C21	C22	C23	121.4 (9)
C21	C26	C25	120.7 (9)
C22	C21	C26	117.6 (9)
C22	C23	C24	118.7 (12)
C23	C24	C25	120.5 (11)
C24	C25	C26	121.1 (11)
C31	C32	C33	120.9 (8)
C31	C36	C35	120.9 (9)
C31	P2	C41	103.6 (4)
C32	C31	C36	118.0 (8)
C32	C33	C34	121.0 (9)
C33	C34	C35	119.1 (10)
C34	C35	C36	120.2 (9)
C41	C42	C43	120.1 (9)
C41	C46	C45	120.3 (8)
C42	C41	C46	117.9 (7)

C42	C43	C44	121.6 (8)
C43	C44	C45	119.5 (9)
C44	C45	C46	120.5 (8)